CR 137752

STUDY OF ON-BOARD COMPRESSION OF EARTH RESOURCES DATA

FINAL REPORT

Contract No. NAS 2-8394
TRW No. 26566

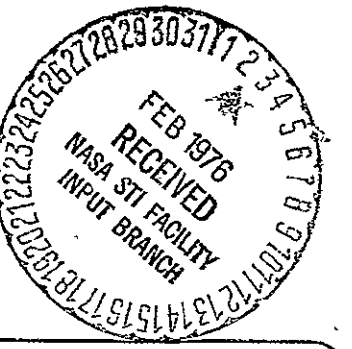

SEPTEMBER 1975

Prepared for

NASA AMES RESEARCH CENTER
Moffett Field, California 94035

TRW
SYSTEMS GROUP
ONE SPACE PARK • REDONDO BEACH, CALIFORNIA 90278

CR 137752

STUDY OF ON-BOARD COMPRESSION OF EARTH RESOURCES DATA

FINAL REPORT

Contract No. NAS 2-8394
TRW No. 26566

A. HABIBI

SEPTEMBER 1975

NASA TECHNICAL MONITOR
Edgar M. Van Vleck

Prepared for

NASA AMES RESEARCH CENTER
Moffett Field, California 94035

TRW
SYSTEMS GROUP
ONE SPACE PARK • REDONDO BEACH, CALIFORNIA 90278

1. INTRODUCTION

NASA's LANDSAT (ERTS) program has provided a wide variety of users the opportunity to explore the utility of satellite-based earth resources observation. Although the full range of applications has not yet been addressed, the potential of such systems to earth resource management has been definitely established. Even at this early stage, many commercial and governmental agencies have expressed strong interest in the operational use of earth observations. The LANDSAT experiment has also shown that converting this potential into an operational system in which practical earth resource management can be accomplished requires extensive investments in communications, data handling, and data processing. These investments are continually increasing along with user requirements for increased spatial and spectral resolution, earth coverage, and data timeliness which imply sensor output and data processing rates of hundreds of megabits per second.

The objective of on-board data compression (source encoding) is to reduce costs and/or systems constraints incurred by high data rates in the sensor-to-ultimate user data handling chain. When the data rate and volume are reduced at the sensor, obvious benefits result. These include reduced on-board storage, simpler data transmission, simpler ground data recording, and fewer data tapes to archive. This is accomplished by exploiting statistical dependencies which exist between data samples in order to reduce the information rate.

Data compression has been the subject of much research and a large number of papers over many years. In spite of the progress made in this field, few spacecraft missions have been able to justify on-board data compression with its attendant risks in reliability and data alteration, and its cost in terms of size, weight, and power. The situation, however, has changed recently. Digital logic has become smaller, more reliable, less expensive, and much less power consuming for a given amount of processing. It now appears practical to actually implement an operational data compression system.

One of the principal considerations in selecting the most feasible data compression technique is the need for broadbased applicability. Earth observation experiments are characterized by general purpose sensors which

are used by hundreds of investigators for many different purposes. Such a variety of users requires that the designer provide an information management system as broadly useful as possible within the cost constraints. Achievement of this maximum utility in terms of cost benefits and cost avoidance is a major tradeoff item.

1.1 NEED FOR DATA COMPRESSION OF EARTH RESOURCES DATA

By surveying the almost continuous studies of user needs for earth resources data, it is possible to judge trends in data requirements. One recent survey [150] of these studies related data types, such as ocean survey, meteorology, agriculture, forestry, geology, and mineral resources to user community uses ranging from sea surface effects (temperature, roughness, etc.) to terrain mapping, atmospheric pollution, and severe storm warning. Additional factors such as data uses, data destination, data perishability, frequency of observation, and resolution can then be used to form candidate missions and sensor groupings to meet emerging needs. Figure 1.1 presents a summary of typical sensor/mission groupings.

MISSION \ SENSORS	IMAGING SENSORS	SPECTROMETERS	VISIBLE AND INFRARED RADIOMETERS	PASSIVE MICROWAVE RADIOMETERS	SYNTHETIC APERTURE RADAR
TERRESTRIAL SURVEY ENVIRONMENTAL QUALITY	x	x			
OCEAN SURVEY METEOROLOGICAL	x	x	x		
TERRESTRIAL SURVEY/ ENVIRONMENTAL QUALITY	x	x			x
OCEAN SURVEY/ METEOROLOGICAL			x	x	
TRANSIENT ENVIRONMENT PHENOMENA MONITORING			x		
TERRESTRIAL SURVEY ENVIRONMENTAL QUALITY	x	x			x
OCEAN SURVEY/ METEOROLOGICAL		x		x	
METEOROLOGICAL			x	x	x

Figure 1.1. Mission/Sensor Grouping

CONTENTS

CONTENTS (Continued)

CONTENTS (Continued)

ILLUSTRATIONS

ILLUSTRATIONS (Continued)

TABLES

1. INTRODUCTION

NASA's LANDSAT (ERTS) program has provided a wide variety of users the opportunity to explore the utility of satellite-based earth resources observation. Although the full range of applications has not yet been addressed, the potential of such systems to earth resource management has been definitely established. Even at this early stage, many commercial and governmental agencies have expressed strong interest in the operational use of earth observations. The LANDSAT experiment has also shown that converting this potential into an operational system in which practical earth resource management can be accomplished requires extensive investments in communications, data handling, and data processing. These investments are continually increasing along with user requirements for increased spatial and spectral resolution, earth coverage, and data timeliness which imply sensor output and data processing rates of hundreds of megabits per second.

The objective of on-board data compression (source encoding) is to reduce costs and/or systems constraints incurred by high data rates in the sensor-to-ultimate user data handling chain. When the data rate and volume are reduced at the sensor, obvious benefits result. These include reduced on-board storage, simpler data transmission, simpler ground data recording, and fewer data tapes to archive. This is accomplished by exploiting statistical dependencies which exist between data samples in order to reduce the information rate.

Data compression has been the subject of much research and a large number of papers over many years. In spite of the progress made in this field, few spacecraft missions have been able to justify on-board data compression with its attendant risks in reliability and data alteration, and its cost in terms of size, weight, and power. The situation, however, has changed recently. Digital logic has become smaller, more reliable, less expensive, and much less power consuming for a given amount of processing. It now appears practical to actually implement an operational data compression system.

One of the principal considerations in selecting the most feasible data compression technique is the need for broadbased applicability. Earth observation experiments are characterized by general purpose sensors which

are used by hundreds of investigators for many different purposes. Such a variety of users requires that the designer provide an information management system as broadly useful as possible within the cost constraints. Achievement of this maximum utility in terms of cost benefits and cost avoidance is a major tradeoff item.

1.1 NEED FOR DATA COMPRESSION OF EARTH RESOURCES DATA

By surveying the almost continuous studies of user needs for earth resources data, it is possible to judge trends in data requirements. One recent survey [150] of these studies related data types, such as ocean survey, meteorology, agriculture, forestry, geology, and mineral resources to user community uses ranging from sea surface effects (temperature, roughness, etc.) to terrain mapping, atmospheric pollution, and severe storm warning. Additional factors such as data uses, data destination, data perishability, frequency of observation, and resolution can then be used to form candidate missions and sensor groupings to meet emerging needs. Figure 1.1 presents a summary of typical sensor/mission groupings.

MISSION \ SENSORS	IMAGING SENSORS	SPECTROMETERS	VISIBLE AND INFRARED RADIOMETERS	PASSIVE MICROWAVE RADIOMETERS	SYNTHETIC APERTURE RADAR
TERRESTRIAL SURVEY ENVIRONMENTAL QUALITY	X	X			
OCEAN SURVEY METEOROLOGICAL	X	X	X		
TERRESTRIAL SURVEY/ ENVIRONMENTAL QUALITY	X	X			X
OCEAN SURVEY/ METEOROLOGICAL			X	X	
TRANSIENT ENVIRONMENT PHENOMENA MONITORING			X		
TERRESTRIAL SURVEY ENVIRONMENTAL QUALITY	X	X			X
OCEAN SURVEY/ METEOROLOGICAL		X		X	
METEOROLOGICAL			X	X	X

Figure 1.1. Mission/Sensor Grouping

The sensors listed are typical of the major classes of earth resources sensors to be used in the post 1975 time frame. Among these, the highest data rates are achieved by the imaging sensors, which are often multispectral, and the synthetic aperture radar. One convenient way to look at the data rates of imagers is from the standpoint of the user oriented requirements shown in Figure 1.2. When projected into the 1980's these sensors lead to spacecraft missions with instantaneous composite data rates in excess of 700 Mbps and data volumes approaching 10^{12} bits per orbit. These high data requirements are solidly based on known earth resources user community needs. Economic and/or political vicissitudes notwithstanding, the necessity of considering data compression tradeoffs in future earth resources mission studies is obvious. This report seeks to provide concrete results on multispectral data compression upon which to base such tradeoffs.

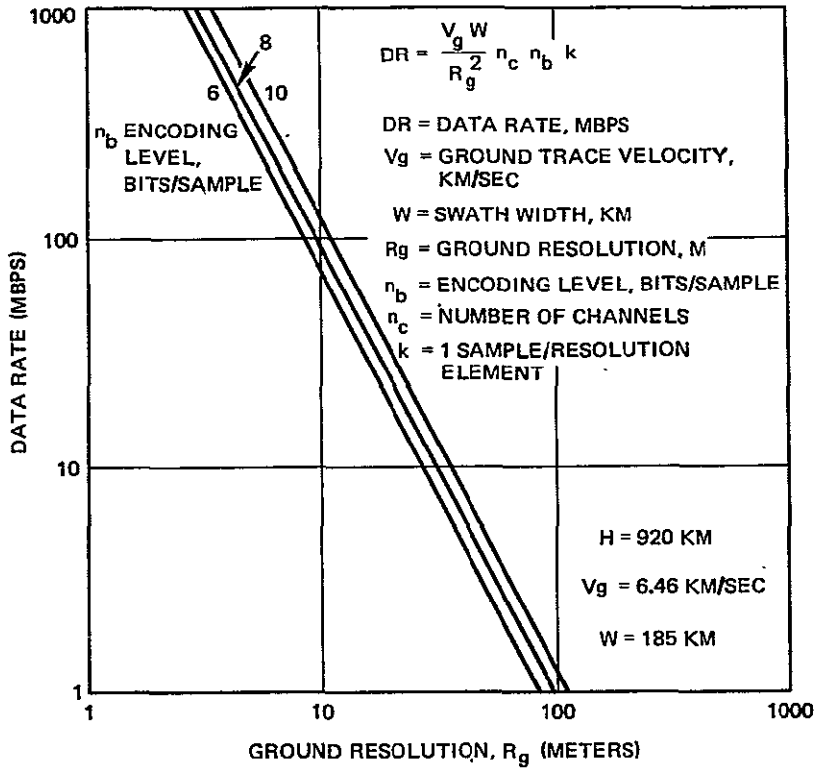

Figure 1.2. Data Rate vs Ground Resolution for Imaging Sensors

1.2 EXPECTED BENEFITS OF DATA COMPRESSION IN NASA EARTH RESOURCES PROGRAMS

The ultimate aim of data compression is to increase the cost-effectiveness of data management in operating earth resources systems. In most cases, the incremental cost of adding data compression is modest. Benefits, however, are usually realized by designing the data management system with integral data compression, not as an add on. There is little impact, for example, in reducing the data rate on an existing communications link if the released capacity cannot be used elsewhere to reduce cost. Cost benefits, in general, are quantitatively related to the compression ratio which is achievable within fidelity constraints. Although the exact relationships and demonstrability of cost savings may be complex, reductions substantially related to the compression ratio are expected. Some of the more obvious cases in which data compression will yield immediate benefits to NASA operating data management systems are:

- High data rate recording at low cost ground stations
- Relaying of data at moderate to high rates, via common carriers (e.g., domestic satellite) for quick look or fast reaction needs
- Maintenance of digital data bases on image analysis computer systems (disks, tapes, drums, etc.)
- Handling, transportation, and capital costs associated with digital (computer) tape distribution and recovery.

It must be recognized that the compression scheme used should be carefully matched to the application. General user applications, such as data archiving, will usually attain only modest compression (factors of 2 to 5). Specific users, however, who require only data subsets with specific characteristics, or who are satisfied with some loss of resolution either spectrally or spatially, can realize cost benefit ratios of 10 to 100. Achievement of some gains is immediately possible in the former case. Information preserving techniques developed under previous NASA studies [91] can be implemented to reduce the cost of archiving and recalling data. In this case, special care is taken that the cost associated with reconstructing compressed data files is minimum because this operation will be repeated often. Compression, on the other hand, is performed only once, upon archiving, and can thus be more complex.

Two examples of data compression benefits to NASA programs are as follows:

Earth Observatory Satellite

One feature of this program is the ability to directly transmit imagery data to low cost user stations for their own processing. Cost considerations, however, dictate a reduced data rate from the 240 Mbps provided to primary stations. A 12 to 1 compression on-board the spacecraft would allow reception of full resolution data at a reduced rate. The only alternatives are various subsampling approaches such as sending 1/4 resolution in each spatial direction. This decreased resolution would severely limit the utility of the imagery to users, even to the point of jeopardizing the practicality of low cost stations.

Goddard Space Flight Center to Sioux Falls Link

The EOS system can produce imagery totaling 10^{12} bits per day. After GSFC processing, this data must be transmitted to the EOS data center at Sioux Falls, S.D. A continuous 10 Mbps link would be required for this transmission for which costs via domestic comsat can exceed $1,000,000 per year. A 4 to 1 compression ratio could provide approximately $750,000 in annual savings.

1.3 PURPOSE OF THE STUDY

The purpose of the study was to provide NASA with comprehensive trade-off data and specific recommended methods of on-board data compression for use in planning and configuring both present and future earth resources programs. This study forms a natural second step to previous NASA funded studies of data compression techniques for multispectral imagery which were more limited in scope and considered only a few specific algorithms. General Electric [142] and Philco-Ford [143] restricted their investigations to rather elementary schemes which were very simply implementable for on-board use. Purdue University [104] considered more complex (transform) techniques and demonstrated their performance on both aircraft and satellite multispectral scanner data. TRW Systems [90] and Purdue University [44] performed parallel studies under the ERTS (now LANDSAT) program to compress multispectral scanner imagery using errorless codes for both archiving and on-board application.

These studies exhibited a number of very basic differences. For one, they were forced to use different data bases due to the sequencing of NASA programs and thus a meaningful comparison of results was difficult. Furthermore, they did not, in general, include important systems parameters such as the effects of channel noise and sensor peculiarities on individual algorithm performance. And finally, the use of differing criteria of optimality and fidelity caused difficulty in applying their results to on-going NASA programs.

The present study is much more comprehensive and unified. It applies a common set of data, criteria, and system parameters and considers a broad range of data compression techniques. The aim was to find the techniques most suitable for multispectral imagery and which inject minimum distortion as measured by a variety of fidelity criteria. Most unique among the criteria was classification accuracy which recognized that many end users employ only specific processing of their data products. Subjective evaluation of typical imagery products was also used. An additional objective was to obtain parametric results which could be used by NASA in future program planning. This included a requirement to deliver all computer simulations to both the Ames and Marshall NASA Centers.

1.4 STUDY APPROACH

The study approach is summarized in the block diagram of Figure 1.3. It starts by surveying the current literature on image bandwidth compression to select the methods which are relevant to the compression of multispectral imagery. The multispectral data is then analyzed statistically. The results are used to select a set of candidate bandwidth compression techniques from the collection of relevant methods. The candidate methods are compared using various criteria of optimality such as mean square error (MSE), signal-to-noise ratio, recognition accuracy, as well as their computational complexity. The comparisons are carried out based on the theoretical performance, experimental performance, and the system considerations of the candidate methods. Based on these results, the candidate methods are funneled down to three recommended methods which are subject to further analysis. The recommended techniques are compared using the above criteria in addition to the subjective quality of the reconstructed imagery. The performance of the recommended techniques was also examined in the presence of

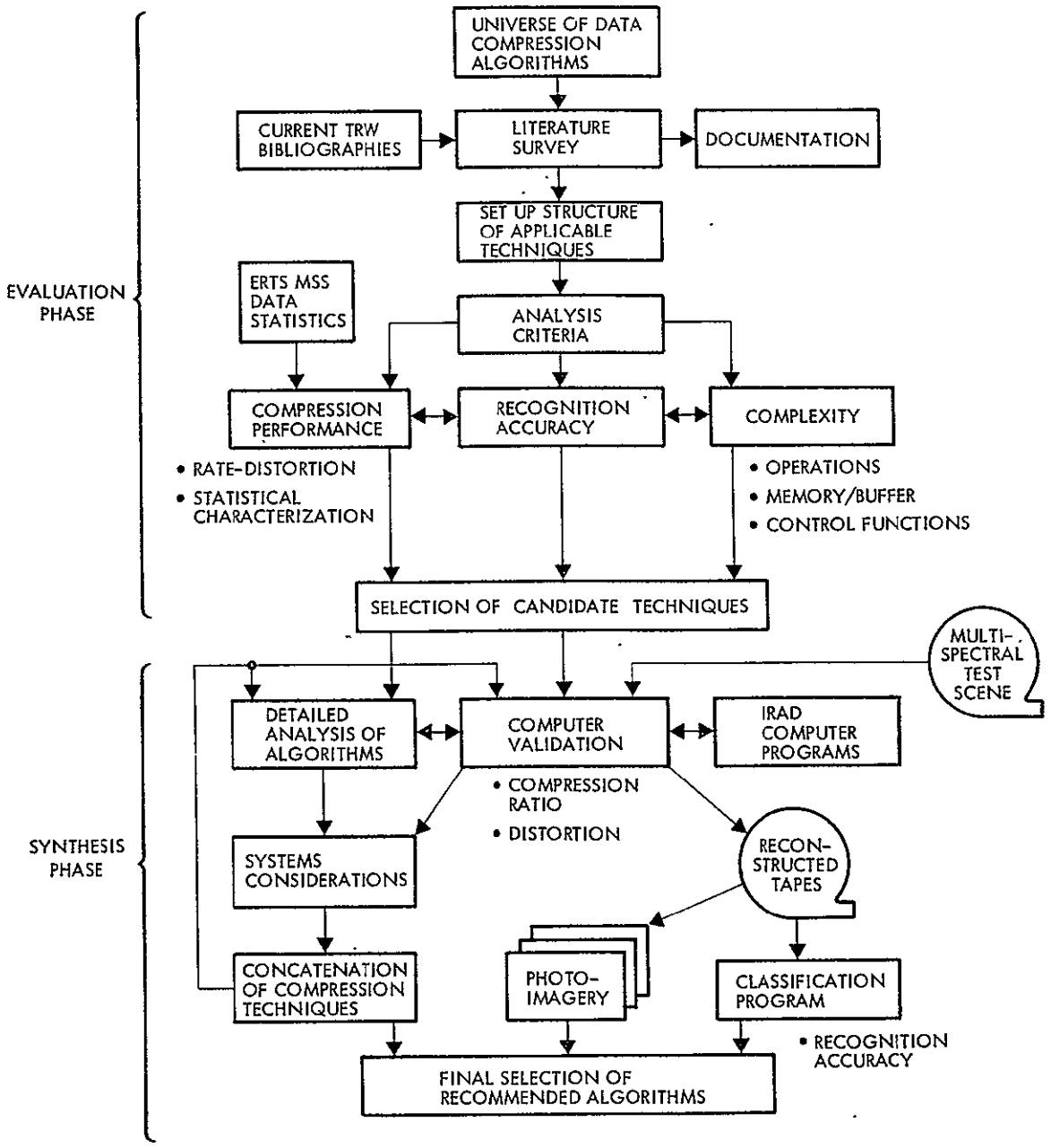

Figure 1.3. Flow Diagram of the Study

channel noise and a variable rate (Huffman) encoder which further reduces the bit rate without affecting the system performance. Finally, merits and demerits of the recommended techniques are discussed and a number of recommendations made for future NASA data compression activities.

1.5 ASSUMPTIONS AND LIMITATIONS

The study has the following limitations:

(1) Only two sets of multispectral data are used in the analysis and simulation of the various coding algorithms. One is a set of four-channel LANDSAT data, and the other is a section of 12-channel high altitude aircraft data. The four-channel LANDSAT data is used to evaluate the performance of various types of bandwidth compression methods. The 12-channel imagery is used to verify the major results and conclusions arrived at using the simulation results with the four-channel data. Although the four-channel data is quite representative of earth resources data, using one set of data limits the reliability of our simulation results to some extent. The alternative approach would have been to use a number of diversified data types, but this would have been impractical in view of the large number of algorithms which have been examined, each performing at several bit rates. This shortcoming is not significant in view of the agreement between the theoretical and experiment results and the fact that the performance of the recommended techniques is verified using the 12-channel aircraft data. In addition, the bandwidth compression software developed under this study has been transferred to NASA Ames Research Center at Moffett Field, California and Marshall Space Flight Center in Huntsville, Alabama. This software could be used to evaluate the algorithm performance on any multispectral data which may be considered significantly different from the above mentioned imagery.

(2) The study considers largely nonadaptive image coding methods for compressing the bandwidth of the multispectral data. This is because nonadaptive image coding methods are better established and tested, they are easier to implement, and in general are less data dependent. In addition, they operate at a fixed output bit rate. This eliminates the need to use a buffer storage and buffer control at the transmitter. However, in recent years a number of adaptive algorithms for coding images have been developed which, in general, perform better than the nonadaptive methods. But they are more data dependent, require buffer storage and buffer control at the transmitter, and are more complex. The addition of a Huffman encoder to the nonadaptive coding methods makes these methods adaptive. This is only one of many ways that bandwidth compression techniques can be adapted to the statistics of the data.

(3) The study includes the complexity of various coding methods and presents tables for comparing the complexity of various coding methods in terms of the number of arithmetic operations and the storage requirements for the various coding algorithms. It does not, however, consider the design complexity and part counts for the various coding methods. A hardware implementation study that would specify the design complexity of the various coding algorithms is beyond the scope of this study.

1.6 SIGNIFICANT RESULTS

The most significant results of the study are summarized as follows:

- Fixed transformations matched to sensors are adequate for spectral processing (e.g., Haar for LANDSAT data)
- For spatial processing at low rates (0.5 to 1.5 bits/pixel), hybrid encoder using a Cosine-DPCM system is optimal. For high rates (>1.5 bits/pixel), a two-dimensional DPCM system technique is optimal.
- The gain due to the addition of entropy coding is 10% for hybrid techniques and 25% for the two-dimensional DPCM technique.
- Cluster coding methods:
  - Best performer at low bit rates
  - Good subjective results for composite color imagery
  - Relatively poor subjective results for individual bands
  - Classification accuracy is not satisfactory for certain users.

2. STATE-OF-THE-ART-SURVEY

This section is a survey of the literature relevant to data compression of remotely sensed earth resources imagery. The survey is divided into three basic segments. The first is a general description of remote sensing, its applications, requirements, and methods. This section is essential to determine which special properties of remotely sensed imagery may be taken advantage of in the compression process and what compression requirements exist. The second category includes the reason for data compression, and the techniques which are relevant to remotely sensed imagery. This section also includes approaches to measuring the error between the original image and the reconstruction of the compressed image. In the final section, the techniques and applications of automatic classification to remotely sensed imagery are described. The last segment is essential since it is by its ability to preserve useful information that a data compression technique must be judged.

Several bibliographies and surveys have been sources of references for this report and should be mentioned here. They are the "Bibliography on Digital Image Processing and Related Topics," by Pratt [2], "Progress in Picture Processing: 1969-71," by Rosenfeld [3], "A Bibliography on Television Bandwidth Reduction Studies," by Pratt [99].

The bibliography documented in Appendix C is also interesting. In addition to the normal reference information, keywords from the article and a brief description of its contents are presented for nearly every reference.

2.1 REMOTE SENSING

One of the areas where images have been found to be very useful sources of information is remote sensing. Essentially, remote sensing is the field concerned with acquiring data about objects while remaining at a distance from them. Although many forms of remotely sensed data, other than imagery, exist, pictures have been very valuable. The word "photograph" has purposely been avoided here because remotely sensed imagery can be obtained in a number of ways besides conventional photography. Among the tools used for obtaining imagery are side looking radar, return beam vidicon tubes, and multispectral scanners [10].

Two questions immediately arise when the use of remotely sensed imagery is proposed. The first one is, why use remotely sensed data? The second is, why use imagery?

There are several reasons for using remotely sensed data. The first and most obvious is that it may not be possible or safe to go near the object of interest. This situation applies to much of man's exploration of space. In fact, many of the developments in remote sensing have been related to the study of space - - from the telescope to space probes carrying sophisticated instruments. For earth resources study, however, the utility of remote sensing is somewhat less obvious. The usefulness comes from the perspective provided, the frequency with which measurements can be made, the large areas which can be covered, and finally from the fact that on the earth there are still many inaccessible places.

Having a high vantage point can be valuable for studies in many fields [7]. Perhaps the most readily apparent are the geographical and geological applications of remotely sensed data. Due to the large scale of geological formations, good persepctive requires that measurements be made from great distances. Other important areas for remote sensing in the past have been forestry and road planning, primarily because of inaccessibility. In agriculture [9], assessment of crop conditions has been made easier using remote sensing techniques, and in archaeology it has been found that patterns in the earth caused by buried ruins of man-made structures can be seen from high above, but are invisible from ground level. Water pollution [8], because of the large areas which must

be covered, also can be studied usefully with remotely sensed data.

In answer to the question "why use imagery," it should first be stated that not all remote sensing methods use imagery. For example, techniques developed to measure water temperature in bodies of water [6] and to measure amounts of air pollution [13] use spectroscopy and scattering of laser radiation, respectively. However, a great percentage of remote sensing is done using imagery. Some of the reasons for the use of pictures are the following. First, all remote sensing measures radiation of some sort emanating from the object under investigation. Many methods are used to record the energy of the radiation. The most familiar is exposing photographic film. Generally, the user of sensor data exploits two kinds of information: the amount of radiation and the direction from which the radiation comes. Using an image format, all the pertinent information can be conveyed. Furthermore, humans are well practiced at separating patterns visible in a scene or picture. It is usually these patterns which provide the information sought by the user. Another key value of imagery is its versatility. That is, the same image which is useful to an agriculturist studying crop type and diseases may be useful to a soil scientist studying soil conditions, or a geologist studying rock formations, or a hydrologist studying drainage patterns.

While imagery has been usefully exploited in remote sensing for a number of years, extremely high altitude imagery has not been available for civilian purposes until recently. The advantages of satellite photography have been discussed and studied [14] using pictures taken by Gemini astronauts, but it has remained for the Earth Resources Technology satellite (LANDSAT) project to provide an important test [11].

Among the reasons put forth in support of satellite-obtained imagery are the large areas which can be covered in a short time, the frequency with which overflights of particular areas can be repeated, the great number of disciplines for which the imagery can provide useful data, and the synoptic view of large areas which is available. Of course acquisition of such imagery is extremely expensive since it requires launching a satellite as well as having appropriate tranducers and communications equipment aboard. The LANDSAT project was designed to test the value of satellite imagery for the study of earth resources.

Since, in many respects, LANDSAT is typical of what can be expected of an earth resources satellite, we describe it in some detail here. LANDSAT was launched July 23, 1972. LANDSAT, which orbits the earth at an altitude between 900 and 950 kilometers, has two kinds of sensors. One is a set of three return beam vidicon tubes, and the other is a multispectral scanner. Each of the vidicon tubes records eletromagnetic energy in a different narrow spectral band. The multispectral scanner records the energy in a different narrow spectral band. The multispectral scanner records the energy in four separate bands from .5 to 1.1 microns. Since the multispectral scanner is probably more typical of future multi-spectral sensors, we describe it in further detail. Essentially, using an array of optical fibers, energy is fed to photomultipliers for the three shortest wavelength bands (.5 to .6, .6 to .7, and .7 to .8 microns) and to silicon photo diodes for the .8 to 1.1 micron band. The outputs of the photomultipliers and photodiodes are analogue signals which are immediately digitized and multiplexed. The output of the multiplexer goes either to a modulator for direct transmission to the earth or is recorded on magnetic tape for subsequent transmission.

A moving mirror aboard the spacecraft permits the recording of one picture line of approximately 3200 points perpendicular to the vehicle's path using only one optical fiber per spectral band. In order to allow for return of the mirror and maintain approximately the same resolution in the directions parallel and perpendicular to the satellite's path, six lines are swept out at a time using six photosensors in each spectral band. Motion of the LANDSAT satellite along its flight path makes possible recording of successive sets of six picture lines. Each fiber passes to its respective photosensor light coming to it from an imaginary four-sided pyramid extending from the fiber at its apex down to the earth at its base. The width of the square base of this pyramid is approximately 79 meters. Since the bases of the adjacent pyramids overlap, the resolution of the multispectral scanner is slightly less than the width of the base. In fact, the vertical distance between picture elements represents a greater distance on earth than the horizontal distance between picture elements. Also, the images are not rectangular because as the satellite travels southward, recording succeeding image lines, the earth rotates

eastward, causing each new line to be slightly further west than the last.

Correction of geometric distortion of LANDSAT imagery done at TRW is discussed in [12]. On the ground, computer compatible tapes are produced for distribution to users. Based on the method of recording, quantizing, and transmitting the image it had been estimated [11] that the error in radiance recorded on the user-distributed tapes due to causes other than quantization, is comparable with the quantization error.

However, the following source of error should be noted: As described above, each spectral component was recorded using six photosensors. These photosensors became less uniform in their behavior as the flight progressed. Consequently, error due to the lack of calibration of these sensors became significant. An on-board calibration procedure using a lamp and calibration wedge had been planned and has been used to linearly equalize the sensors. However, the calibrator has not been entirely successful. (See Algazi et al. [18]). Striping with a six line periodicity occurs in much of the later multispectral scanner imagery. Several methods have been proposed for correcting the streaking a posteriori, with reasonable success.

2.2 DATA COMPRESSION

Several factors determine the data rate required of a high altitude earth resources multispectral sensor [123]. They are observational frequency (hours to months), field of view (1 mile to 1500 miles), ground resolution (50 feet to 20 miles), spectral resolution (0.2μm to .5μm), spectral coverage (.1μm to 2.2μm), radiometric resolution (2 bits/sample to 10 bits/sample). The resulting data rate can be between 20 and 300 megabits per second.

These high data rates make data compression desirable before data transmission. The large amounts of data which must be archived on the ground also make groundbased data compression desirable.

Until now the cost of implementation of data compression schemes has generally outweighted their advantages. Reductions in size, cost, and power consumption, as well as improvements in reliability of digital logic, are making data compression increasingly practical. In order that

data compression be possible, one or both of two separate conditions must be satisfied. The first condition is that the data have some structure or redundancy. This means the data at any point in the image does not take on all values with equal likelihood or that the value at any point is not totally independent of the data at every other point. By knowing something about the data structure, data compression can be accomplished without losing any of the information the data contains. Hence data compression which relies on knowledge of data structure is called information-preserving or error-free data compression. Comparison of a number of such techniques has been done at TRW and appears in [90], [91]. The second condition which leads to compression is that the image user have interest in only a certain portion or aspect of the data collected. In this case, data which is of no value to the user can be discarded, again resulting in data compression. Since information discarded is permanently lost, compression based on user interest is called information-destroying data compression. It can now be seen that information-preserving data compression depends on a property of the data, and information-destroying data compression depends on a property of the user. In an actual application both types of data compression may be used.

Two major types of structure can be exploited for information preserving data compression of multispectral image data as shown in Figure 2.1. The first type is spatial correlation due to properties of the scene being scanned and the scanning mechanism itself. The second type of structure is correlation between the spectral components of a scene. A relatively high spatial redundancy occurs and the ratio of spectral band intensities per picture element (pixel) remains relatively constant, since the reflectivity and incident radiations are reasonable uniform. Suppose that a cloud shadow is cast over a segment of the desert. When the shadowed region is encountered by the scanner, intensities in all spectral bands should simultaneously decrease and remain at some lower value until the shadow boundary is crossed. If the scanning system is such that contiguous pixels represent the intensities of overlapping ground elements, then even higher spatial correlation exists between pixels.

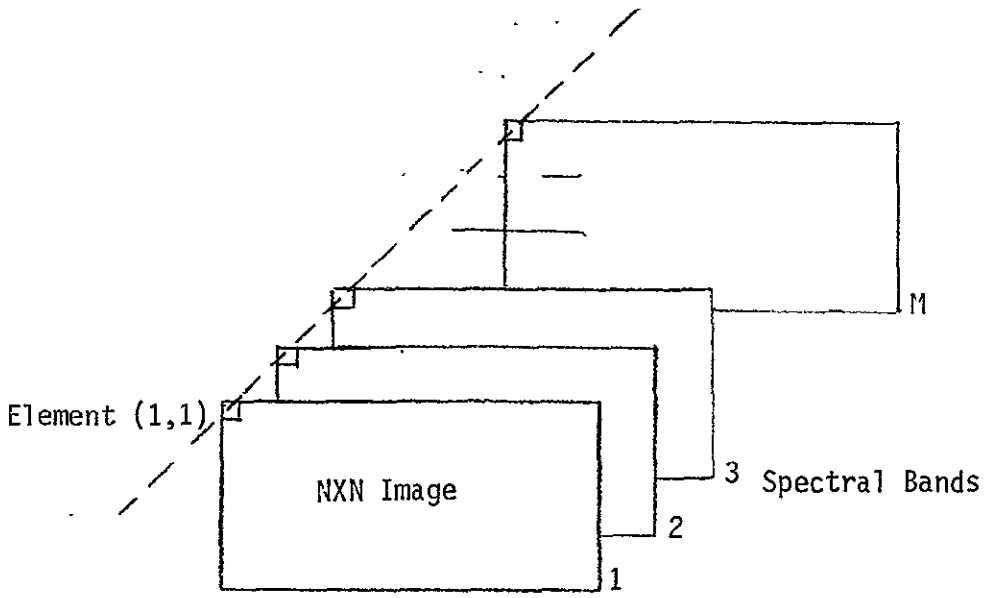

Figure 2.1. Multispectral Image Data

Information-destroying schemes have been regarded with disfavor for earth resources applications because image users have been unable to specify in advance which aspects of the data are of importance to them and which aspects are unimportant. With the increase in data rates, the need to use some sort of information-destroying compression will increase, particularly for "quick look" uses. At the same time, users of earth resources imagery are gradually determining their needs more accurately. These two factors make increasing use of information destroying compression probable.

2.2.1 Fidelity Criteria

In order to determine whether a particular information-destroying compression algorithm preserves sufficient information for a particular use, a criterion must be defined by which the information loss can be measured. Several approaches to the definition of such a criterion have been widely discussed. One approach is the definition of a measure of error between the original image and the reconstruction of the compressed image. Such a measure is called a distortion measure [54], [121]. Given such a measure and the source statistics, it is possible to determine the maximum compression which can be obtained with a particular amount of distortion. The functional relationship between the amount of distortion

and the achievable compression of the source data is given by the rate distortion and the achievable compression of the source data is given by the rate distortion function. Unfortunately, although the rate distortion function specifies the minimum data rate which will yield less than a specific amount of distortion, it does not reveal what encoding method will achieve the minimum rate. It does, however, provide a basis for judging any particular coding scheme. A summary of the evaluation of performance appears in [40]. The various aspects of rate distortion theory are discussed in [29]. A method for bounding rate distortion functions for cerain memoryless sources is given in [69]. The rate - distortion function for a class of processes is derived in [113].

The basic problem which is inherent in any use of rate distortion theory, is the difficulty in choosing an appropriate measure of distortion. This problem has been studied by several authors in attempts to obtain reasonable measures for particular applications[88], [112], [127]. These measures have primarily been developed to account for the behavior of human visual systems and as such include weighting of spatial frequencies. For earth resources imagery, however, human sensitivity is not of the same importance as in television, for example. Computer classification, as well as the ability to greatly magnify portions of an image, make desirable the definition of a distortion measure independent of spatial frequency. Because of its mathematical convenience, a number of authors have used mean square error as a measure of distortion. This measure was used in [115] to compare line by line encoding and two-dimensional encoding. Vector valued distortion measures have also been studied. For such measures, rate-distortion functions have been derived as well. These functions give the source rate required to keep each element in the distortion vector below some value.

Another criterion which can be used to judge whether a particular information-destroying compression algorithm preserves sufficient source information is the algorithm's effect on classification accuracy. For example, if each raster point in the image is to be classified as corresponding to some crop or land use, based on the recorded brightnesses in the several spectral bands, the increase in the several spectral bands, the increase in classification errors resulting from performing

classification on the reconstruction of the compressed data rather than on the original image is a measure of the relevant information lost due to compression.

The increased probability of misclassification can be used as a distortion measure, but, unfortunately, the complexity of the classification procedure generally precludes calculation of the corresponding rate distortion function.

2.2.2 Data Compression Techniques

A number of data compression techniques have been used for various types of data. In this discussion we will limit ourselves to those methods which are relevant to imagery, with emphasis on multispectral high altitude imagery. Most of the methods which have been shown to perform well consist of concatenations of several techniques.

Entropy Coding

Entropy coding is one of the most basic approaches to data compression. Many compression schemes use such coding in the last stage of the coding procedure. Combination of entropy coding with other techniques will be discussed in subsequent sections. Entropy coding is applicable whenever certain data values occur more frequently than others or the data can be converted into a form in which certain values occur more frequently than others, such as through differentiation. A code is used which has a short code word length for the frequently occurring values and a long code word length for infrequently occurring values. The average word length can thereby be minimized. This approach is similar to that used in Morse code where the frequent letter "e" is coded with one dot and the infrequent "z" is coded with two dashes and two dots. To make effective use of entropy coding, the statistics of the data must be known and the frequency of occurrence of certain data values must be significantly higher than the frequency of others. Since codewords have variable length, it is necessary that there be some means by which succeeding codewords can be separated by the decoder. Some variable length codes can be uniquely decoded without separation between succeeding codewords. Such codes are said to be "comma free."

The optimal entropy code, given the probability of occurrence of each data value, is the Huffman Code [54]. This code is comma free and can readily be determined from the probabilities of the data values.

A near optimal entropy code, which is likewise comma free, is the Shannon-Fano Code. It also requires knowledge of the data value probabilities but can be developed more easily than the Huffman code.

One approach to the problem of determining the source statistics is to read in a block of data and make a histogram of the data values. Then one of several possible variable length codes can be chosen based on these statistics [95], [106]. An additional codeword specifying which code has been chosen is then required. Rice coding is an example of this technique in which the data is first transformed into a form where certain values are more likely than others and then the transformed data is read in a block at a time. The transformation which has been studied the most involves differencing of succeeding elements. Since spatial correlation exists in most imagery, the difference between adjacent elements tends to be small. Hence the frequency of small difference values is much larger than the frequency of large difference values. Thus Rice coding can be applied to the data differences. Other data transformations such as the Fourier Transform or Hadamard Transform can be treated in a similar fashion. Using data differences, Rice and Plaunt [106] obtained data rates no more than .5 bits greater than the first-order data entropy (the minimum obtainable). Studies of the application of such techniques to earth resources imagery have been done at TRW [90], [91].

A general treatment of Universal Codes (block codes which adapt to obtain a performance measure arbitrarily close with increasing block length) is given in [43].

Since codewords are of variable length for all entropy codes, the source coder output rate is not constant. Consequently, a buffer is required in order that the output rate is constant. A number of studies of the properties of such buffers have been made [33], [74]. Buffer considerations have been studied at TRW as well, and appear in [90], [91].

Quantization and Sampling

When a continuous signal is sampled and quantized, there is generally information loss. If the signal is bandlimited,then sampling at the Nyquist rate (twice the highest frequency component present in the signal) without quantization will make possible perfect signal reconstruction when infinite samples are obtained [111]. However, sampling is only for a finite time. Furthermore, for convenience of handling and for noise protection, quantization is normally desirable in sampled systems. The sampled and quantized signal expressed in binary form is said to be coded by pulse code modulation (PCM). PCM is commonly used for the output of multispectral scanners whose sensors are arrays of photodiodes or photomultipliers. Sampling is inherent due to the discrete nature of the sensor array. Quantization can be done in equal increments (called linear quantization) or with varying size increments. For example, steps sizes can vary logarithmically or as a Gaussian wave. Step sizes can also be designed to minimize some error measure [89].

The distortion introduced when a signal is sampled and quantized as well as optimum sampling and quantization are discussed in [28], [53], [55], [56], [59], [70], [72], [89], [129]. Adaptive quantization is discussed in [31], [108].

The Nyquist rate for scanned sampling is generally higher than the highest two dimensional frequency. As a result, scan-sampling below the Nyquist frequency can be accomplished by using comb filters to eliminate the aliased signal [58].

Permutation codes can be used for block quantization [28], [30], as follows. A block of data values are recorded. The n_1 largest recorded values are represented by one codeword. The n_2 next largest values are represented by another codeword. This procedure is continued until all values are represented by some codeword. The number of values to be represented by each codeword is chosen adaptively depending on the data, as is the number of codewords to be used for any block. These codes have been shown to be very good for low rates and can be made good for high rates if long block lengths are acceptable.

Delta Modulation

In delta modulation the signal is sampled and a decision is made to transmit a positive step or a negative step depending on whether the reconstructed signal is larger or smaller than the original signal. The step size is always constant (see Figure 2-2). Thus for each sample only one bit is transmitted. An initial value must also be transmitted. Consequently, if the fixed size is Δ, the delta coded signal requires a minimum of N steps to change in magnitude by $N\Delta$. The result is that if the original signal has a large change at some point, the delta modulator cannot keep up with the signal. This shortcoming is called "slope overload." To eliminate or reduce slope overload, several adaptive approaches have been tried. One is to sample at a high rate in comparison with the Nyquist frequency. Another approach is to change the value of Δ according to the number of times in a row the delta modulator obtains the same direction of change [37]. This scheme requires a delay and feedback. A third approach is to transmit large differences using differential pulse code modulation (discussed below) and small changes using delta modulation [50]. Other approaches are discussed in [15]. Delta modulators have been combined with other compression techniques such as PCM [60] and their signal to quantizing noise properties studied [94], [95].

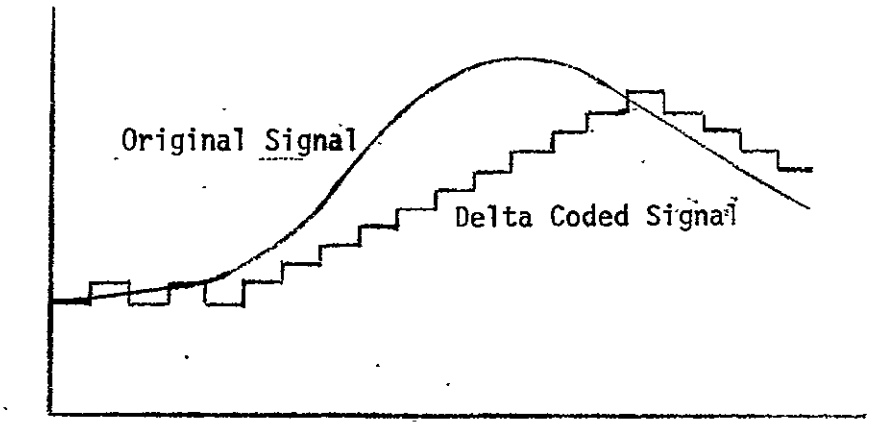

Figure 2.2. Delta Modulation

Predictive and Interpolative Encoding

An important set of compression techniques falls in the category of predictive and interpolative encoding. Generally, these techniques in some way use data that has already been obtained to estimate other data. It is the difference between the estimate and the actual value which is actually encoded. Predictive and interpolative coding methods are distinguished by their method of estimating new data. In the interpolative case, estimates are made of values between already measured points. In the predictive case estimates are made of data values which are not between already recorded data values. For example, a zero order predictive encoder predicts that the next data value will be equal to the most recently measured data value. It then encodes the difference between the next data value and its prediction, i.e., the most recently measured data value. This type of predictive encoder is very popular and when the difference is quantized is called differential pulse code modulation (DPCM).

DPCM can be used for data compression because signals generally change slowly compared with the sampling rate, and consequently the difference between succeeding elements tends to be small. Thus fewer bits are required to encode the differences than to encode the actual signal values. When few bits are used to encode the differences, the scheme has a susceptibility to slope overload similar to that discussed in the previous section [123]. To overcome the problem of slope overload, nonlinear quantization has been used [51], coding which takes advantage of the eye's lack of sensitivity to small changes in the neighborhood of large changes has been investigated [75], and block Huffman coding of DPCM data has been studied [106]. Decoding of DPCM data essentially requires integration. Consequently, errors tend to propagate [26], [47]. This sensitivity of DPCM to channel errors makes other predictive schemes of interest [35]. DPCM is also sensitive to sensor nonuniformity such as that described in Section 2.

A number of studies and comparisons of a variety of predictive and interpolative coding schemes have been made [22], [27], [34], [38], [39], [41], [42], [45], [71], [81], [84], [92], [105].

Transform Coding

The object of the ideal transform coding system is a linear mapping of a block of correalted sample values into a smaller set of statistically independent coefficients. A rate reduction is then accomplished by sorting and quantizing the transformed scene depending on data activity.

Transforms are usually applied to square blocks of data, although they can be used with other blockings as well or on a line-by-line basis. A survey of various transform techniques appears in [128]. A comparison of various transform techniques in both performance and complexity appears in [22], [66], [110]. The application of transform techniques to color television is covered in [102]. If the picture is broken up into square blocks, adaptive coding can be used to take advantage of block non-stationarities. DPCM, described in the previous section, can be viewed as a transform technique [65]. A comparison of DPCM and various transform techniques appears in [62].

The following transforms have received the major attention:

(1) Eigen-Function (Karhunen-Loeve) Transform [40]. This transform, also known as the KL transform, the eigenvector transformation, the principal components transformation, and the Hotelling transformation, results in uncorrelated (and hence if the data is assumed Gaussian, independent) transform values. While theoretically optimal in the mean square sense, this technique is often impractical to implement due to the excessive computation required and the uncertainty in covariance matrix determination, since, in practice, the correlation matrix of sample values must be known or estimated (i.e. scene statistics are required to use it). This matrix must be diagonalized to find the eigen-values and eigenfunctions and then the transform performed (a matrix multiplication that is quite time-consuming for large block lengths). There is no fast algorithm for this transformation, in contrast with the Fourier and Hadamard transforms. Adaptive block quantization using this transform has been studied in [125]. Application to multispectral imagery is discussed in [104].

(2) Fourier Transform -The Fourier transform values are asymptotically (in block size) uncorrelated and for moderate video block sizes (say 32x32 or larger) have been found to be essentially so. Hence, the Fourier transform is almost as good as the Karhunen-Loeve transform without requiring knowledge

of scene statistics. In addition, it can be rapidly computed with the Fast Fourier Transform (FFT) algorithm [57], which requires on the order of $2N^2\log_2 N$ operations for an NxN block, compared with N^4 operations for the KL transform. By adaptively quantizing in blocks,this transform has been shown effective in [19]. Previous work appears in references [24], and [25].

(3) Cosine Transform. The Cosine transform is a modified form of the Fourier transform where the original sequence of data is first used to generate an odd or an even sequence [140]. In the discrete case this gives a sequence of N points for generating an odd or even sequence respectively. The discrete Fourier transform of the longer sequence of data is normalized to give a set of 2N-1(or 2N) real values. This transform possesses the attractive feature of the Fourier transform in addition to the fact that it has continuous boundary conditions and it performs even closer to the KL transform for Markov sequences.

(4) Hadamard (Walsh Function) Transform. This transform is computed using only additions and subtractions and is hence faster than the Fourier transform. A tutorial appears in [10]. Unfortunately, the transform values are not asymptotically uncorrelated, although in some sense they are less correlated than the original data. Hence, the method applies only where Fourier transform implementations are too complex. Data compression is achieved by reducing the signal dimensionality while simultaneously maintaining sufficient subjective image quality. A fast Hadamard transform (FHT) algorithm reduces the number of operations required in NxN matrix multiplication to $N\log_2 N$ operations. The operations are simpler than with the Fourier transform since only additions and subtractions are required. In [16], there has been described a simple factorization of the Hadamard matrix that reduces the FHT algorithm to the equivalent of seven Fortran statements. An implementation of the algorithm for image bandwidth compression has been designed by TRW [17]. The Hadamard and KL transforms have been compared in [61], [76]. Real time implementation is considered in [52] and [93]. Computer experiments on two-dimensional Hadamard transforms were done in [82].

Several other transforms have also been studied:

(5) Other Transforms. The Haar transform also has a fast computational algorithm [23], and like the Hadamard transform, offers greater simplicity

than the Karhunen-Loeve and Fourier techniques. Relations between the Haar and the Hadamard Transforms have been examined in [48].

(6) The discrete linear basis transform has been proposed in [68]. In simplicity and compression it is between the Hadamard and KL transform according to the study. The discrete linear basis is defined a priori, independent of the scene statistics as are the Hadamard and Fourier transforms, and unlike the KL transform. Additions, subtractions, and multiplications are required for its implementation.

(7) The Slant transform is described in [100], and [10], Basis functions for this transform are sampled and quantized "saw tooth" waves. Additions,multiplications, and subtractions are required to implement this transform. Because the slant transform has basis functions which change gradually along an image line, it is suitable for representing gradual brightness changes. This transform has produced good results in simulation using sampled imagery.

Rate reduction techniques which are used in conjunction with transform coding can be classified under the terms sampling, quantizing, and coding. Sampling techniques attempt to exploit the clustering of correlated data in the transform domain. Transform sampling techniques which have been proposed include checkerboard sampling, random sampling, zonal sampling, and threshold sampling [23]. The checkerboard and random sampling technique give poor results in practice because of the convolution of their transforms with the reconstructed image and because they indiscriminately remove some large energy transform samples. Nonadaptive zonal filtering is also not useful for images which contain both low and high frequency energy. The most practical technique which has been investigated is threshold sampling, or threshold coding, in which samples are included only if they lie above a predetermined threshold. Another technique is frequency-dependent threshold coding which is also quite promising, yielding good comparison for low distortion applications.

Quantizing techniques fall into two general categories: 1) distribution of bits among different frequencies according to power level, and 2) distribution of quantization levels at a given frequency. The simplest, but not optimal, distribution of levels is uniform. In [61] the distribution of bits among frequencies is studied. Experiments with the bit distribution

for orthogonal transform coding appear in [110]. The logarithmic quantizer is one means of nonlinearly quantizing the transform domain samples. Its principal advantage is that it can be implemented by continuous arithmetic operations followed by linear quantization.

Frequency domain coding has been studied in [25]. The effects of frequency-dependent bit distributions, high resolution quantizing with code truncation, and a combination of the two techniques were investigated. The performance gains achieved vary from 16.7% to 35%. Some distortion occurred with all of the techniques due to the "convolution effect." A technique which should be investigated further is the use of fixed source (M-ary) codes to coding in the transform domain. Particular promise is shown by the Rice algorithm, a form of universal coding. TRW and JPL have studied implementations of the Rice algorithm [90], [91]. Concatenation of transform coding followed by predictive coding of adjacent coefficients does not appear to be useful because the coefficients in the transform have low redundancy, and the transform is not positively definite. The resulting dynamic range and rapid sign changes result in the need for impractical edge detection coding methods. However, block transform techniques followed by predictive encoding between blocks are considered in [68]. DPCM for coding the error between the original signal and the reconstruction of the transformed signal is discussed in [44].

Block length and dimensionality are important choices in any of the transform techniques. There is a tradeoff between achievable performance and subjective quality, because the distortion criteria permit wide variability in averaging over blocks. The "Gibbs phenomenon" due to transform truncation in subsection processing can be reduced by spectral windows or through a scheme proposed by Algazi [18].

Convolutional Coding

In order to describe the application of convolutional coding to source coding, it is useful to first discuss the difference between source coding and channel coding. This is necessary because convolutional coding is generally applied to the channel coding problem. Source coding, as we have already mentioned, is the process of compressing the data stream coming from the source in order to reduce the amount of data which must be transmitted or stored. Source coding normally results in the removal of redundancy from the data. Channel coding is the process of adding redundancy to a signal in order to protect against channel errors.

Convolutional coding is commonly used as a way of adding redundancy to a data stream for the purpose of channel coding. In its simplest form, the convolutional coder convolves a data sequence with two or more different functions, each convolution producing a separate data sequence. These data sequences are interleaved, forming a new, long sequence. The decoder then reconstructs from the output sequence the actual shorter input sequence. If channel errors have occurred, the decoder finds the most likely original sequence given the channel corrupted output sequence.

We now observe that the decoder acts in some sense as a compressor: It takes long sequences as input and produces as output short sequences. Hence, a decoder for a convolutional code can be used as a source encoder. The difficulty is that several long streams of data are mapped into the same short stream of data. Therefore distortion occurs in the compression process. Methods for applying convolutional encoding to the source coding problem are discussed in [20], [21], [26]. The average "Hamming distortion" obtained in encoding binary memoryless sources with certain convolutional codes is given in [73].

Most of the results which are given for convolutional codes have been generalized to constant rate tree codes, but simulations have been limited to convolutional codes.

Clustering Techniques

Clustering techniques group certain data values or points together and transmit only a value representative of the group. Consequently,

however, one defines the various groups, clustering preserves intergroup differences and destroys intragroup differences. Hence, clustering techniques are inherently information-destroying. Clustering methods differ among themselves primarily in how the groups or clusters are chosen.

These clusters can be predefined or be adaptively selected based on the structure of the signal. Quantization is itself a trivial example of a clustering procedure wherein all signal values within half a quantization level of a prespecified level are represented by the same value. Applications to multidimensional data such as multispectral data have been developed [46]. Both of these methods choose clusters adaptively based on the data structure. The former method first clusters in each dimension separately and then refines the estimates using the multidimensional data. The latter method iteratively attempts to find N clusters which minimize the percentage error between the reconstructed cluster image and the original image. Another example of a clustering technique appears in [85], and is called plateau coding. In this case, a luminance and two chrominance signals are to be transmitted. A threshold is specified and the luminance signal is scanned. Whenever the luminance change is larger than the threshold, a flag is set. Between each pair of flags only the average value of each chrominance signal is transmitted.

Feature Extraction

As a final compression technique, we discuss feature extraction. Feature extraction has the potential for very high compression. This potential must be weighed against the requirement that the user be able to very specifically define his requirements. The principal behind feature extraction is that only measurements directly related to the users' needs must be transmitted. For example, if a user were interested in determining the total area covered by water in a specific region, he would require only that the location of edges of bodies of water be transmitted, together with information about which side of the edge is water and which side is not. Although feature extraction has not been practical up to now, in a system which is adaptable to the individual user, such techniques hold great promise.

Feature extraction before classification of multispectral data has been done and is discussed in [104], [135], [137]. More general overviews of feature extraction appear in [83] and [130]. At TRW the possibility of using spectral signatures of various classes to estimate boundaries of the classes has been studied [79]. Once the boundaries have been found, only the location of the boundaries and the codeword for the class surrounded by the boundary need be recorded.

2.2.3 Classification

As has been pointed out in the previous two sections, earth resources satellites produce vast quantities of data. In addition to presenting a data transmission problem, this presents to the users the problem of taking advantage of all the data. In order to extract the desired information from satellite imagery, a number of approaches to automatic classification have been tried. By comparing classifier performance on an original image and on the reconstruction of the compressed image, we can determine the effect a particular compression technique has on the extraction of useful information. In order to judge the compression technique we must make the comparison described for each classification task to which the imagery will be subjected.

In this section we briefly describe several techniques which have been applied to the classification of high altitude imagery.

General discussions of pattern classification without specific reference to earth resources imagery appear in [130], [133] among others.

Three kinds of information are available in imagery; radiometric, cartographic and temporal. Radiometric information is obtained from the recorded brightness in each spectral band. Cartographic information is contained in the spatial distribution of the brightnesses. Temporal information exists when images of the same area recorded at different times are available. Use of multitemporal imagery for automatic classification must generally be preceded by registration of the various images (reduction to the same scale and orientation, followed by superposition). Studies of registration appear in [131], [132]. All three types of information have been used in classifiers.

The most commonly used classifier operates strictly on radiometric information [134], [135]. A programming package for clustering and classifying multispectral data, developed at TRW, is described in [136]. A modified version of this program, called COSMIC, is available through NASA-JSFC. For each point in the image, the spectral response (spectral signature) is classified as belonging to one of some finite number of categories. These categories generally include crop type, soil type, land use, and so on. Some systems allow clustering into classes which are defined solely by the data structure and are not prescribed a priori.

Radiometric classifiers are sometimes extended to apply to multitemporal as well as radiometric information. This is particularly useful in crop classification since crops change their reflectance properties in a fixed time sequence as they mature.

Classification techniques that use spatial information are discussed in [137], [138]. The first technique optically computes the Fourier Transform of a small area of an image, then samples and quantizes the transform. Using a computer, classification of the area according to land use is done based on the value of some parameters of the transform. The second technique operates directly on digitized imagery. Various features are defined which are linear combinations of neighboring elements. The values of these features are used for land use classification.

3. SELECTION OF BANDWIDTH COMPRESSION METHODS RELEVANT TO MULTISPECTRAL IMAGERY

The previous section has compiled a comprehensive list of references applicable to the compression of sampled imagery data for purposes of transmission or storage reduction. In this section these are specialized to those which are relevant to on-board compression of multispectral earth resources data. The techniques are described and listed by categories organized so as to increase the efficiency of their comparative evaluation. This listing forms the basis for all subsequent evaluation and synthesis in the report leading ultimately to three specific recommended compression techniques.

In selecting compression methods which are relevant to on-board compression of earth resources data, each class considered in the literature survey is discussed in turn below. Descriptions of the techniques themselves may be found in the literature survey (Section 2). All of the relevant classes are listed in tree form in Table 3.1.

3.1 GENERAL COMMENTS

A survey of the literature in bandwidth compression techniques shows that the search for efficient techniques of compressing the bandwidth of pictorial data has led various researchers to a common approach to the problem. Briefly, this approach is processing the correlated data (images) to generate a set of uncorrelated or as nearly uncorrelated as possible set of signals which in turn are quantized using a memoryless quantizer. The quantized signal is then encoded using either fixed or variable length code words and is transmitted over a digital channel. This is the general approach taken in designing differential pulse code modulators (DPCM) and the techniques that use unitary transformation and block quantization as well as errorless coding methods such as entropy coding of the difference signal, contour tracing algorithms, and many other techniques discussed in the literature review.

Table 3.1 Multispectral Imagery Data Compression Techniques

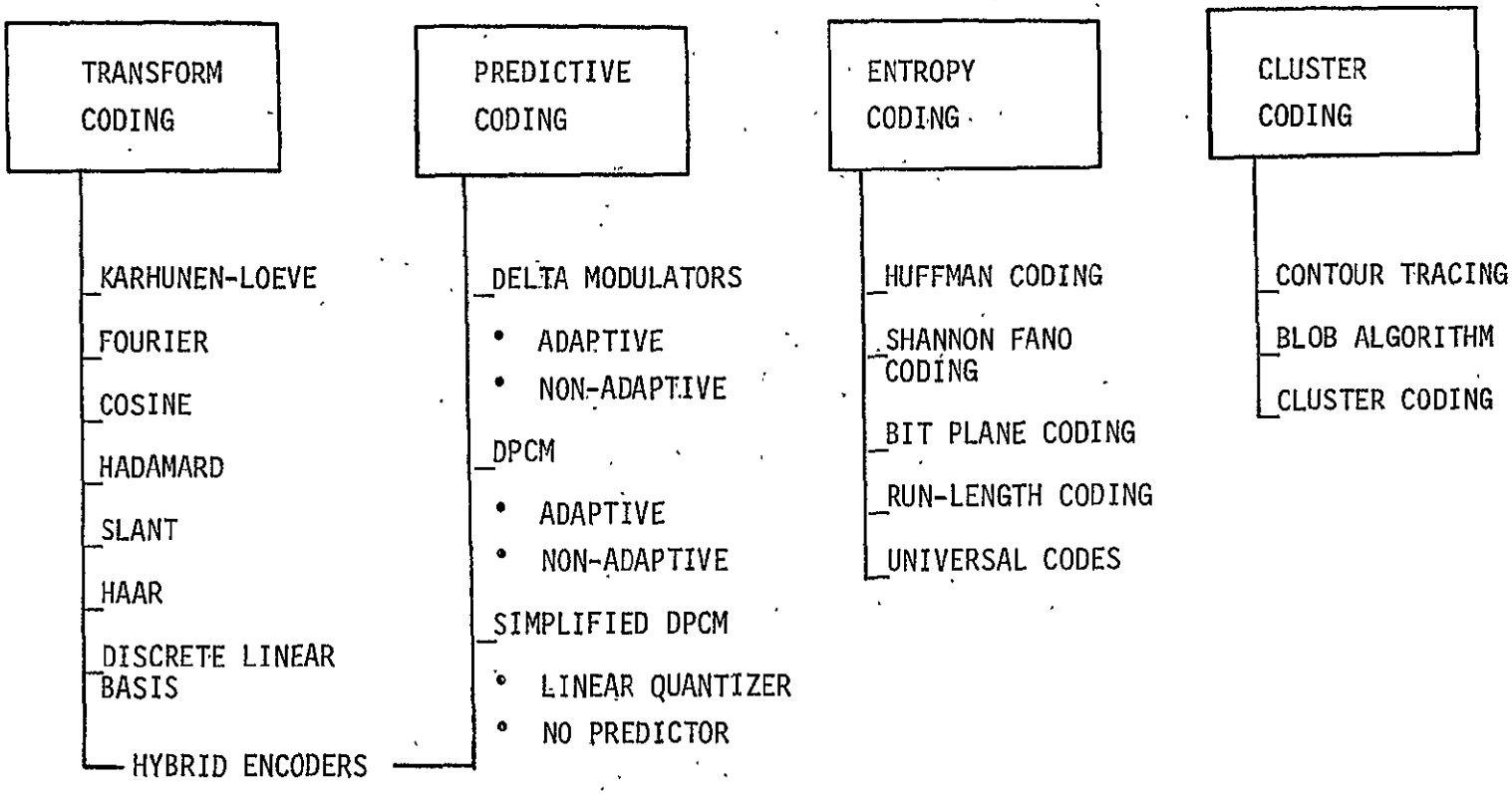

The same general approach is applicable to on-board compression of multispectral earth resources imagery. However the addition of one additional dimension (spectral) to the 2 spatial dimensions introduces subtleties into generating uncorrelated signal sets including different correlation functions in the two domains. In extending intraframe (spatial only) coding techniques to multispectral data, at least two variants may be made:

- Concatenation of two techniques, one applied spectrally, the other spatially
- Extending a technique to one higher dimension.

Selection of applicable techniques must thus be kept sufficiently general to include all variants. Among the more important criteria for use with earth resources data are ability to achieve low distortion without introducing artifacts and sensitivity to variations in sensor design.

3.2 ENTROPY CODING

These methods have been used for compressing the bandwidth of multispectral imagery as well as imagery data from weather satellites. Entropy coding methods are most useful for archiving applications since they can be used to reduce the bandwidth of imagery without introducing any distortion. Variations of entropy coding methods are Huffman Coding, Shannon-Fano Coding, Bit Plane Coding, Run-Length Coding and the Universal Codes. They are all relevant in compressing the bandwidth of multispectral imagery.

3.3 QUANTIZATION AND SAMPLING

These methods are not included since compression of bandwidth at a fixed resolution, which would be the case of satellite data, implies increased quantization error. Large quantization error results in contouring error in the reconstructed imagery. In video (television) data, the effect of contouring error is often reduced by adding dithered noise to the signal before quantization and subtracting it from the reconstructed signal [141]. This is not recommended for earth resources data since for many users a small distortion is much more acceptable than the introduction of artificial information or artifacts.

3.4 DELTA MODULATORS AND PREDICTIVE CODING

These methods have been used with wide success in a large variety of image applications. They are very easy to implement. They require very little storage capacity and perform well at relatively high bit rates. These methods are listed under the three general categories of delta modulators, DPCM, and simplified DPCM systems.

3.5 INTERPOLATIVE ENCODING

These methods have not been included. This is because interpolative methods are sensitive to data statistics [39]. They do not perform as well as other methods such as DPCM, and the more efficient interpolative encoding methods are rather complex to implement.

3.6 TRANSFORM CODING

These methods have been used successfully in compressing the bandwidth of video data. They are fairly insensitive to data statistics and channel noise. Included here are the Karhunen-Loeve, Fourier, Cosine, Hadamard, Slant, Haar and Discrete Linear Basis transforms as being relevant to multispectral imagery. Table 3.1 also lists hybrid encoders that use a cascade of a unitary transformation with a bank of DPCM systems [140]. This sytem combines the attractive features of both transform coding and the DPCM systems thus achieving good coding capabilities for any imagery data including MSS imagery without many of the limitations of each system.

3.7 CONVOLUTIONAL CODING

These methods have not been included since they are still in the stage of theoretical development. Some attempts have been made to use convolutional coding for bandwidth compression of speech signals, but as yet there is no literature available on the application of convolutional coding to imagery data.

3.8 CLUSTERING AND FEATURE EXTRACTION

These techniques are particularly relevant to the compression of multispectral data since they may be used to achieve bandwidth compression as well as data classification simultaneously. Three variations of this technique which are currently in use are contour tracing, the BLOB algorithm, and the cluster coding methods which are listed in Table 3.1.

4. ANALYSIS OF MSS-LANDSAT DATA

The bandwidth compression methods which are relevant to the bandwidth compression of multispectral imagery are listed in Table 3.1. Selection of this list from a variety of image bandwidth compression techniques listed in the literature survey was discussed in Section 3. To narrow the list to a still smaller number of techniques, first the MSS data was analysed, then, considering the characteristics of the MSS data, a list of bandwidth compression techniques most appropriate for MSS data was selected.

In this section first we describe the MSS data, and then list its most important characteristics. Section 5 will utilize these characteristics in funnelling down the list of bandwidth compression techniques to the candidate algorithms.

4.1 DESCRIPTION OF MSS DATA

The multispectral scanner on-board LANDSAT-1 records the energy in four separate bands from 0.5 to 1.1 microns. The four bands correspond to red, green, and two near infrared bands. The outputs of the scanner are analog signals which are immediately digitized and multiplexed. The output of the multiplexer is either directly transmitted to the earth or it is recorded on a magnetic tape for subsequent transmission. A moving mirror permits the recording of one picture line of approximately 3200 points perpendicular to the vehicle's path using one optical fiber per spectral band. To allow for return of the mirror and to maintain about the same resolution in both directions, six lines are swept out at a time using photosensors in each spectral band. As discussed in Section 2.1, the resolution of a multispectral scanner is different in horizontal and vertical directions. This is because the vertical distance between picture elements represents a greater distance on earth than the horizontal distance between picture elements.

4.2 STATISTICAL MODELING OF MSS DATA

Multispectral data can be modeled by a stochastic process $f(x,y,k)$ which is a function of three discrete variables x, y, and k; x and y refer to spatial variables, and k is the spectral variable. In

theoretical studies of image bandwidth compression methods, one often models the data with a stochastic process having statistics identical to those of the imagery so that one can evaluate the average performance of various encoders. This approach to the analysis of algorithms used for coding video data is often carried out by assuming that the stochastic model $f(x,y,k)$ is Markov on all three variables x, y, and k. This would imply that the auto-covariance of the assumed stationary process $f(x,y,k)$ is exponential in all three dimensions [62], i.e.,

$$R(x,\hat{x},y,\hat{y},k,\hat{k}) = e^{-\alpha_1|x-\hat{x}|-\alpha_2|y-\hat{y}|-\alpha_3|k-\hat{k}|} \qquad (4.1)$$

This is a desirable assumption since it simplifies the analysis of the problem to a considerable degree. The results are valid on most naturally obtained video data that show ordinary movements in both spatial and temporal directions. Considering this model for MSS data, one proceeds with correlation measurements which specify α_1,α_2, and α_3 in (4.1). These measurements also verify the correctness and the accuracy of the above model.

Measurements of the spatial correlation of the data reveal that the correlation of the data in the horizontal and the vertical directions is indeed exponential. Estimates of values for α_1 and α_2 are given in Table 4.1 along with other statistics regarding the representative MSS data shown on Figures 4.1 and 4.2. The spectral convariance of the representative MSS data is shown in Table 4.2 The entries of this table show that the spectral correlation does not reduce exponentially by moving across the bands. Indeed various bands show similarities and differences which are totally different from interframe behavior of other video data encountered in television or in reconnaissance flights. Table 4.2 shows the following spectral characteristics for the MSS-LANDSAT data:

- Large positive correlation between the red and the green bands
- Large positive correlation between the two infrared bands
- Small negative correlations between the red and the two infrared bands.

Table 4.1. Statistics of the Representative MSS-LANDSAT Data

DATA PARAMETERS	RED	GREEN	IR#1	IR#2
Max (Amplitude)	84	103	96.0	52
Min (Amplitude)	24	15.0	10.0	2.0
AVE (Amplitude)	47.83	52.17	59.58	26.83
α_1	0.011	0.039	0.089	0.089
α_2	0.019	0.076	0.156	0.156

Table 4.2. Spectral Correlation Matrix of the Representative MSS-LANDSAT Data

	RED	GREEN	IR#1	IR#2
RED	1.000	.866	.276	-.141
GREEN	.866	1.000	.288	-.177
IR#1	.276	.288	1.000	.654
IR#2	-.141	-.177	.654	1.000

This behavior is characteristic of LANDSAT multispectral imagery. This point was verified by similar measurements on two additional LANDSAT images.

ORIGINALS

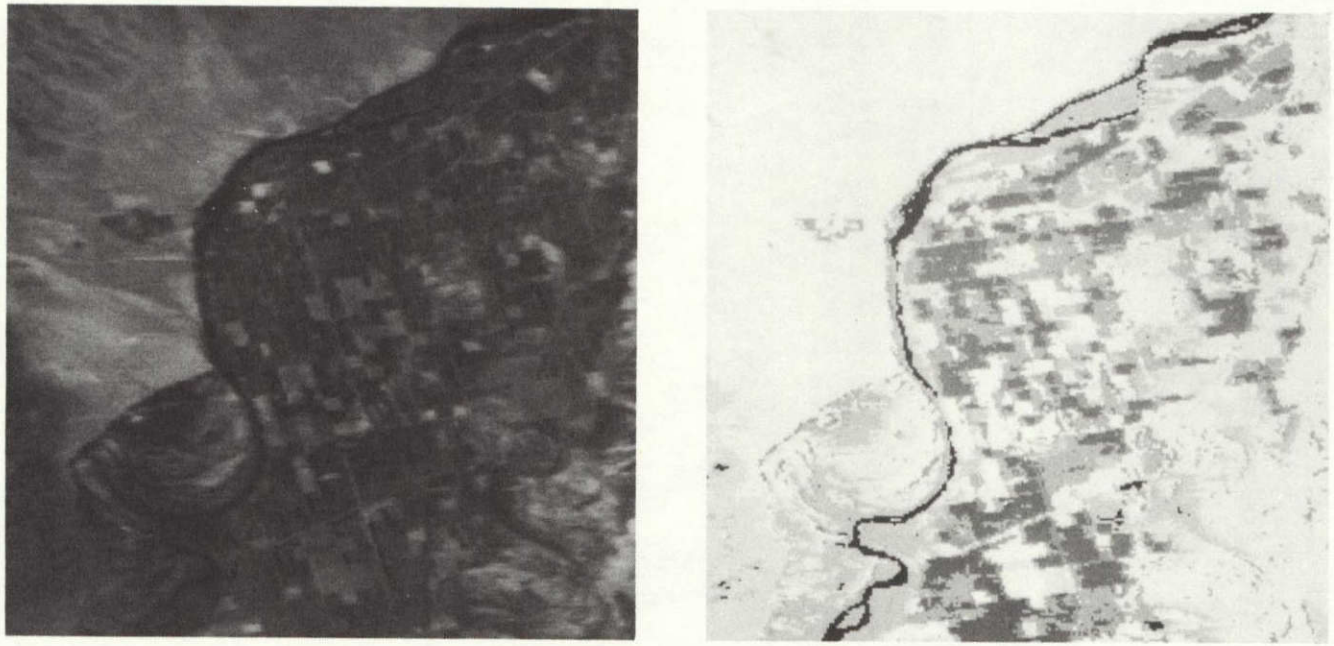

Figure 4.1. Representative MSS Data

ORIGINAL BANDS

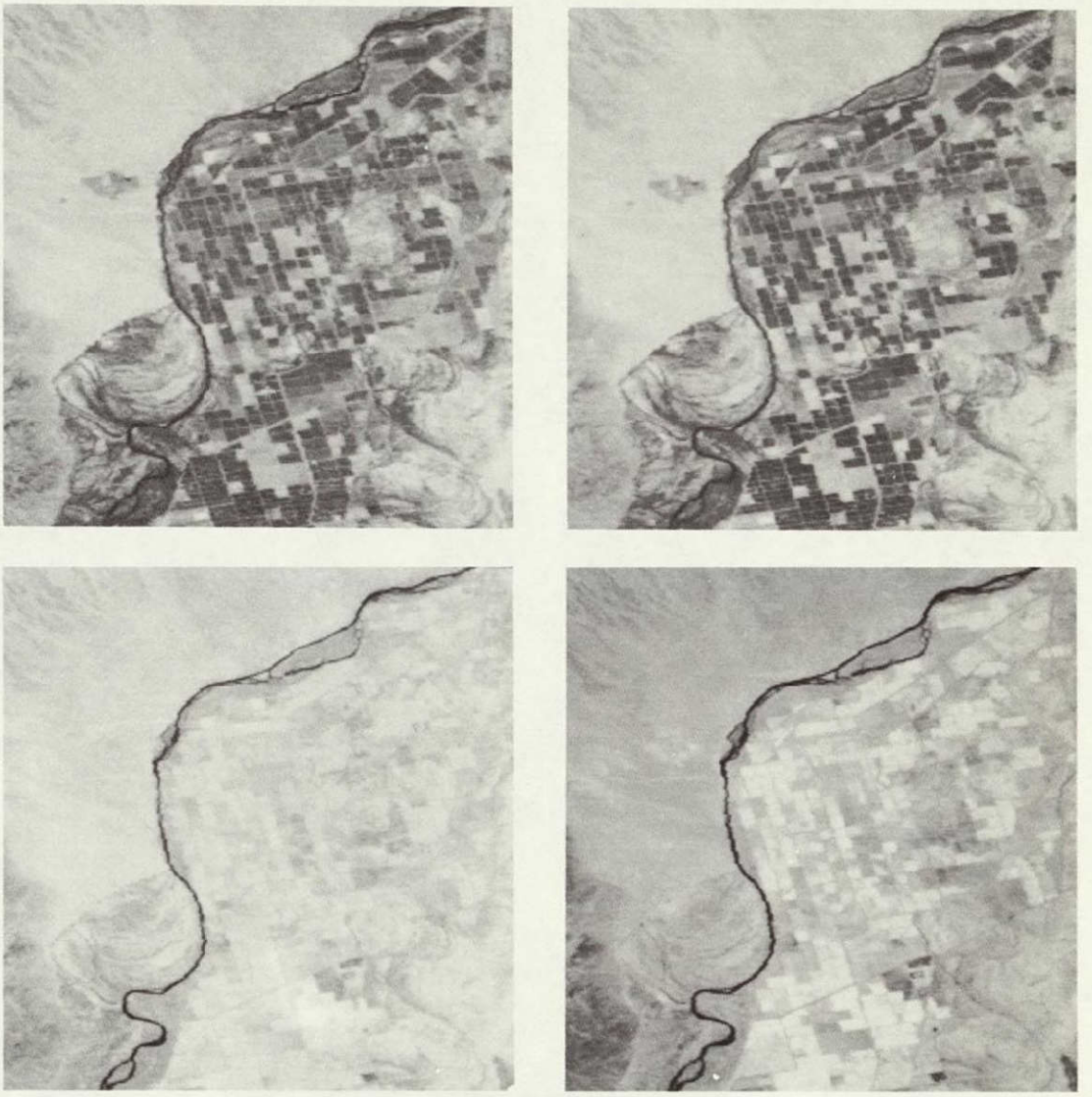

Figure 4.2. Representative MSS Data

5. SELECTION OF CANDIDATE BANDWIDTH COMPRESSION TECHNIQUES

In Section 3 the relevant bandwidth compression techniques were selected. They are listed in Table 3.1 in four categories. In this section we examine each coding method which is listed in general form on Table 3.1, and utilize the characteristics of the MSS data discussed in Section 4 to get a list of specific bandwidth compression techniques most suitable for MSS data. These candidate techniques were studied and compared in detail and were funnelled down to three multispectral bandwidth compression techniques which we finally recommend.

5.1 ENTROPY CODING

A study of entropy coding methods for compressing the bandwidth of MSS data was performed at TRW. The salient points of the study were that the entropy coding methods can be used to compress the bandwidth of MSS data by a factor of about 2 to 1 without any degradation and the compression technique can be fabricated for on-board processing using an acceptable number of parts and within reasonable weight, power, and size limitations. For details of the study the readers are referred to reference [91]. Because of this comprehensive study we will not consider entropy coding methods in compressing the bandwidth of MSS data individually. Instead, entropy coding methods will be considered in cancatenation with other bandwidth compression techniques. This is because entropy coding further reduces the bit rate of a bandwidth compression technique that generates an uneven distribution of symbols at the output receiver. Here the object is to study the improvements in the performance of each bandwidth compression technique as a result of concatenating it with the entropy coding methods. For this reason only the Huffman encoder is considered. Other methods listed in this category have a similar performance and are in general more complicated to implement.

5.2 TRANSFORM CODING

MSS data is three-dimensional. As discussed in Section 4.1, it possesses spectral as well as spatial correlation. Three-dimensional transform coding methods take advantage of the correlation of the data

in all three dimensions to compress its bandwidth. Among the transforms listed in Table 3.1, we chose three-dimensional Fourier, Cosine, Hadamard, and Slant transforms for further study. The three-dimensional KL transform is rejected because of its great implementational complexity. The three-dimensional Haar transform is rejected due to its performance, which has been shown to be lower than that of other transforms such as the Hadamard transform. The discrete Linear Basis transform is rejected because it has a performance rather similar to the performance of the Slant transform and also because it has been used to compress the bandwidth of MSS data in other studies [68].

In addition to the above three-dimensional transforms, two techniques that use a combination of different types of transforms are also considered. These are the three-dimensional bandwidth compression techniques that use a combination of KL-2 Dimensional Fourier and KL-2 Dimensional Hadamard transforms. In both systems the KL transform is in the spectral domain. These methods are selected because the correlation of the MSS data in the spectral domain is not exponential, thus the KL transform is expected to result in substantial improvements over other unitary transforms such as Hadamard or Fourier.

5.3 DELTA MODULATORS AND PREDICTIVE CODING

In the class of predictive coding methods, only DPCM systems are considered. Delta modulators are rejected because for bit rates higher than one bit per picture element they require sampling the analog signal at a higher sampling rate. Thus, the implementation requires a variable sampling of the sensor outputs which increases the complexity of the system enormously. Besides it has been shown that the performance of both delta modulators and adaptive delta modulators is suboptimal to the performance of two-dimensional DPCM encoders for imagery data [63].

Simplified DPCM encoders are used in the actual design of a system to approximate the performance of DPCM encoders. The loss in performance of the bandwidth compression systems due to this simplification is rather small. This problem has been studied in recent literature extensively [84].

In addition to DPCM and transform coding techniques, the hybrid encoders

that combine transform coding systems with DPCM encoders give good performance for both intra and interframe coding of television signals. These systems can be divided in three categories:

- Systems that performs a two-dimensional transform of each band of the MSS data and use a bank of DPCM encoders to process the transformed data across the individual bands.
- Systems that take a transform across the spectral bands and use a two-dimensional DPCM encoder to process the data in the spectrally transformed domain.
- Systems that follow a spectral transformation in the spectral domain of MSS data by a second transform in the horizontal direction (scan direction) and use of a DPCM encoder in the vertical direction.

From the hybrid system in the first category, we studied systems using two-dimensional Hadamard and Cosine transforms in combination with a DPCM encoder. From the second category we studied the system using KL-2 Dimensional DPCM encoder. From the third category, two systems combining KL-Hadamard-DPCM and KL-Cosine-DPCM encoders were selected for further study.

The reason for including a choice between Cosine (or Fourier) and Hadamard (or Slant) transforms is the different approaches that can be taken in the design of these systems. Where Hadamard and Slant transforms are always implemented using all-digital circuitry, the Cosine and Fourier transforms can be implemented using analog transversal filters that utilize the chirp-Z algorithms [141].

5.4 CLUSTER CODING

Among the cluster coding methods listed in Table 3.1, we selected a coding technique that uses a Swain-Fu distance to generate an image of clusters and utilized that for a combined bandwidth compression and classification procedure. This method was selected because a similar method (using ISODATA for clustering) has been used with success at Jet Propulsion Laboratory. Comparing its performance with other bandwidth compression methods was of considerable interest to the results of this study.

The contour tracing algorithm was rejected because it has been shown

that its performance, when applied to the imagery data directly, is not as good as other bandwidth compression systems [149].

The BLOB algorithm was rejected because in its present form [147] it is not optimal for multispectral data; it could be extended to multispectral data but this makes the technique rather complicated.

5.5 LIST OF CANDIDATE TECHNIQUES

The candidate techniques selected in this section fall into six categories. The number of individual techniques considering various transforms is actually 12.

1. Three-dimensional transform coding algorithms
   a) 3D Fourier transform with block quantization.
   b) 3D Hadamard transform with block quantization.
   c) 3D Slant transform with block quantization.
   d) 3D Cosine transform with block quantization.
2. Mixed three-dimensional coding algorithms
   a) KL transform in the spectral and 2D Fourier transform in the spatial domain.
   b) KL transform in the spectral and 2D Hadamard in the spatial domain.
3. Two-dimensional spatial transformations with DPCM encoding in spectral domain
   a) 2D Hadamard transform with DPCM coding in spectral domain.
   b) 2D Cosine transform with DPCM coding in spectral domain.
4. One-dimensional KL transform in spectral domain cascaded with two-dimensional DPCM encoder in the spatial domain.
5. One-dimensional KL transform in spectral domain followed with
   a) Cosine transform and DPCM in spatial domain.
   b) Hadamard transform and DPCM in spatial domain.
6. Cluster coding algorithm using Swain-Fu distance for clustering.

The following sections compare these methods based on their analytical and simulation performance as well as their complexity of implementation.

6. CRITERIA FOR COMPARING BANDWIDTH COMPRESSION TECHNIQUES FOR MULTISPECTRAL IMAGERY

To evaluate the performance of a particular bandwidth compression method, one must determine whether the bandwidth compression method preserves sufficient information for a particular application. To do this, a criterion of optimality must be defined by which the information loss is measured. To measure the distortion in imagery data, a variety of criteria of optimality has been used. These criteria are necessarily user-dependent. One such criterion is the weighted mean square error used in conjunction with video data. This measure weighs the error at various frequencies according to the characteristics of human vision. The imagery data used for applications involving pattern recognition and pattern classification use other measures such as the classification accuracy of the compressed imagery. In addition to these criteria which are used to evaluate the performance of a bandwidth compression technique, a different set of criteria exists which relate to the complexity, cost, and the sensitivity of various image bandwidth compression techniques. These criteria are discussed under the general heading of system considerations. They are also of varying degrees of importance depending upon the particular application.

In this study for criteria of optimality we use mean square error, peak-to-peak signal-to-noise ratio, recognition accuracy of reconstructed imagery and the system considerations of the various bandwidth compression methods.

6.1 MEAN SQUARE ERROR (MSE)

Mean square error is the most frequently used criterion of optimality in data compression as well as in most other estimation and filtering problems. This is partly due to the inherent simplicity of this criterion which allows for closed-form analytical solutions and partly to the fact that many sensing systems respond directly to the energy contained in the stimulus and that the energy and mean square error are closely related. Many image bandwidth compression results are in terms of mean square error or weighted mean square error.

Experiments with the mean square error have shown that it does have some correlation with the subjective quality of the reconstructed imagery. Limited experiments show a value of about 50% for this correlation. In general, mean square error shows a better correlation with the subjective quality of the bandwidth compressed imagery at low levels of degradation. This correlation also depends on the type of the degradation as well as the location at which degradation occurs. Human vision is less sensitive to uncorrelated error. It also shows less sensitivity to the error at high brightness levels and the error at highly detailed areas.

6.2 SIGNAL-TO-NOISE RATIO (S/N)

A criterion closely related to mean square error is the signal-to-noise ratio. Indeed this criterion can be considered a normalized form for the MSE. Peak-to-peak signal to root mean square (RMS) value of the noise as well as RMS signal-to-noise ratio are widely used by the television industry as a measure of television signal quality.

In this study both the MSE and peak-to-peak signal-to-RMS-noise ratios are used to evaluate and compare various bandwidth compression methods. These quantities are calculated for each band as indicated by equations (6.1) and (6.2).

$$\varepsilon^2 = \frac{\sum_{j=1}^{M} \sum_{i=1}^{N} (X_{ij} - \hat{X}_{ij})^2}{M N} \tag{6.1}$$

$$S/N = 20 \log_{10} \frac{P}{\varepsilon} \tag{6.2}$$

where

$\hat{X}_{ij}$ = sample in each band of original imagery

X_{ij} = sample in each band of reconstructed imagery

P = peak-to-peak signal value

ε^2 = mean square error

An average for all spectral bands is used to make the evaluation and the comparison of the bandwidth compression methods. The software used to perform the calculation of the MSE and signal-to-noise ratio is documented in Appendix E.

6.3 RECOGNITION ACCURACY

Many important uses of the earth resources data rely heavily on the use of computerized pattern classification and pattern recognition of the multispectral earth resources imagery. For many pattern classification applications, the multispectral data is first used to obtain a clustered image. This clustered image is then used for image data extraction and classification. Thus, it is of importance that a particular bandwidth compression method not result in significant changes in the resulting clustered imagery. Thus a criterion of performance which can be employed for evaluating various coding algorithms is the performance of various encoders in retaining the classification accuracy of the clustered imagery. That is, the clustered image obtained from the encoded multispectral data should be identical to the clustered picture obtained from the original set of multispectral data.

In order to test the degree of preservation of classification accuracy, a set of programs was developed for TRW's Interdata 80 image processing facility. These programs, which are described in Figure 6.1, make it possible to do classification on multispectral imagery, to compare results obtained for compressed and uncompressed data, as well as to display the imagery itself, the clustered imagery, and the difference between pairs of clustered images. A flow diagram showing the sequence in which these programs are used in obtaining a measure of preservation of classification accuracy is shown in Figure 6.2 and is explained here.

Multispectral imagery, either reconstruction of compressed imagery or original imagery, is accepted as input. This imagery is assumed stored as a set of separate, monochrome images which may be "packed" (two picture element values for every sixteen bits) or "unpacked" (one picture element for every sixteen bits). If the data is packed, it can be unpacked using the program STRIP. Once unpacked data has been obtained, the several spectral bands are interleaved by program MIXER. In the interleaved form, those

CLUSE	Finds centroids of clusters given multiband data.
CLASF	Classifies each pixel in a multiband image based on which of several centroids produced by CLUSE it is radiometrically closest to.
CMPR	Compares classification obtained on two sets of data corresponding with the same spatial area.
EQUCLU	Determines which clusters correspond with one another given two clustered images of the same area.
EXTRCT	Extracts every fourth row and column from a picture.
SCALE	Scales imagery from 0 to 255 for display.
FW1	Displays a picture on the Dicomed/film recoder. (A Dicomed Image Recorder is discussed in Appendix D.)
STRIP	Unpacks pictures stored one pixel per 8 bit byte to one pixel per two bytes.
MIXER	Interleaves several narrow band images.
DEMIX	Reverses the action of MIXER.
PACK	Packs pictures stored one pixel per 2 bytes to one pixel per byte.

Figure 6.1. Programs Belonging to Classifier Package

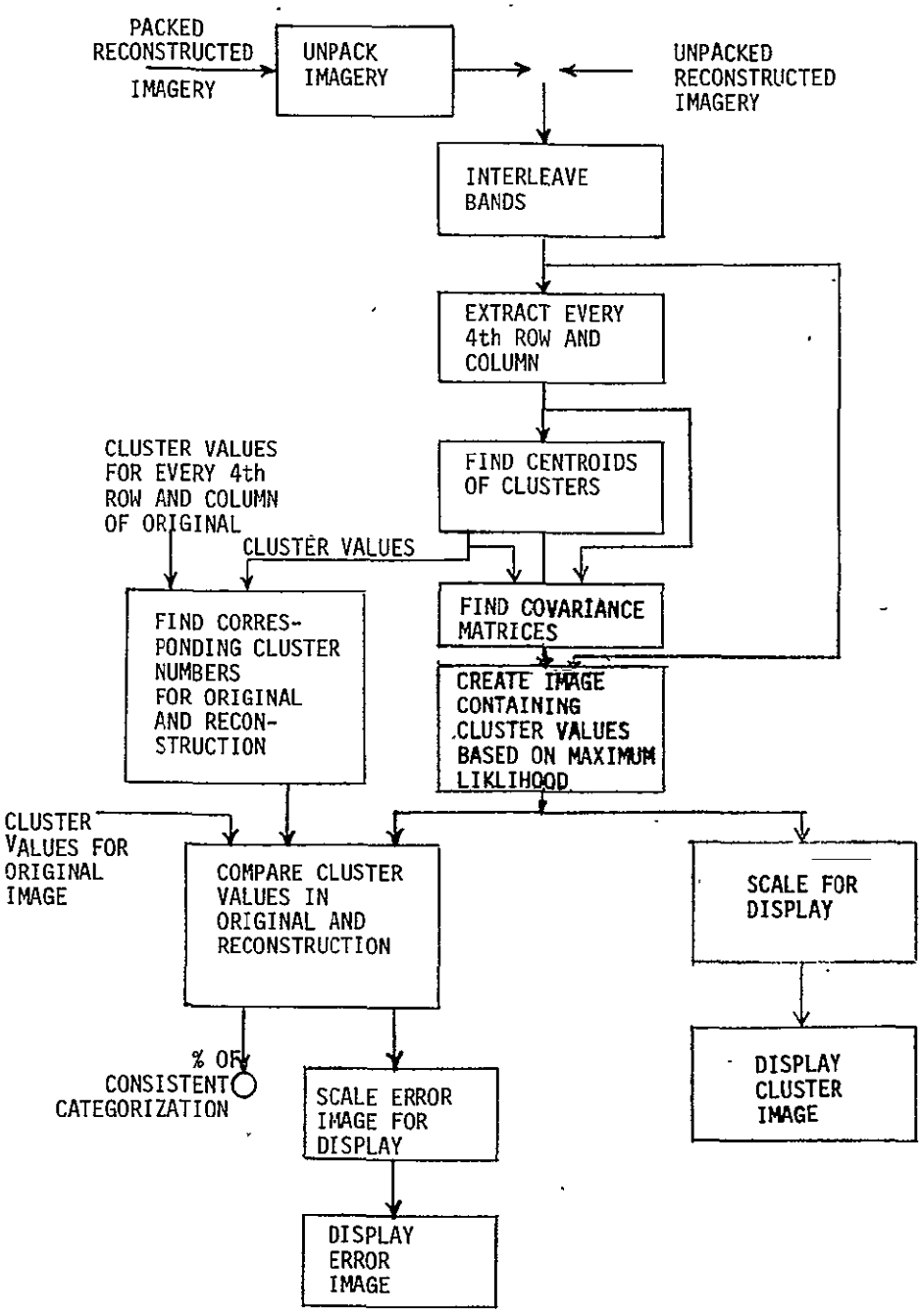

Figure 6.2. Measuring Preservation of Classification Accuracy

data from the several spectral bands which correspond with the same picture element are stored consecutively as shown in Figure 6.3.

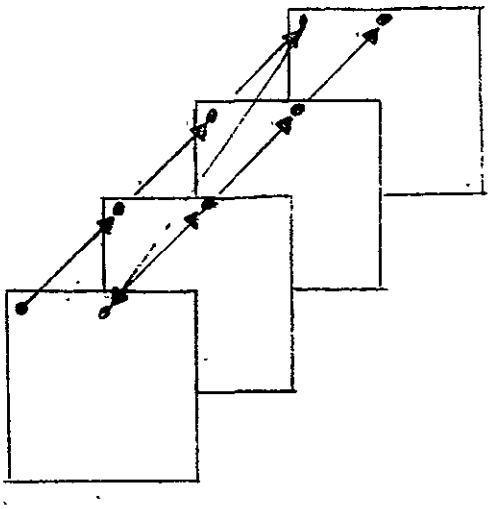

In the interleaved image, the data is stored in the sequence indicated by the arrows.

Figure 6.3. Interleaving

At this point we are almost ready to calculate the centroids of the clusters. Unfortunately, calculation of the centroids is an interactive process which is quite time-consuming. Hence, it is desirable to sample the available imagery and determine the centroids using a subset of the picture elements. For convenience we have chosen to use every fourth row and column of the imagery in determining the centroids. The subset of sample values is extracted using program EXTRACT. The pixels which are retained are shown in Figure 6.4

Using the clustered subset we obtain the centroids of the clusters using an adaptation of the clustering program provided by NASA Ames Research Center. By "centroid" is meant the following: Each cluster has a particular mean value in every spectral band. The centroid of a cluster is the set of mean values for that cluster. Figure 6.5 shows pictorially the meaning of centroid for the case of only two spectral bands.

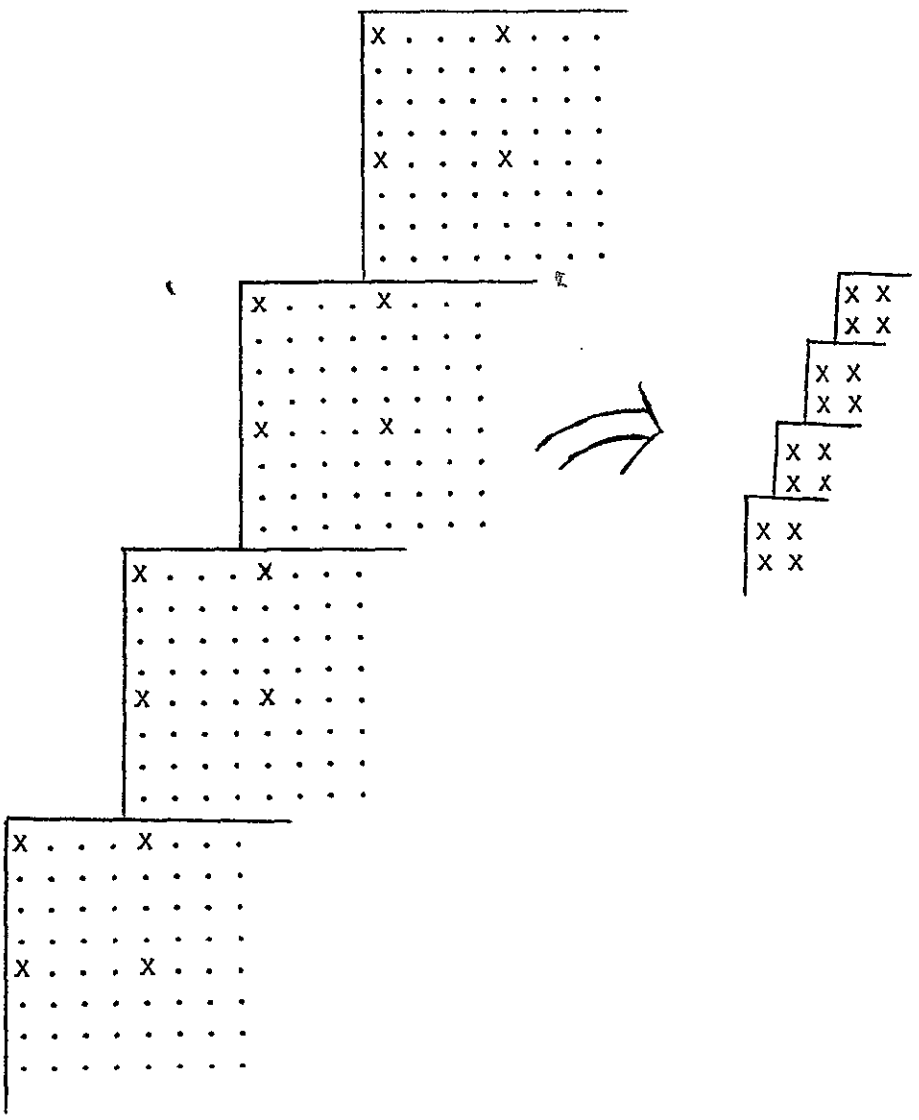

Figure 6.4. Extraction of Every Fourth Row and Column Before Clustering

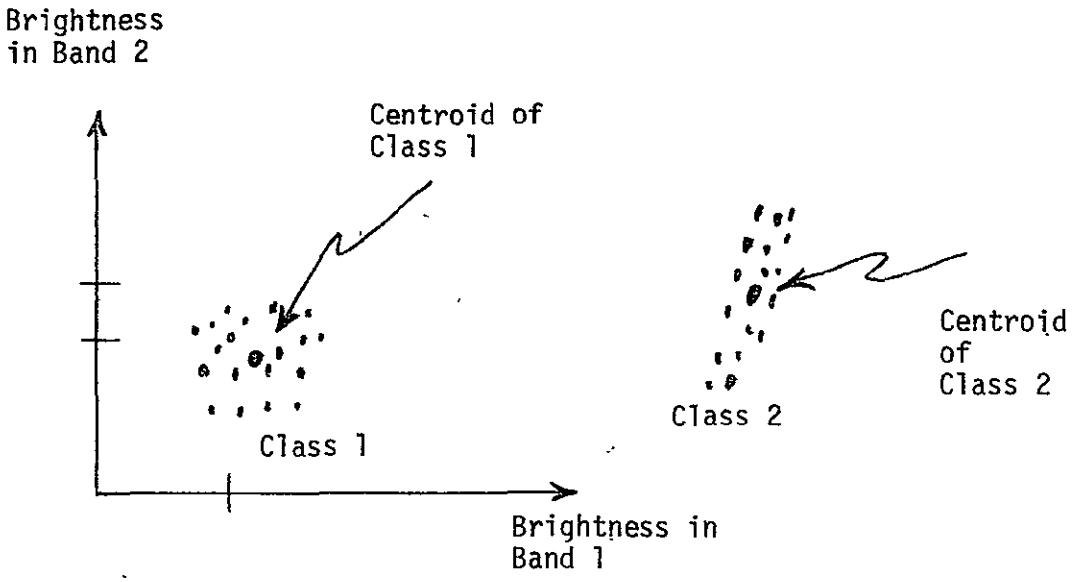

Figure 6.5. Meaning of Centroid. Each class has a centroid equal to the average location of data in that class.

The centroid-finding program, called CLUSE, block diagram is shown in Figure 6.6.The program's steps can be summarized as follows: A particular number of clusters is selected. More or less arbitrarily, a set of initial centroid values is chosen. Each sample value is assigned to the category corresponding to the closest centroid. Then the centroids of the sample values belonging to each class are computed. Once again, the data samples are mapped into those categories having the closest of the new centroids. This entire process is repeated until very few of the sample values change category on one of the iterations. At that point, the so called "Swain-Fu" distance between each pair of classes is measured. If the minimum distance between classes is less than some prescribed distance, the two closest classes are merged and the whole process is repeated with one fewer class. Otherwise the clustering algorithm terminates. A minimum number of clusters is also specified in order that merging not continue indefinitely.

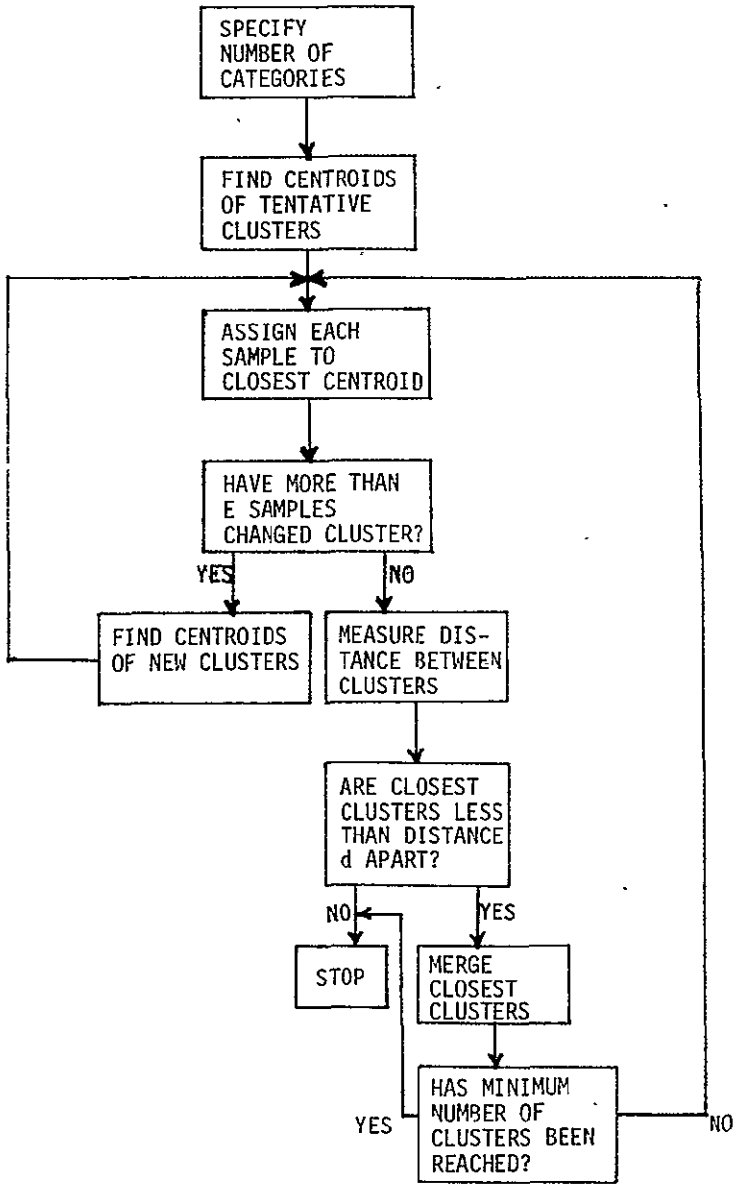

Figure 6.6. Clustering Technique Used

After completing determination of the cluster centroids, the entire 256 x 256 image is classified using program CLASF. This is accomplished by determining to which centroid each sample is closest. The output of this program is an image in which the value corresponding with any pixel is the number of the cluster to which it belongs. The cluster values can then be scaled linearly to occupy the entire contrast range of the display.

In order to compare the clusters obtained on the original imagery and on the reconstruction of the compressed imagery, we first determine the correspondence between clusters in the two sets of imagery. To illustrate what is meant by finding a correspondence between clusters, consider the case when cluster 1 in the original image represents water, and in the reconstruction water is represented by cluster 3. It is the purpose of program EQUCLU to ascertain the correspondence between clusters 1 in the original and 3 in the reconstruction in the case of our example, and more generally to obtain a good mapping from clusters in the reconstruction to clusters in the original. In order to save time this program does not determine the cluster correspondence which will minimize the difference in classification but instead first minimizes the difference in classification for the subarea of pixels belonging to the cluster with the most elements, then minimizes the difference in classification error for the subarea of pixels belonging to the cluster with the next greatest number of elements, and so on.

Once the cluster correspondence is determined, program CMPR compares the clusters obtained for the original imagery and the reconstruction and determines the percentage of differently classified picture elements.

6.4 SYSTEM CONSIDERATIONS

In addition to the criteria of optimality which are used to evalute and compare the performance of various techniques, there exists a different set of criteria which deals with the systems aspects of the various techniques. This set of criteria is particularly important in design and operation of the system under imperfect conditions of the real world. These criteria are discussed in the following.

6.4.1 Computational Complexity

The complexity of any technique is eventually measured in terms of the total number of parts, weight, power, and the size of that particular technique. However, before one can specify the above design parameters one must specify the number of operations and the memory which is required for implementing a particular bandwidth compression technique. Since the number of operations and the storage required for a particular bandwidth compression method is directly related to the design parameters such as the total number of parts, weight, power, and the size, one could use the computational complexity as a measure of eventual complexity of the system. In this study we have defined the computational complexity in terms of number of adds and multiplies and the number of memory units per picture element.

6.4.2 Sensor Imperfections

A number of different sensor phenomena contributes to degraded compression performance compared with that expected for an ideal sensor. In order to explain those sensor properties which adversely affect compression, first two types of multispectral sensors which are most likely to be used for future satellite based gathering of earth resources data are studied. They are the thematic mapper and high resolution pointable imager (HRPI). The most important sensor parameters which may affect the bandwidth compression performance of the selected techniques are:

- Photodiode Nonuniformity
- Signal-to-Noise Ratio
- Radiometric Nonlinearity
- Spectral Misregistration
- Geometric Distortion due to Satellite Attitude Variations
- Geometric Distortion due to Scan Pattern
- Data Rate.

The effect of these parameters on various bandwidth compression methods is analyzed by measuring the impact of the above imperfections

on the correlation of the data and relating that to the expected performance of the selected bandwidth compression algorithms.

6.4.3 Channel-Error Effect

A different type of imperfection present in most communication systems is the channel error. This in general includes perturbation of the transmitted signal due to atmospheric turbulence, natural and man-made interference, and thermal noise present in the transmitter and receiver of the system. In digital communication systems, the overall effect of the above imperfections is expressed in terms of bit error rate (BER) which is the percentage of binary integers which are detected erroneously. Naturally this depends on the type of the receiver and the modulation technique that is used in a particular communications system. A fixed bit-error rate affects some bandwidth compression methods more severely than others. For instance, in a transform coding system the channel error occurring at a particular transform component distorts a specific frequency component of the image. This degradation appears at all points in the image having a contribution from that particular frequency component. As such it has a different effect on a human observer than an equal perturbation occurring in the spatial domain directly, as happens in DPCM systems.

In this study we will simulate the effect of the noisy channel by a binary symmetric channel with bit error rates ranging from 10^{-4} to 10^{-2}. The effect of the channel error in selected bandwidth compression algorithms is evaluated by how it affects mean square error signal-to-noise ratio, classification accuracy, and the subjective quality of the reconstructed imagery at various bit rates.

7. COMPARISON OF SELECTED BANDWIDTH COMPRESSION TECHNIQUES

This section discusses and compares the 12 bandwidth compression techniques listed in Section 5. Analytical and experimental techniques are used. The analytical results are based on the expected performance of these methods using mean square error as the criterion of optimality. The experimental results are obtained by simulating these bandwidth compression methods on a digital computer and using them to compress the bandwidth of two typical multispectral images. The simulated methods are compared based on their performance on multispectral LANDSAT images and on a 12-channel high altitude aircraft image at various bit rates. In comparing the simulated bandwidth compression methods, the criteria of optimality are:

- Mean square error
- Peak-to-peak signal-to-noise ratio
- Recognition accuracy
- Subjective quality of the reconstructed imagery
- Implementation complexity, sensor effects, and channel-error effects.

The software developed under this study was transferred to NASA Ames Research Center and Marshall Space Fight Center for use with other multispectral data in the comparison and evaluation of the 12 different bandwidth compression methods.

7.1 THEORETICAL PERFORMANCE

Section 4 discussed modeling and some of the statistical characteristics of two sets of multispectral data. One was a sample of LANDSAT imagery and the other was a sample of 12-channel high altitude aircraft data. Due to the fact that our typical MSS data and in particular the LANDSAT data exhibit a different type of correlation in the spectral and spatial domains, the analysis of the problem is divided in two parts. Section 7.1.1 discusses the use of various transforms in the spectral domain and Section 7.1.2 multidimensional coding in the spatial domain. Section 7.1.3 discusses cluster coding of multispectral data.

7.1.1 Transforms in the Spectral Domain

The general form of a transformation of a process f(x,y,k) in the spectral domain is modeled as

$$u_i(x,y) = \sum_{k=1}^{K} f(x,y,k)\mu_i(k) \tag{7.1}$$

$$f(x,y,k) = \sum_{j=1}^{K} u_i(x,y)\mu_i(k) \tag{7.2}$$

where $u_i(x,y)$ for i=1,2,...,k refers to various two-dimensional signals in the particular domain which is represented by the discrete basis vector $\mu_i(k)$. Various transformations that one can use will generate different sets of transformed data $u_i(x,y)$. One can adapt one of many types of these transformations for multispectral imagery depending upon the applications and uses of the data as well as the degree of complexity that one is willing to accept. In what follows we discuss a number of these transformations using mean square error as the criterion of performance of the coding algorithms.

Karhunen-Loeve Transformation

Using mean square error as a criterion of performance, the Karhunen-Loeve transformation is the optimum transformation that one can use on a set of arbitrarily correlated data to generate an uncorrelated signal. This also holds true for multispectral data. In this case, $\mu_i(k)$; k=1,2,...,K are the K components of the i^{th} eigenvector of the covariance matrix of the multispectral data f(x,y,k), i.e., $\mu_i(k)$ are the eigenvectors of the covariance matrix C where

$$C_{k\ell} = \frac{1}{N^2} \sum_{y=1}^{N}\sum_{x=1}^{N} \left[f(x,y,k) - \frac{1}{K}\sum_{j=1}^{k} f(x,y,j) \right] \left[f(x,y,\ell) - \frac{1}{K}\sum_{j=1}^{k} f(x,y,j) \right] \tag{7.3}$$

The eigenvectors for the covariance matrix of the representative multispectral data are shown on Table 7.1. The corresponding eigenvalues of the covariance matrix are also listed on Table 7.1. Figure 7.1 shows the percentage accumulative energy in each band after the Karhunen-Loeve transformation. This curve in a sense indicates the significance of each band at the transformed domain and the mean square error that would result by not transmitting the signal in that particular band. Naturally the total energy in all four bands is the same for all transformations. The shortcoming of the Karhunen-Loeve transformation is that the coding system requires a knowledge of the auto-covariance of the data. The performance of the system is dependent upon the accuracy of this information. This is a serious shortcoming since it requires the on-board encoder to measure the auto-covariance adaptively and update the basis vectors accordingly. This is not an impossible task, especially as the number of spectral bands are rather limited. However, the on-board transmitter will be much simpler if a deterministic set of basis vectors is used instead. For this reason, we considered the theoretical performance of a number of other transformations in comparison with the Karhunen-Loeve transformation in their capacity to reduce the bandwidth of the multispectral data.

Table 7.1. Eigenvalues and Eigenvectors of the Covariance Matrix of the Multispectral Data

Eigenvalues	$\mu_1(x)$	$\mu_2(x)$	$\mu_3(x)$	$\mu_4(x)$
0.724	.496	.069	-.865	-.021
0.214	.846	.141	.492	.151
0.040	.195	-.869	.054	-.452
0.022	-.033	-.470	-.078	.879

Hadamard Transformation

A unitary transformation which is simple to implement but which still performs rather close to Karhunen-Loeve transformation in a number of applications is the Hadamard transform. The performance of this transformation on the representative data is also shown in Figure 7.1. The

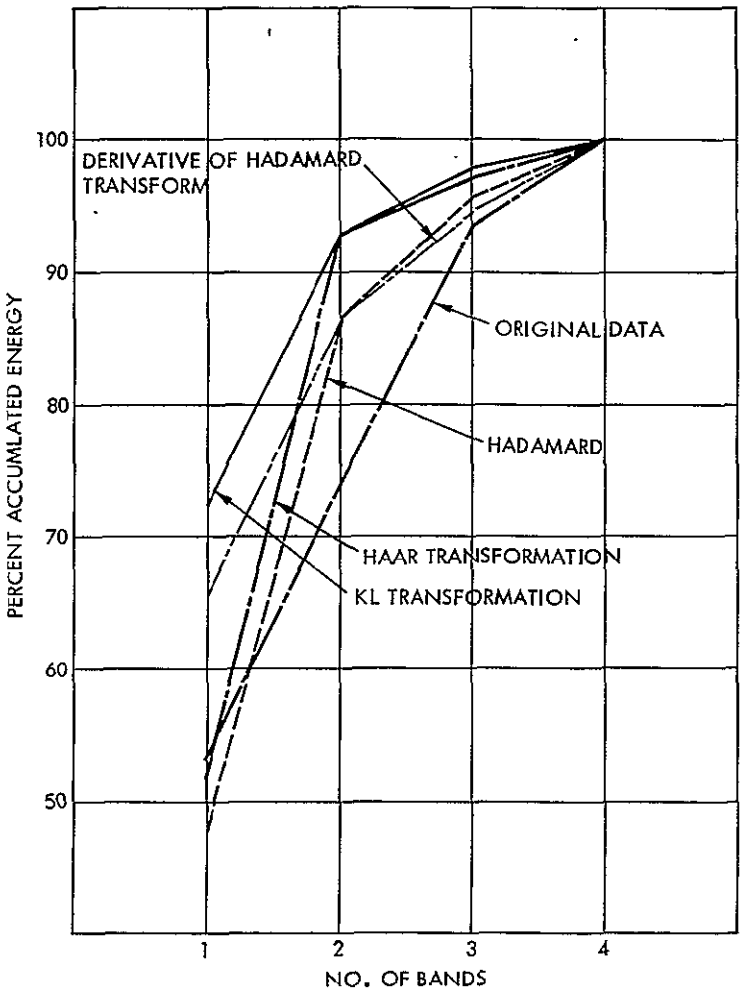

Figure 7.1. Percent Accumulated Energy vs No. of Bands for Various Spectral Transformations

performance of the Hadamard transform on the multispectral data is significantly inferior to the performance of the Karhunen-Loeve transform. This is because the multispectral data does not have the correlation properties of Markovion processes. Other unitary transformations, such as Fourier, Cosine, and Slant transformations with properties similar to those of the Hadamard transform, also display performance substantially inferior to that of the Karhunen-Loeve transformation in their ability to compress the energy into a small number of coefficients. For this reason, we considered other linear, unitary transformations that form a better match with the statistics of the multispectral data. Two of these are discussed below.

Haar Transform

Considering the general properties of the multispectral data outlined in the beginning of Section 4, one would guess that a transformation uncorrelating two bands at a time performs better than the Hadamard transform in uncorrelating the multispectral data. Naturally one would choose to make two infrared bands and the red and the green bands as uncorrelated as possible. This is because of the large mutual correlations between these bands. One such transformation is performed by operator Δ where

$$\Delta = \begin{bmatrix} 1 & 1 & 0 & 0 \\ 0 & 0 & 1 & 1 \\ 1 & -1 & 0 & 0 \\ 0 & 0 & 1 & -1 \end{bmatrix} \tag{7.4}$$

This transformation is unitary, ($\Delta^{-1} = \Delta^{T}$) i.e.,

$$\Delta^{-1} = \frac{1}{2} \begin{bmatrix} 1 & 0 & 1 & 0 \\ 1 & 0 & -1 & 0 \\ 0 & 1 & 0 & 1 \\ 0 & 1 & 0 & -1 \end{bmatrix} \tag{7.5}$$

Δ is simpler to implement than the Hadamard transform. Indeed a 4 x 4 Hadamard operator H_4 is obtained by two consecutive applications of the Δ operator; i.e.,

$$H_4 = \Delta^2 \tag{7.6}$$

For this reason Δ is called a derivative of the Hadamard transform. Its performance is shown on Figure 7.1. It is superior to that of the Hadamard transform using only one or two bands. It becomes inferior if more than two bands are utilized.

A second linear transformation considered is the Haar transform which is denoted by D. This operator and its inverse are defined as

$$D = \begin{bmatrix} 1 & 1 & 1 & 1 \\ 1 & 1 & -1 & -1 \\ \sqrt{2} & -\sqrt{2} & 0 & 0 \\ 0 & 0 & \sqrt{2} & -\sqrt{2} \end{bmatrix} \tag{7.7}$$

and

$$D^{-1} = \frac{1}{4} \begin{bmatrix} 1 & 1 & \sqrt{2} & 0 \\ 1 & 1 & -\sqrt{2} & 0 \\ 1 & -1 & 0 & \sqrt{2} \\ 1 & -1 & 0 & -\sqrt{2} \end{bmatrix} \tag{7.8}$$

The performance of the Haar transform is also shown on Figure 7.1. It performs significantly better than Hadamard and Δ transforms. Its performance is very close to that of the Karhunen-Loeve transform. The residual correlation remaining in the data after application is shown on Table 7.2.

Table 7.2. Residual Correlation in the Multispectral Data after Haar Transform Operation

.471	0.026	.002	.078
.026	.409	-.002	.078
.002	-.002	.034	-.006
.078	.078	-.006	.086

Based on these results, we use Haar transform on the spectral data as an alternative to the Karhunen-Loeve transform prior to using other methods of bandwidth reduction in the spatial domain. It generates slightly inferior results which may be acceptable in view of its simplicity.

7.1.2 Multidimensional Coding of Multispectral Data

Following the spectral transformation on K spectral bands of the multispectral data one obtains K bands of data $u_i(x,y)$, $i=1,2,\ldots,K$ as defined by (7.1). Each band must be coded and transmitted. A total of M_b binary digits is used for all four bands. The receiver combines the coded bands $u_i^*(x,y)$ $i=1,2,\ldots,K$ to reconstruct $f^*(x,y,k)$ which is different from the original multispectral data $f(x,y,k)$ because of coding and possibly transmission errors. The spectral transformation generates $u_i(x,y)$; $i=1,\ldots,K$ which is almost uncorrelated with a maximum compaction of energy in the first k of the K components. The allocation of M_b binary digits to the K bands of $u_i(x,y)$ is such that the total resultant error for all spectral bands is minimum.

To achieve this performance, we proceed with appropriate transformations in the spatial domain and make the proper bit allocations. This will be shown for all three candidate techniques individually.

Multidimentional DPCM

The block diagram of a DPCM system is shown in Figure 7.2. The transmitter is composed of a predictor and a quantizer. The predictor uses n previous samples to predict the present value of the input signal. The difference between this and the actual value of the signal, called the differential signal, is quantized and is transmitted over an error-free digital channel. At the receiver, a similar predictor uses n previously transmitted values of the quantized differential signal to reconstruct a facsimile of the signal at the transmitter. It is conceivable to design a system that would minimize a measure of the overall error between the input and the output of the coding system. However, the analysis of such a system is hampered by the nonlinear character of the quantizer. Therefore, the optimization problem is solved in two stages. First, a best linear predictor is designed ignoring the quantizer; then a quantizer optimized for the distribution of the differential signal is

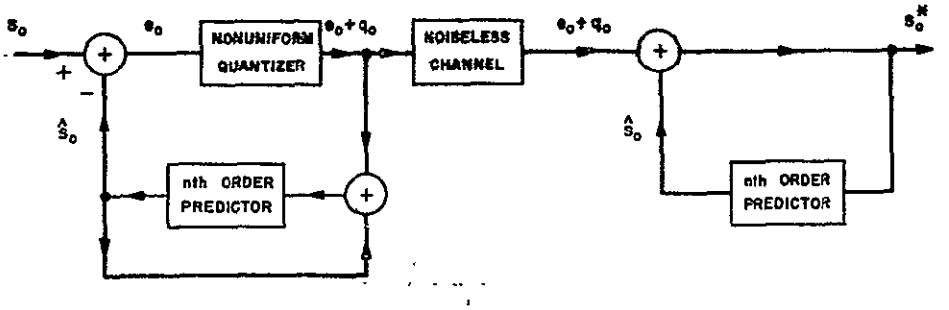

Figure 7.2 DPCM System

employed. It has been shown that if the quantizer is outside the prediction loop, the performance of the system for a Gaussian-Markov process is not any better than the performance of a PCM system [65]. Since the predictor was designed neglecting the effect of the quantizer, including the quantizer in the prediction makes the predictor suboptimum. As a result, the differential signal becomes more correlated; also, its distribution changes, thus degrading the performance of the quantizer. This effect becomes more crucial as coarser quantizers are employed. O'Neal [62] has given a heuristic discussion that shows this system actually gives a higher signal to noise ratio than a PCM system.

Consider a set of correlated random variables $\{S_i\}$ with mean zero and variance σ^2. The set could represent a set of picture elements where the mean is subtracted. The linear predictor estimates the next sample value S_0 by $\hat{S}_0$ based on the previous n sample values as

$$S_0 = \sum_{i=1}^{n} A_i S_i \tag{7-9}$$

the differential signal corresponding to S_0 is $e_0 = S_0 - \hat{S}_0$. The best estimate in the least mean squared error (MSE) sense is one where the weighting coefficients A_i are solutions of the n algebraic equations

$$R_{0i} = \sum_{j=1}^{n} A_i R_{ij}, \quad i = 1, 2, \cdots, n \tag{7-10}$$

where

$$R_{ij} = E(S_i S_j) \tag{7.11}$$

then the mean squared value of the error is

$$\sigma_e^2 = \sigma^2 - \sum_{i=1}^{n} A_i R_{oi} \tag{7.12}$$

As $n \to \infty$ the sequence of error samples can be made completely uncorrelated [96]. However, if the sequence of samples $\{S_i\}$ is the n^{th} order Markovian process, then using only n samples in forming estimates S_o will make the resulting sequence of error terms uncorrelated. In this case, a further increase in the number of samples employed in forming the optimum predictor will not improve the quality of the estimate.

Experimental results indicate that for most typical pictures, the probability density function of the differential signal e_i is Laplacian (two-sided exponential) probability density function [62]. For a Laplacian, Smith [145] has determined the least MSE quantizer. It is a uniform quantizer with pre- and post-quantization transforms z(e) and $e^*(z^*)$ that are defined as

$$z(e) = \frac{E_o[1 - \exp(-me/E_o)]}{1 - \exp(-m)} \tag{7.13}$$

$$z(-e) = -z(e)$$

and

$$e^*(z^*) = \frac{-E_o}{m} \ln\left[1 - \frac{z^*}{E_o}(1-\exp(-m))\right], \tag{7.14}$$

$$e^*(-z^*) = -e^*(z^*)$$

respectively, where

E_o = maximum value of e,

$m = \frac{\sqrt{2E_o}}{3\sigma_e}$, z^* quantized value z.

and

σ_e = variance of the differential signal

The function E_0 is the maximum value that the differential signal can obtain. That, in turn, is the maximum value of the normalized (zero mean and unit variance) picture elements. Note that using a value smaller than this quantity for E_0 means clipping some elements of the differential signal which corresponds to a coarse quantization in the tail area of the density curve and a finer quantization of the samples in the midrange. Since the tails of the differential signal density correspond to large variations in the values of picture elements, it follows that using a smaller values for E_0 would produce poor results in the edges and a better result in the region of finer variations of the encoded picture. Thus, E_0 is a parameter which affects the edge quality in the encoded picture. The optimum value for E_0 is one that gives a good compromise between degration of edges and finer variations in the encoded picture.

To compress the bandwidth of multi-dimensional data such as multi-spectral imagery one must first decide on the order n of the DPCM system that should be utilized. Then each data point S_0 is predicted using a weighted sum of n adjacent data points $S_1, S_2, \ldots, S_n$. For monochrome imagery it has been shown that a two-dimensional DPCM encoder performs near its optimum level of performance when only three adjacent elements are utilized in predicting S_0. These elements are the element directly to the left of S_0, the element directly above S_0 and the element diagonally across from S_0. These elements are shown on Figure 7.3 by S_1, S_2, S_3, respectively. For three-dimensional data one must utilize elements from the previous frame as well as the previous line. Although a comprehensive study of the use of a three-dimensional DPCM system is not available,* from

*For multispectral imagery, the application of a DPCM encoder across the spectral bands is not advisable because of the limited number of spectral bands available. For television data, some results of a three-dimensional DPCM encoder are available [146]. However, these results favor other coding methods such as transform and hybrid coding schemes.

the study of two-dimensional DPCM systems it can be inferred that for a near optimal level of performance, one needs to include seven adjacent points in predicting each element. These samples are indicated on Figure 7.4 by S_1 through S_7.

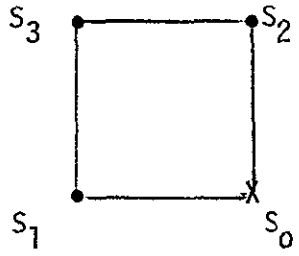

Figure 7.3

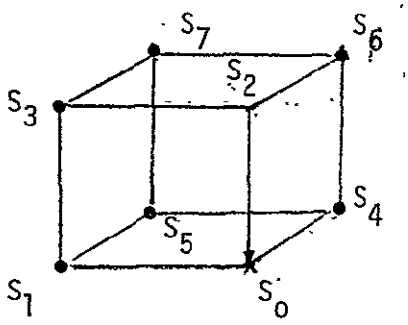

Figure 7.4

Multidimensional Transform Coding

In three-dimensional transform coding algorithms, the spectral transformation is followed by two consecutive transformations in the horizontal and the vertical directions. Experimental and theoretical results have shown that the performances of the three-dimensional coding algorithms are rather insensitive to the particular type of transformations used in the spatial domain. In implementing the coding system, it is the ease of implementation and weight-power requirements which dictate the choice of the particular transformation. It is also shown that different types of transformations can be cascaded without a substantial change in the quality of the encoded picture. The spatial transformations of various bands $u_i(x,y)$ $i=1,\ldots,k$ can be modeled as

$$u_{ijk} = \sum_{y=1}^{N} \sum_{x=1}^{M} u_i(x,y)\, \mu_j(x)\, \psi_k(y) \qquad (7.15)$$

$$u_i(x,y) = \sum_{k=1}^{N} \sum_{j=1}^{M} u_{ijk}\, \mu_j(x)\, \psi_k(y) \qquad (7.16)$$

The coding of the coefficients u_{ijk} introduces quantization error in the transformed domain. This error is minimum when the total number of M_b digits assigned to u_{ijk} is such that the quantization error for all coefficients with a variance smaller than this constant need not be transmitted, thus they do not require any encoding. This is achieved by assigning m_{ijk} bits to u_{ijk} coefficients such that

$$m_{ijk} = \frac{M_b}{mnk} + 2\left[\log \sigma^2_{ijk} - \frac{1}{mnk} \sum_{\ell=1}^{k} \sum_{q=1}^{n} \sum_{p=1}^{m} \log \sigma^2_{pq\ell}\right] \qquad (7.17)$$

where σ^2_{ijk} is the variance of u_{ijk} and k, m, and n are the number of coefficients selected for transmission out of K coefficients in the spectral domain, M coefficients in the horizontal domain, and N coefficients in the vertical domain, respectively. The above bit assignment algorithm is optimum in a mean square error sense, but in a system where one is interested in substituting one transformation for the other, making the above bit assignment becomes rather tedious. Besides, making the bit assignment is a complicated task for a hybrid encoder which combines a unitary transformation with a DPCM encoder following the above procedure. For this reason we will consider a two-step bit assignment procedure which is equivalent to the above, but can be simulated more simply.

Two-Step Bit Assignment Procedure. In a two-step bit assignment procedure, one first decides on a number of binary digits out of a total of M_b bits which would be assigned to each one of the spectral bands (M_i, i = 1, 2,...,k). Then M bits are assigned to the various coefficients which are obtained by applying two-dimensional transformation to the i^{th} band of the multispectral data. These consecutive bit assignment algorithms are modeled as

$$M_\ell = \frac{M_b}{k} + 2\left(\log \lambda_\ell - \frac{1}{k} \sum_{\ell=1}^{k} \log \lambda_\ell\right) \qquad \ell = 1, 2,...k \qquad (7.18)$$

and

$$m_{ij\ell} = \frac{M_\ell MN}{mn} + 2\left(\log \hat{\lambda}_{ij} - \frac{1}{mn}\sum_{q=1}^{n}\sum_{p=1}^{m}\log \hat{\lambda}_{pq}\right) \tag{7.19}$$

where $\hat{\lambda}_{ij}$ are the variances of the coefficients in the two-dimensional transform domain, and λ_ℓ, $\ell = 1 \ldots, K$, are the variances of elements in the one-dimensional transform domain. To make the combination of (7.18) and (7.19) equivalent to (7.17) under the assumption of separable covariances which implies $\sigma^2_{ij\ell} = \lambda_\ell \hat{\lambda}_{ij}$, it can be shown that (7.18) should be modified as

$$M_\ell = \frac{M_b}{k} + 2\left(\log \lambda_\ell^{\frac{mn}{MN}} - \frac{1}{k}\sum_{\ell=1}^{k}\log \lambda_\ell^{\frac{mn}{MN}}\right) \tag{7.20}$$

where MN is the total number of samples in the spatial domain, and mn is the total number of samples which are selected for transmission. The ratio $\frac{mn}{MN}$ depends upon the average number of bits per picture element use for coding the data. From past experience these ratios for typical pictures at various bit rates are:

Average Bit/Pixel	mn/MN
0.5	1/4
1.0	1/2
2.0 or more	1.0

Multidimensional Hybrid Coding

In the hybrid coding of transformed spectral bands $u_k(x,y)$, the sampled image is divided into arrays of M by N samples such that the number of samples in a line of $u_k(x,y)$ is an integer multiple of M. One-dimensional unitary transformation of the data and its inverse are modeled by the set of equations

$$u_{ki}(y) = \sum_{x=1}^{M} u_k(x,y)\ \Phi_i(x) \qquad \begin{matrix} i = 1, 2, \ldots, M \\ y = 1, 2, \ldots, N \end{matrix} \tag{7.21}$$

$$u_k(x,y) = \sum_{i=1}^{M} u_i(y)\ \Phi_i(x) \tag{7.22}$$

where $\Phi_i(x)$ is a set of M orthonormal basis vectors. The correlation of the transformed samples $u_{ki}(y)$ and $u_{ki}(y + \tau)$ is given by

$$C_{ik}(\tau) = \sum_{x=1}^{M} \sum_{\hat{x}=1}^{M} R_k(x, \hat{x}, y + \tau)\ \Phi_i(x)\ \Phi_i(\hat{x}) \tag{7.23}$$

where $R_k(x, \hat{x}, y, \hat{y})$ is the spatial autocovariance of the k^{th} band of multispectral data.

Note that this equation indicates (1) the correlation of samples in each column of the transformed array is directly proportional to the correlation of sampled image in vertical direction, (2) the correlation of samples in various columns of the transformed array is different. Thus, a number of different DPCM systems should be used to encode each column of the transformed data. The block diagram of the proposed system is shown in Figure 7.5. A replica of the k^{th} band of the original image $u_k^*(x,y)$ is formed by inverse transforming the coded samples, i.e.,

$$u_k^*(x,y) = \sum_{i=1}^{n} v_{ki}(y)\ \Phi_i(x),\ n \leq M \tag{7.24}$$

The mean square value of coding error for the k^{th} band is

$$\varepsilon_k^2 = E\ \frac{1}{MN} \sum_{y=1}^{N} \sum_{x=1}^{M} \left[u_k(x,y) - u_k^*(x,y)\right]^2 \tag{7.25}$$

Using (7.21) to (7.24) and assuming that $q_{ki}(y)$, the quantization error encountered in the i^{th} DPCM system is uncorrelated with $u_{ki}(y)$, the coding error, ε_k^2, is

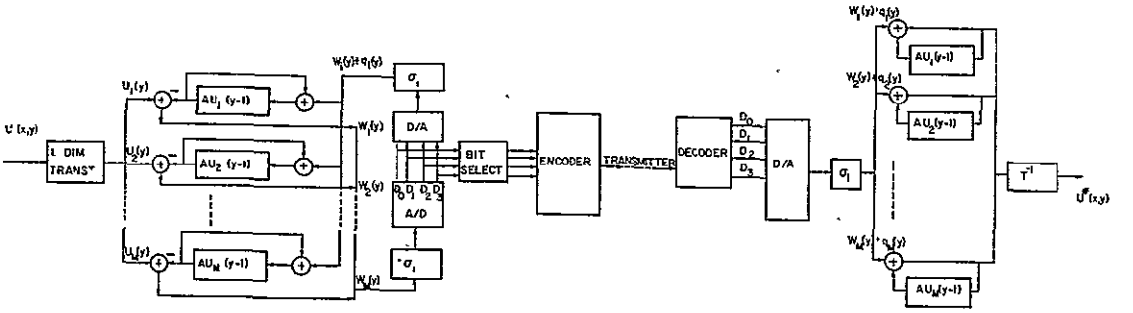

Figure 7.5. Hybrid System

$$\varepsilon_k^2 = R_k(0,0,0,0) - \sum_{i=1}^{n} C_{ik}(0) + E\,\frac{1}{MN}\sum_{y=1}^{N}\sum_{x=1}^{n}\left[u_{ki}(y) - v_{ki}(y)\right]^2 \tag{7.26}$$

where the first two terms are introduced because of using n (rather than M) DPCM systems. Study of DPCM systems has shown that

$$E\left[u_{ki}(y) - v_{ki}(y)\right]^2 = E\,q_{ki}^2(y) = G(m_{ki})\,e_{ki}^2 \tag{7.27}$$

where e_{ki}^2 is the variance of the differential signal for the k^{th} band in the i^{th} DPCM system, and $G(m_i)$ is the quantization error of a variate with a unity variance in a quantizer with $(2)^{m_i}$ levels.

Analysis of a Lloyd-Max quantizer has shown that $G(m_i)$ can be approximated fairly accurately by

$$G(m_i) \cong be^{-am_i} \tag{7.28}$$

where the best fit for a Gaussian variate is obtained using an = 0.5 ℓn 10 and b = 1.0. Study of other quantization techniques has indicated similar

results for various probability density functions [64]. For a Laplacian random variable, values of a = 0.5 ℓn 10 and b = 2 are more appropriate. Experimental results have shown that the differential signal in the DPCM systems have a Laplacian histogram.

From published results [62] the variance of the differential signal in a DPCM system with the m^{th} order linear predictor for the k^{th} band is

$$e_{ki} = C_{ki}(0) - \sum_{j=1}^{m} A_{kij} C_{ki}(j) \tag{7.29}$$

where A_{kij} are related to $C_{ki}(j)$ by m algebraic equations.

Substituting (7.21) and (7.22) in (7.20), ε_k^2 is

$$\varepsilon_k^2 = R_k(0,0,0,0) - \sum_{i=1}^{n} C_{ki}(0) + \frac{b}{M} \sum_{j=1}^{n} e^{-am_{ki}} e_{ki} \tag{7.30}$$

where the error is defined in terms of n and m_i, i = 1,..., n. Treating m_i as continuous variables and minimizing ε_k^2 with a constraint $\sum_{i=1}^{n} m_{ki} = M_k$ will give

$$m_{ki} = \frac{M_k}{n} + \frac{1}{a}\left(\ell n\, e_{ki}^2 - \frac{1}{n}\sum_{j=1}^{n} \ell n\, e_{kj}^2\right) \tag{7.31}$$

where n is chosen such that ε_k^2 is minimum* and the quantizer in the i^{th} DPCM system will have $(2)^{m_{ki}}$ levels. m_{ki} as obtained from (7.25) is modified as discussed in [62]. Note that expressions (7.24) and (7.25) are similar to those obtained for coding the transformed data by memoryless quantizers, the difference being that here the variance of the differential signal rather than the variance of the transformed data is used.

*Ready and Wintz minimize ε_k^2 with respect to both n and m_i. It gives the same end result requiring less computation [104].

Figure 7.6 shows the theoretical value of the coding error as given by (7.30) in terms of the peak-to-peak signal to RMS noise ratio for a discrete random field with an autocovariance

$$R(x, \hat{x}, y, \hat{y}) = e^{-\alpha|x - \hat{x}| - \beta|y - \hat{y}|} \tag{7.32}$$

using Karhunen-Loeve, Hadamard, discrete Fourier, discrete Cosine, and Slant transformations fpr $\alpha = 0.0545$, $\beta = 0.128$. These curves are obtained using a bank of n DPCM encoders with one-element predictors. The quantizers in the DPCM systems are of instantaneous-companding type and are designed for a Laplacian probability density function of the differential signals in the DPCM systems.

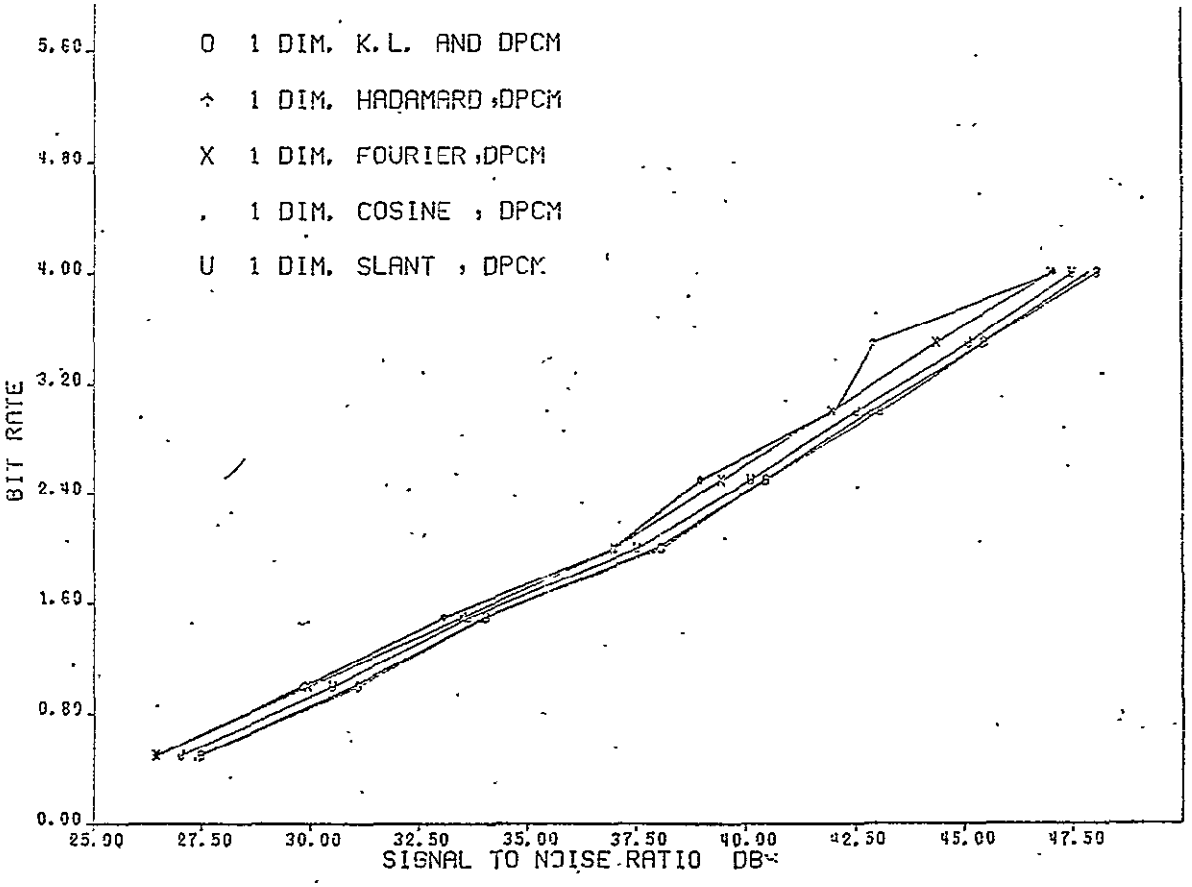

Figure 7.6. Bit Rate vs the Signal-to-Noise Ratio for the Proposed One-Dimensional Hybrid Systems for the Discrete Random Field

Figure 7.7 shows that increasing the block size M improves the theoretical performance of the proposed one-dimension systems; however, the improvement becomes negligible for values of M larger than 8. This makes this coding system less sensitive to the block size than the standard transform coding systems which use memoryless quantizers.

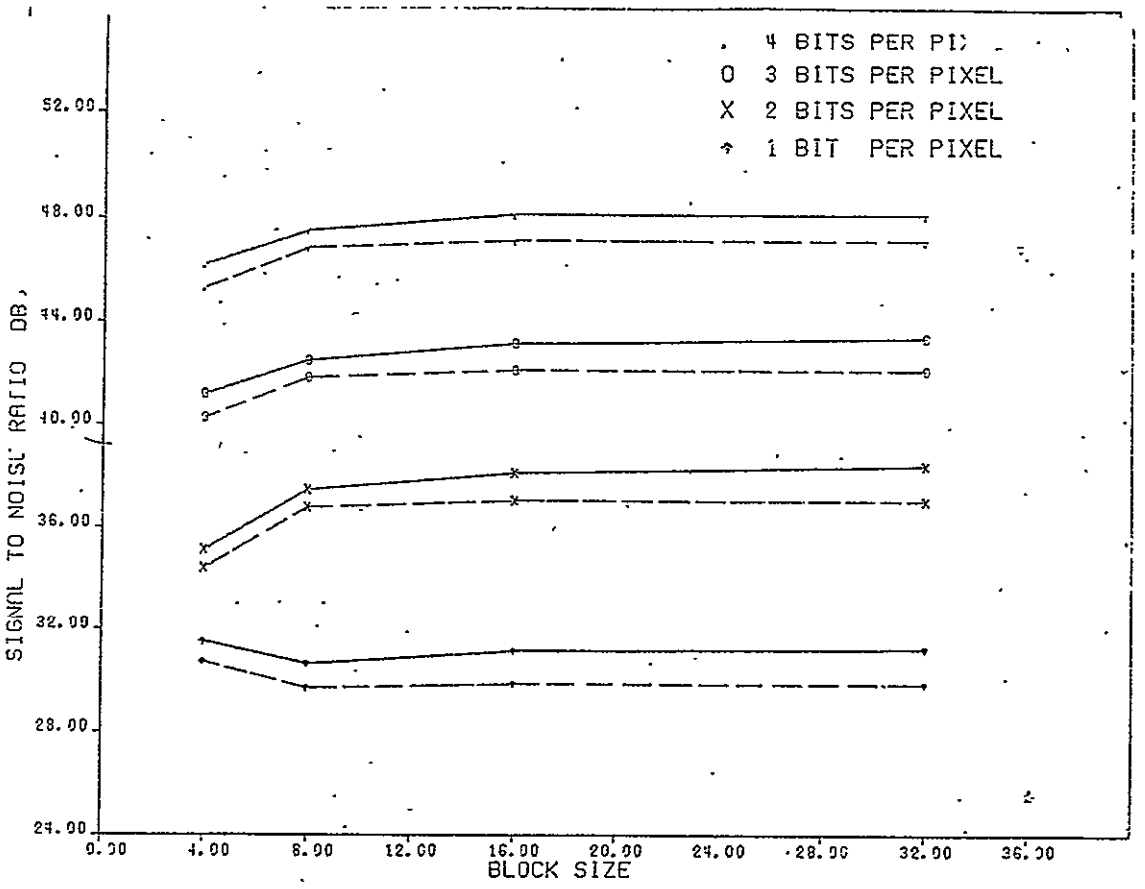

Figure 7.7. Theoretical Performance of the Proposed One-Dimensional Encoders vs Block Size M. The Solid and the Dashed Lines Refer to the Karhunen-Loeve and the Hadamard Transforms, Respectively

7.1.3 Cluster Coding of Multispectral Data

Many important uses of the earth resource data rely heavily on the use of computerized classification and recognition of multispectral imagery. For many classification applications, the multispectral data is first used to obtain clustered imagery. The clustered imagery is then used for image data extraction and classification. Therefore, the bandwidth compression method must not produce significant changes in the resulting clustered imagery. A criterion employed for evaluating various coding algorithms is the performance of various encoders in retaining the classification accuracy of the clustered imagery. That is, the clustered image obtained from the encoded multispectral data should be identical to the clustered image obtained from the original set of multispectral data. This presents an alternative approach to compressing the bandwidth of the multispectral imagery which involves classifying the multispectral data on-board the space vehicle and transmitting only the clustered imagery. The problem with this approach is that there are many users who are interested in information contained in the individual bands as well as the classified imagery. For this reason, in addition to the classified picture which contains an arbitrary number of clusters, additional information should be transmitted such that individual bands of the original data can be reconstructed. Naturally, the number of binary digits used to transmit the classified imagery and the additional information required for reconstructing the various spectral bands should be smaller than the number of binary digits needed for transmitting the original bands. This type of bandwidth compression algorithm has been discussed in recent literature [147, 148]. In the following sections we will compare the performance of a cluster coding method with other candidate methods of bandwidth compression.

Clustering

Clustering techniques group data values into classes. This grouping of data can be used for data compression if one represents each class by one value and transmits only the number of the cluster to which a particular data value belongs.

The concept of a "measurement space" is useful in explaining clustering procedures. We define a measurement space as it applies to this application. For the case of multispectral ERTS (LANDSAT) data, for each picture element

we obtain four measurements (recorded energies in each of four narrow spectral bands). The four measurement values can be represented by a 4-tuple. This 4-tuple can be plotted as a point in a four-dimensional space. This space is called the measurement space. Two picture elements recording approximately the same energy in each band are represented by points which lie close together in the measurement space. An example of sample points in a two-dimensional measurement space is illustrated in Figure 6-5.

The many clustering techniques differ in the criteria by which they define similarity and dissimilarity of data samples. One of the most common measures of dissimilarity is mean square error. If one fixes the number, N, of classes, the minimum mean square error clustering reduces to selection of a representative, m_j, of each class such that

$$J_e = \sum_{i=1}^{N} J_i \text{ is minimized} \tag{7.33}$$

where

$$J_i = \sum_{x \in \text{cluster } i} || x - m_i ||^2 \tag{7.34}$$

Equivalently, the average Euclidean distance in the measurement space from a sample to its cluster representative is minimized. We have used a clustering techniques that selects cluster representatives that reduce the mean square error resulting from representing all elements of a cluster by one value. Because it is essentially a hill climbing procedure, the technique can find only the locally minimum mean square error clusters and consequently depends on the initial choice of cluster representatives.

The cluster representatives are referred to as centroids because each one is the "center of mass" (in the measurement space) of the sample values belonging to that class. The iterative for each measurement technique for finding the centroids is summarized as follows.

A particular starting number of clusters is selected. More or less arbitarily, a set of initial centroid values are chosen. In our case, the

initial centroids are chosen to lie along the line of maximum variance of all the sample data in the measurement space. Their spacing is proportional to the standard deviation in the specified direction. Each sample value is assigned to the category corresponding to the centroid closest in the sense of Euclidean distance. Then the centroids of the sample values belonging to each class are computed. Once again, the data samples are mapped into those categories having the closest of the new centroids. This entire process is repeated until less than a prespecified percentage of the sample values change category on one of the iterations. Clusters having the two closest centroids are merged and the iterative procedure is repeated with the smaller number of clusters.

The centroids are real numbers; thus, they must be quantized and encoded. We have used the rather inefficient pulse code modulation (PCM) scheme for coding the centroids for the preliminary results reported here. The ij^{th} block in clustered imagery can be coded using $[\log_2 C_{ij}]^+$ binary digits where C_{ij} is the number of clusters in block indexed by i,j and $[\log_2 C]^+$ is the smallest integer larger than $\log_2 C_{ij}$. Using $[\log_2 C]^+$ bits for coding the ij^{th} block in the classified imagery is a rather inefficient use of binary digits, since it does not exploit any part of the spatial correlation in the clustered imagery. Several methods for efficient coding of the clustered imagery exist. One is using contour tracing combined with statistical coding algorithms such as Huffman encoding of directionals and gray levels. The other is use of differential encoders combined with the statistical coding algorithms. These modifications reduce the bit rate essential for transmitting the clustered imagery and the centroids, which, in turn, corresponds to a further bandwidth compression of the multispectral imagery.

The average bit rate per sample per band of the ij^{th} block of imagery R_{ij} for the cluster coding algorithm using PCM transmission of centroids and the clustered imagery is calculated as follows. Let 2^P stand for the number of levels used in quantizing each centroid element and B refer to the number of bands in the multispectral imagery then

$$R_{ij} = \frac{[\log_2 C_{ij}]^+}{B} + \frac{P\, C_{ij}}{N^2} \tag{7.35}$$

where N^2 is the number of samples in each block of the multispectral imagery.

Equation (7.35) shows that the bit rate is directly related to the number of clusters in the classified imagery in each block and the number of levels that one uses for quantization of centroids. It is inversely related to the number of samples in each block and the number of spectral bands in the multispectral data. Since one has to allow for a large number of clusters in each block to recover the details of multispectral imagery, this coding method is particularly efficient for a large number of spectral bands.

The idea of dividing the multispectral imagery into blocks of N^2 samples and cluster coding each block is not essential for the coding algorithm. Indeed if one is interested only in a classified imagery using the whole image as one block, a very efficient encoder will result. However, if one is interested in the details in various spectral bands, then using a large block size requires allowing the classifier to classify the multispectral data to a large number of clusters. The problem with this approach is the extremely large computer time required for the convergence of the classifier. On the other hand, using relatively small block sizes, detailed information in various spectral bands can be reconstructed rather accurately using a moderate number of classes.

Coding Methodology

Classification of multispectral data discussed in Section 6.3 is a method of quantization in the spectral domain. That is, a number of picture elements in the measurement domain are represented by a single point in the four-dimensional space. This is illustrated on Figure 6.5 for a two-dimensional space. The combination of the clustered imagery and the centroids represents a quantized form of the multispectral data which can be used to reconstruct an approximation of each band in the multispectral data. This operation is similar to quantizing the amplitude of a scalar signal. Reduction of the multispectral imagery to an image of clusters and centroids for each cluster corresponds to exploiting the spectral correlation of the multispectral imagery. The spatial correlation inherent in the multispectral earth imagery is preserved, to some extent, in the form of spatial correlation in the classified imagery. Naturally in addition to spatial

correlation of the classified imagery, both inter- and intracorrelation of the centroids can be used for further bandwidth compression.

The cluster coding algorithm discussed here uses the following steps for encoding and decoding the multispectral data.

- A multispectral image is divided into blocks of 16 by 16 picture elements in each band.

- Using all spectral components each block is classified into a number of classes. The clustered imagery and centroids corresponding to each cluster are the output of this step in the coding operation. The number of clusters in each block can be fixed or it can be allowed to vary, generating different numbers of clusters for various blocks. The latter corresponds to an adaptive bandwidth compression technique that operates at a variable bit rate where the former could be made to operate at a fixed bit rate. Even when the number of clusters is allowed to vary from one block to the other the maximum and the minimum number of clusters in each block can be fixed. This sets a fixed upper bound and a lower bound on the output bit rate which can be used for a more effective control of a storage buffer that has to be used with any variable rate encoder.

- The receiver reconstructs each block of the multispectral imagery by generating the individual bands in each block from the clustered imagery and the corresponding centroids of those clusters. The procedure is to examine each point in the clustered imagery and specify to what class it belongs. Then individual bands corresponding to the particular picture location are reconstructed by choosing their values equal to the centroid of that particular class.

7.2 SIMULATION OF SELECTED BANDWIDTH COMPRESSION TECHNIQUES

Analytical studies of picture bandwidth compression methods give the expected performance of a bandwidth compression method for an ensemble of imagery. This is different from the simulation results for a particular bandwidth compression method. The main drawback of the analytical results is twofold: First, the limited form of the criteria of optimality which is used for evaluation of the performance of the bandwidth compression methods. Second, the effect of inaccuracy of the assumptions which are made in developing the analytical models. This is the major reason for differences between the analytical and the simulated results. The analytical results are in terms of mean square error, or rate distortion functions. Simulation of the bandwidth compression methods enables one to compare the various bandwidth compression methods using other criteria of performance. In addition, this eliminates the inaccuracies of the analytical results and gives results which are closer to the performance of the actual bandwidth compression devices.

7.2.1 Methodology

The methodology for computer verification of bandwidth compression methods is as follows.

(1) Various bandwidth compression methods are simulated in their entirety on a digital computer. The simulated systems can accept a fixed-size multispectral imagery, reduce the bandwidth of this imagery to a particular level, and reconstruct the compressed multispectral imagery.

(2) The original and the reconstructed imagery (at a particular bit rate and using a particular method) are displayed on a COMTAL image display system for side-by-side comparison.

(3) Hard copies of the original and the reconstructed imagery are generated using a Dicomed image writing system. The original and reconstructed imagery are used to generate various measures of the difference between the two sets of imagery. These are mean square error, signal-to-noise ratio, and the classification accuracy (consistency) between the original and the reconstructed imagery. (A detailed description of TRW's image processing facilities is given in Appendix C.)

7.2.2 Description of the Imagery Selected

Since the study involved analyzing and simulating a large number of bandwidth compression methods, it was necessary to restrict performance evaluation to a few images. Two sets of multispectral imagery were selected. One is a 256 x 256 sample of a LANDSAT multispectral image comprised of a red, a green, and two infrared bands. The other is a set of 12-channel high altitude aircraft data. Eight out of the 12 channels were selected for simulation results. These are shown on Figure 7.8. The LANDSAT multispectral imagery is representative in the sense that it includes a variety of scenes ordinarily encountered in earth resources data. It is a particularly difficult scene for bandwidth compression since it involves areas of high detail as well as low detail. It consists of a rather large number of edges as well as flat areas. A bandwidth compression method giving acceptable results using this representative image is expected to produce acceptable results using most other types of imagery.

7.2.3 Program Framework (Flexibility, User Options)

A number of bandwidth compression methods for multispectral data was developed. These bandwidth compression methods are simulated on digital computers using a software package that includes:

(1) Three-dimensional coding algorithms using a block size of 4 x 16 x 16 with a block quantizer. The system has the option of utilizing three-dimensional Hadamard, Cosine, or Slant transformations. The system uses a fixed block quantizer for all three options.

(2) A hybrid coding algorithm using an option of Karhunen-Loeve, Haar, Hadamard, Cosine, or Slant transformation followed by a two-dimensional differential pulse code modulator (DPCM). The transformation is in the spectral domain and the two-dimensional DPCM encoder uses a third-order predictor. The eigenvectors of the Karhunen-Loeve transform and the weightings in the two-dimensional DPCM encoder are fixed. They are based on the statistics of typical data. They could be varied by simply reading a set of new values in the program.

(3) A hybrid coding algorithm which uses an option of Karhunen-Loeve, Haar, Hadamard, Cosine, or Slant transform in the spectral domain followed by an option of Cosine, Slant, or Hadamard transform in the horizontal and

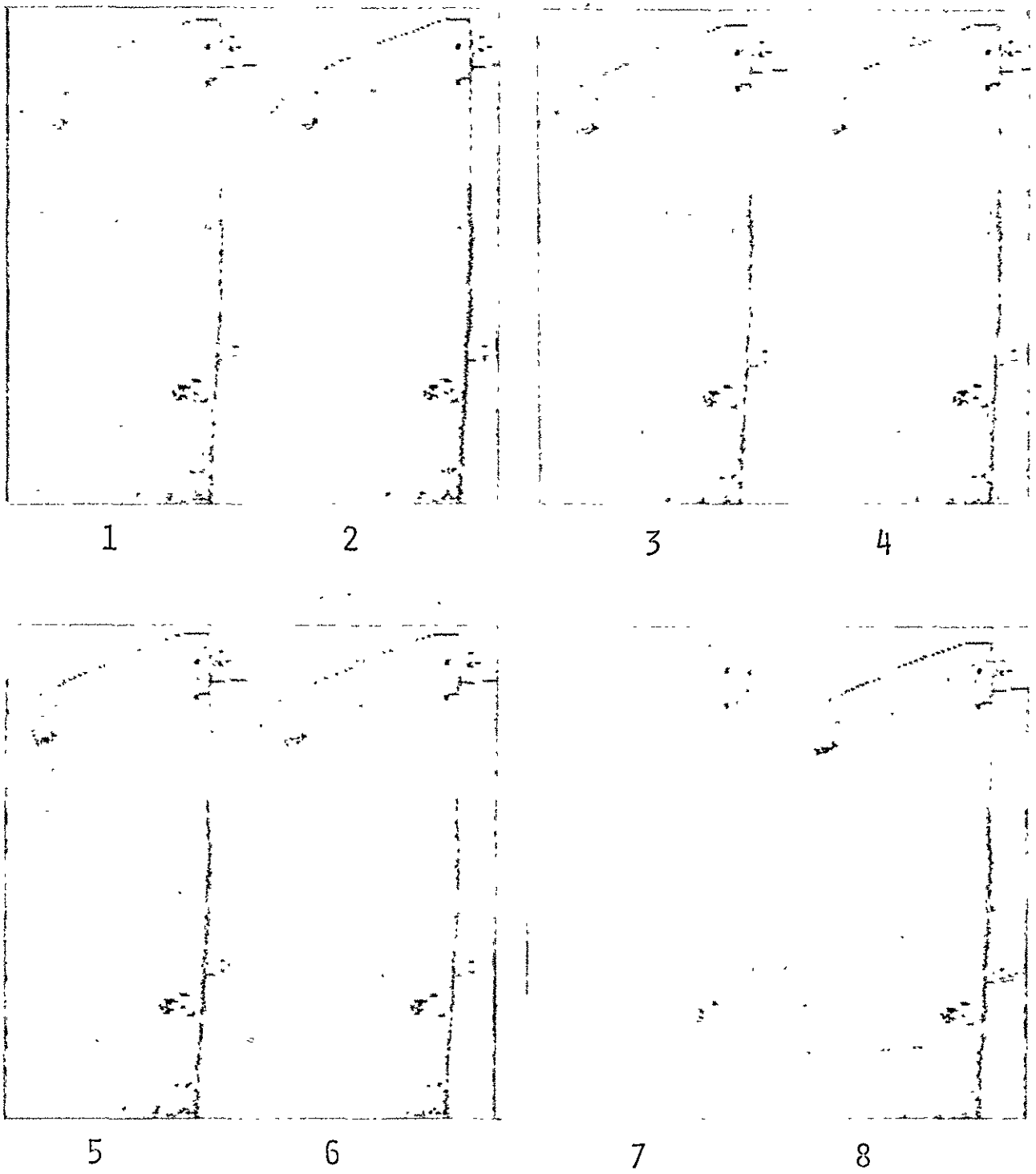

Figure 7.8. 8 Bands of Multispectral Aircraft Image — Each Band Consists of 256 x 128 Samples

block of DPCM encoders in the vertical direction. The block size of the spectral transformation is four, and the block size of the transformation in the horizontal direction is 16. The system uses a fixed set of DPCM encoders for all transformations.

All three coding methods discussed above have a fixed bit rate. They encode the multispectral data at bit rates of 0.5, 1, 2 bits per picture element. The average bit rate can be varied easily by changing the data card in the program.

The above coding algorithms have the option of using a binary symmetric channel at bit error rates of 10^{-2}, 10^{-3}, and 10^{-4}. This can also be varied to any optional value by changing the input data.

In (2) and (3) we also have considered the additional reduction in the bit rate that results by adding an entropy coding algorithm at the output of the DPCM encoders. This results in a reduction in the bit rate without affecting the degradation level in the reconstructed imagery. The addition of the entropy coding method makes the above bandwidth compression methods operate at a variable bit rate. This increases the complexity of the system by requiring buffer storage and buffer control systems.

(4) A cluster coding algorithm using four spectral bands and a block size of 16 x 16. This bandwidth compression algorithm classifies the elements of each block in four spectral bands into a prespecified number of clusters. It also utilizes the Swain-Fu distance to classify each block in four spectral bands to an arbitrary number of clusters. The classified image along with the centroids are used to reconstruct each 16 x 16 block of the multispectral imagery.

7.2.4 Statistical Measures

The statistics of the representative multispectral data utilized in the bandwidth compression methods are the following:

(1) The spectral correlation of the data is utilized in the KL transform of the multispectral data. The correlations for the four bands of LANDSAT and the eight channels of the aircraft data are shown on Table 7.3. The spectral correlation of the LANDSAT data is not exponential, thus the process is not Markovian. The spectral correlation of high altitude data

Table 7.3. Correlation Matrix of the Representative Multispectral Data

(a) LANDSAT Data

1.000	.866	.276	-.141
.866	1.000	.288	-.177
.276	.288	1.000	.654
-.141	-.177	.654	1.000

(b) High Altitude Aircraft Data

1.00	.82	.94	.77	.91	.69	.62	.69
.82	1.00	.85	.92	.85	.85	.79	.81
.94	.85	1.00	.83	.96	.76	.71	.81
.77	.92	.83	1.00	.86	.92	.91	.92
.91	.85	.96	.86	1.00	.82	.77	.87
.69	.85	.76	.92	.82	1.00	.95	.88
.62	.79	.71	.91	.77	.95	1.00	.91
.69	.81	.81	.92	.87	.88	.91	1.00

also does not appear exponential. However, after rearranging the various bands, it can be approximated by an exponential function fairly accurately.

(2) The spatial correlation of the multispectral data, after performing the spectral transformation, is utilized in the various bandwidth compression algorithms. In the system using a two-dimensional DPCM encoder, these correlations are used in obtaining the optimum values for the weightings in the DPCM predictor. In the three-dimensional transform encoder and the hybrid encoder, the spatial correlation is utilized in optimizing the

bit-assignment routine. The spatial correlation of the LANDSAT data after Haar transform is shown in Figure 7.9. This figure shows almost exponential decay of the correlation as a function of distance. Table 7.4 shows the mean and the standard deviation of various bands after Haar transform as well as the optimum weightings in the two-dimensional DPCM system for each band. The table also lists the bit assignment and the standard deviation of the differential signal for each band.

Table 7.4. Statistics of Various Bands after Haar Transform and the Parameters of the DPCM Encoder

Various Bands	A_1 (Horizontal)	A_2 (Vertical)	A_3 (Diagonal)	Average Value	Standard Deviation of the Signal	Standard Deviation of the Differential Signal	No. of Bits/Sample in Each Band (2 Bits/Pel. Average)
Band #1	0.8569	0.5347	-0.4004	186.4	34.71	6.11	3
Band #2	0.8161	0.5808	-0.4096	13.6	30.96	7.13	3
Band #3	0.5143	0.5250	-0.1479	-6.1	14.34	8.29	1
Band #4	0.5271	0.5203	-0.1434	46.3	11.85	6.54	1

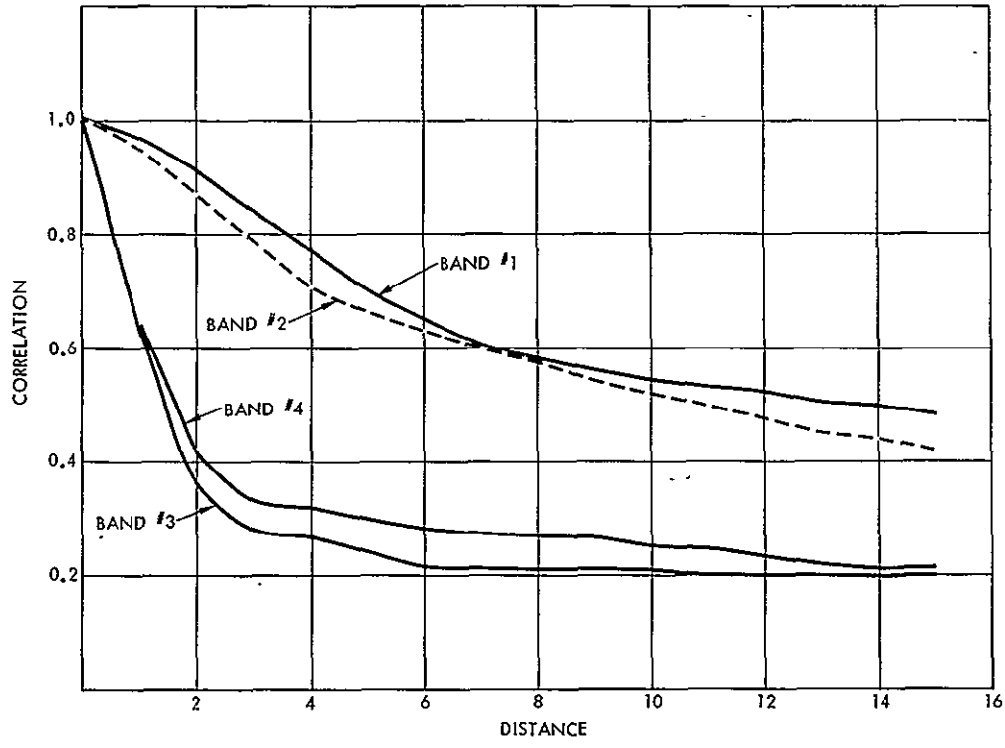

Figure 7.9. Spatial Correlation of Various Bands after Application of Haar Transform in Spectral Domain

7.2.5 Compression and Distortion Results

The simulation results reported below are intended to:

(1) Verify for various methods the compression performance predicted by analytical results.

(2) Compare performance of three-dimensional bandwidth compression methods with those of two-dimensional bandwidth compression methods. Two-dimensional bandwidth compression methods utilize spatial correlation of the imagery data where three-dimensional bandwidth compression methods utilize spectral correlations as well as the spatial correlations.

Since most of our simulation results relate to four-channel LANDSAT data, the performance of a number of bandwidth compression methods is evaluated using multispectral data with a larger number of bands to evaluate the consistency of the results.

Comparative performance of the two-dimensional and the three-dimensional bandwidth compression algorithms is shown in Figures 7.10 and 7.11 in terms of the mean square error and SNR. Each case shows that some improvement in the performance of the bandwidth compression methods is achievable by utilizing spectral correlation of the data. However, the size of this gain is relatively small (about 1.5 dB). Nevertheless, though small, minimal additional complexity is required to achieve it. Further justification for using spectral transformations is that each one of the four channels obtained after a spectral transformation has attributes from all four original spectral channels. Therefore for some users, one channel of this data may be more valuable than any one channel of the original data.

Figures 7.10 and 7.11 show that hybrid encoders perform better than multidimensional cosine transform encoders. This supports the conclusions based on the analytical results that:

- The spectral correlation of the LANDSAT data is not Markovian; therefore, a KL transform or a deterministic transformation matched to the sensor characteristics (such as the Haar transform for LANDSAT data) should be used for spectral operations.
- The combination of a transform-DPCM encoder performs better than a two-dimensional transform encoder.

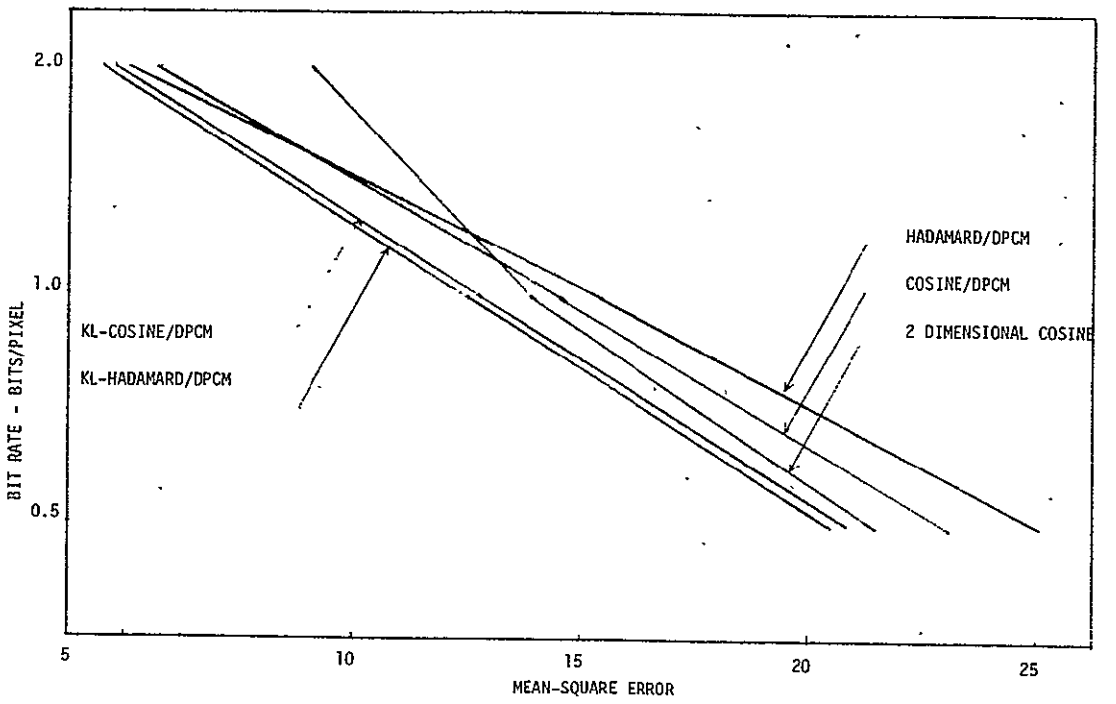

Figure 7.10. Bit Rate vs Mean Square Error for the Two-Dimensional and Three-Dimensional Coding Algorithms

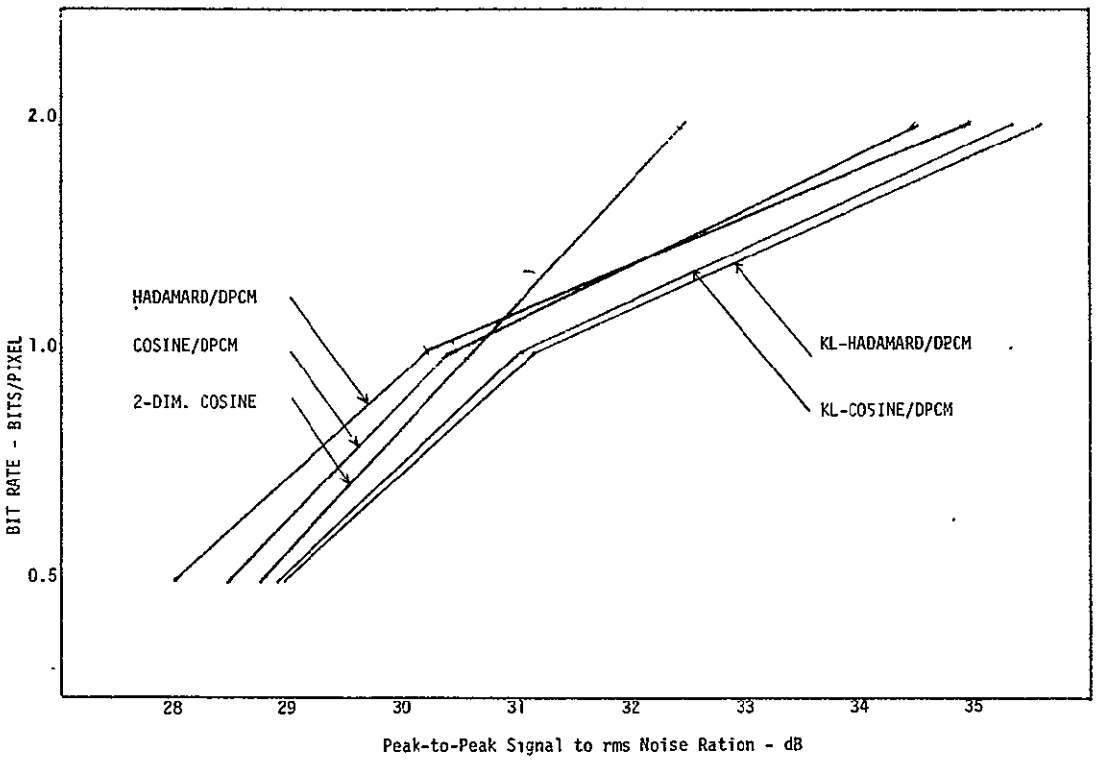

Figure 7.11. Bit Rate vs the Signal-to-Noise Ratio for the Two-Dimensional and Three-Dimensional Coding Algorithm

Figure 7.12 shows reconstructed composite color pictures (consisting of a red, a green, and an infrared band) at 1 and 2 bits/picture elements, corresponding to two- and three-dimensional bandwidth compression methods.

The performance of some of the recommended compression techniques on the eight channels of the high altitude aircraft data is evaluated. The performance of KL two-dimensional DPCM and Haar two-dimensional DPCM systems on the eight-channel data is shown in Figure 7.13. These, as well as other results with the high-altitude data, indicate that:

- The performance of the compression systems on eight-channel data is very similar to the performance of the compression methods on LANDSAT data. This confirms the generality of our results to multispectral data other than LANDSAT data.
- Since the spectral correlation of the data is exponential, the performance of Cosine, Slant, and Hadamard transforms in the spectral domain is better than the Haar transform. However, the difference is so small that the choice of spectral transformation should be based on other considerations. Indeed, using identity transformation instead of the KL transform, there is a loss of about 1.5 dB.

Experimental results relevant to the performance of the recommended compression methods are discussed in Section 9.

1 BIT COSINE - DPCM

1 BIT KL - COSINE - DPCM

2 BIT COSINE - DPCM

2 BIT KL - COSINE - DPCM

Figure 7.12. Bit Rate vs Signal-to-Noise Ratio of KL — 2-Dimensional DPCM and Haar — 2-Dimensional DPCM Systems for Eight Channels of the High Altitude Aircraft Data

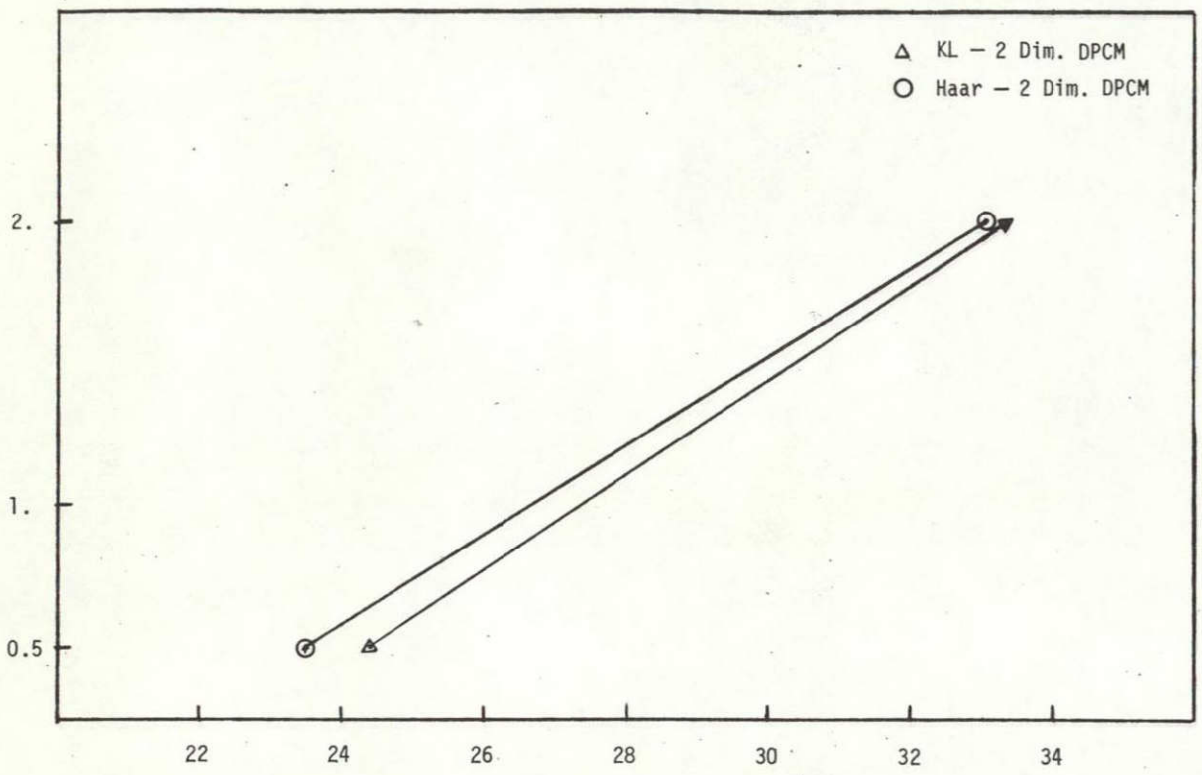

Figure 7.13. Bit Rate vs Signal-to-Noise Ratio of KL – 2-Dimensional DPCM and Haar – 2-Dimensional DPCM Systems for Eight Channels of the High Altitude Aircraft Data

7.3 SYSTEM CONSIDERATIONS

In addition to comparing the performance of the candidate bandwidth compression methods, we have compared the candidate methods based on system considerations. This involves evaluating the candidate methods in terms of their implementational complexity, sensor effects, and the effects of a noisy channel on performance.

7.3.1 Sensor Effects

A number of different sensor phenomena contribute to degraded compression performance compared with that expected for an ideal sensor. These effects may require variations of up to half a bit per pixel in the data rate required to maintain a particular signal-to-noise ratio, based on the results below. In order to explain those sensor properties which adversely affect compression, we first describe the two types of multispectral sensors which are most likely to be used for future satellite based gathering of earth resources data. They are the thematic mapper and high resolution pointable imager.

HRPI

The high resolution pointable imager (HRPI) is still in the planning stage. It is a so called push broom device. An array of photodiodes (4864 long in the Westinghouse proposed HRPI design) records one line perpendicular to the vehicle's path. Motion of the vehicle along its orbit makes possible the recording of succeeding lines. A prism assembly is used to separate incoming energy into four spectral bands, each band recorded with a unique array of sensors. For each image, the HRPI can be oriented vertically downward or at any angle between plus and minus 30° by use of an adjustable mirror aboard the spacecraft.

Thematic Mapper

The thematic mapper collects radiation in each of seven spectral bands by scanning the ground below the spacecraft. Using a system of optics, light entering the input port is fed to a set of photo sensors for each spectral band. Each set of sensors is laid out parallel to the vehicle's path. A mirror scans the earth in a direction perpendicular to the orbital path, producing succeeding image lines as the spacecraft moves in its orbit.

For each spectral band, a set of sensors laid out parallel to the vehicle's path allows sweeping out several lines simultaneously.

Sensor Effects Which Impact Compression

The factors which may affect compression performance can be explained based on the descriptions of the HRPI and thematic mapper. A list of the significant sensor effects is given in Table 7.5. The most critical factor is the variation in gain and bias of the various photodiodes. The photodiode nonuniformity has different consequences depending on the compression technique used. If predictive encoding is used, one can expect that the energy recorded at one photodiode will be less correlated with the energy recorded by the adjacent photodiode than it would be if sensor performance were uniform. Consequently, the error of prediction will have greater variance than for uniform sensors. This in turn implies poorer compressor performance. If transform coding is used instead of predictive coding, high frequency coefficients will tend to have greater energy than in the case of uniform sensors. This will cause the quantizer following the transform to be inefficient.

Table 7.5. Sensor Effects

- Photodiode nonuniformity
- Signal-to-noise ratio
- Radiometric nonlinearity
- Spectral misregistration
- Geometric distortion due to satellite attitude variations
- Geometric distortion due to scan pattern
- Data rate.

In performing a data compression study for NASA Goddard (NAS5-21746) on LANDSAT data, TRW encountered the effect of sensor nonuniformity. Band MSS5 of the LANDSAT multispectral scanner had one sensor which frequently performed quite differently than the other sensors. This caused every sixth line to differ significantly from its neighbor. Thus coding schemes which assumed approximately the same statistics for succeeding lines

suffered degraded performance. It is worth mentioning, however, that for information-preserving compression, a compression ratio of between 1.5 and 2 was still achievable.

Signal-to-noise ratio is an important parameter of a sensor because it determines the fineness with which the input signal should be quantized. The sensor noise and quantization error should be comparable in a well designed system (finer quantization is pointless because the small signal variations are lost in the noise and rougher quantization wastes the sensor's capabilities).

Spectral misregistration tends to reduce spectral correlation and consequently is another factor which may reduce the effectiveness of a data compression technique. The correlation is reduced because misregistration means that corresponding pixels from different spectral bands not only have spectral separation but have spatial separation as well.

The sensor scan pattern is an important source of distortion which may affect compression. Since the distance from the spacecraft to the ground in the vertical direction is shorter than the distance to the ground at an angle, the area on the ground corresponding to each pixel is not the same. In fact, the ground area corresponding to one recorded image line has the shape of a bow tie. Figure 7.14 demonstrates this phenomenon in a highly exaggerated fashion. This effect applies to both the thematic mapper and the HRPI since it depends on the varying distance from the spacecraft to the ground and not on the physical scanning mechanism. As previously noted, the photodiodes record one brightness value for each subarea indicated in Figure 7.14. The data compressor does not depend on the shapes of the subareas but rather on the correlation of the recorded brightness values. The correlation between values in succeeding lines will vary due to the overlapping of succeeding lines (see Figure 7.15).

Fluctuations in satellite attitude may also cause nonuniform distances between succeeding lines in both the thematic mapper and HRPI-produced imagery and within a line in thematic mapper imagery due to its scan.

Radiometric nonlinearity refers to the relation between the sensor's input and its output. If this function is nonlinear, the statistics of the output are not the same as those of the input and consequently the

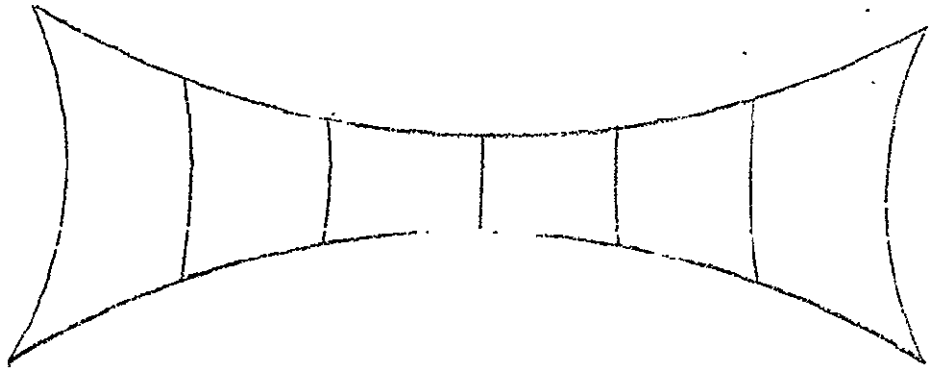

Figure 7.14. Bow Tie Pattern of Ground Area Scanned

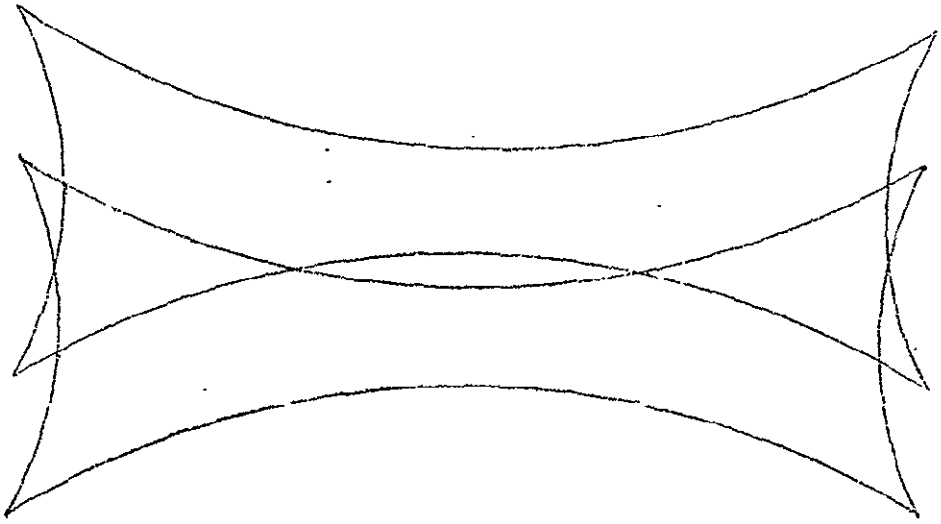

Figure 7.15. Overlap of Succeeding Lines

correlation of the output data sequence is not the same as that of the input sequence. This nonlinearity may not adversely affect compressor performance, however, since it may in fact increase the correlation between the values of the succeeding picture elements.

The data rate out of the sensor has an influence on achievable data compression because at high rates only a limited amount of time is available to perform computations and hence a limit exists on the number and kind of computations.

Relationship of Data Correlation to Compression

We now observe that all of the sensor effects we have described, except data rate, alter either the spatial or spectral correlation of the imagery. Most compression techniques take advantage of this correlation in one form or another since correlation is a good measure of the redundancy in a set of data.

In order to get some idea of the extent to which the various sensor phenomena affect compressor performance, we make several approximations and examine the performance of the optimum compressor of a monochrome image. We assume that such an image is the sample function of a two-dimensional Gaussian random process, $f(x,y)$. We further assume that the correlation function of this process is

$$E\,[f(x_1,y_1)\ f(x_2,y_2)] = k\,\rho^{|x_1-x_2| + |y_1-y_2|} \tag{7.36}$$

where k is a constant and ρ is the correlation coefficient of the process. A somewhat more appropriate assumption would be that

$$E\,[f(x_1,y_1)\ f(x_2,y_2)] = k\,\rho^{\sqrt{(x_1-x_2)^2 + (y_1-y_2)^2}}. \tag{7.37}$$

However, the form of (7.36) is considerably more convenient mathematically than (7.37) and can be expected to give comparable results. It can be shown, under the above assumptions, that the minimum required number of bits to maintain a specific signal-to-noise ratio given a fixed correlation coefficient is

$$\frac{1}{2}\log_2\left[(1-\rho^2)^2\,\frac{S}{N}\right]\ \text{bits/sample} \qquad (7.38)$$

For the thematic mapper and HRPI, we expect 8 bits per picture element and sensor noise to be approximately comparable in size to quantization error. Thus, the SNR of the data leaving the quantizer will be approximately

$$\frac{1}{3}(2^8-1)^2 \cong 2^{15} \qquad (7.39)$$

Hence, if the data were totally uncorrelated, $\frac{1}{2}\log_2 2^{15} = 7.5$ bits would be required to permit perfect reconstruction of the quantized sensor output. If the correlation coefficient is greater than zero, we see from (7.38) that we can reduce the number of bits required by $-\log_2(1-\rho^2)$ bits/sample.

The correlation coefficient for typical multispectral scanner imagery is approximately 0.9. (For the LANDSAT scene processed in this study, coefficients of 0.937, 0.938, 0.883, and 0.901 for MSS4, 5, 6 and 7 were measured.) If, for example, the sensor phenomena reduce the correlation by 10%, then, based on (7.38), 0.86 additional bits would be required to maintain a specific signal-to-noise ratio.

Up to now, the figures we have mentioned have been based on the required rate for the optimal compressor. This curve is closely approached by both transform and predictive techniques. Hence, results similar to those given can be expected to apply. In addition, these results have assumed knowledge of the correlation coefficient. In practice this coefficient will be unavailable. Since transform techniques are less dependent on exact knowledge of the correlation coefficient than predictive techniques, we can expect performance of transform techniques to be less subject to sensor phenomena.

Correlation Reduction Due to Sensor Effects

Based on the EOS System Definition Study performed by TRW for NASA under contract NAS5-20519, the relative radiometric accuracy from cell to cell and band to band will be within 1% for both instruments. This would imply that sensor gain and bias effects as well as sensor nonlinearity would alter the correlation coefficient less than 1%. Spectral registration for the devices is expected to be within one tenth of a picture element.

For a correlation coefficient of 0.9, this means a potential change of $1 - 0.9^{1/10}$ or approximately 1%.

The remaining significant factor in evaluating sensor-caused reduction in the correlation coefficient is related to the bow tie scan phenomenon mentioned earlier. Due to this effect, the ground area represented by thematic mapper pixels may vary by 1.1% and by HRPI pixels by 29%. The HRPI may have such large variations since it can be pointed 30% from the nadir. A 1.1% variation in area should have a negligible effect on the correlation coefficient. To get an approximation to the variation in correlation coefficient for the HRPI, due to the bow tie pattern, we compare the correlation between two adjacent squares directly below the sensor and at 30° from the vertical, the HRPI's range. If we define the ground area directly below the sensor corresponding to one pixel to be of size one, we obtain for the correlation of two adjacent pixels

$$\rho = E \int_0^{\frac{1}{\cos\theta}} \int_0^{\frac{1}{\cos\theta}} f(x,y)\,dx\,dy \int_{\frac{1}{\cos\theta}}^{\frac{2}{\cos\theta}} \int_0^{\frac{1}{\cos\theta}} f(x,y)\,dx\,dy \cos^4\theta \qquad (7.39)$$

where $f(x,y)$ is the energy of the radiation emanating vertically from the ground, and θ is the off-nadir angle of view of the sensor. If we assume that the correlation function of f can be roughly approximated by a separable exponentially decaying function, we obtain

$$\rho = \cos^4\theta \int_{\frac{1}{\cos\theta}}^{\frac{2}{\cos\theta}} \int_0^{\frac{1}{\cos\theta}} \int_0^{\frac{1}{\cos\theta}} \int_0^{\frac{1}{\cos\theta}} e^{-\alpha[|x-\gamma| + |y-\mu|]}\,dx\,d\nu\,dy\,d\mu \qquad (7.40)$$

Solving this integral we obtain

$$\rho = \frac{2}{\alpha}\cos^4\theta\left[\frac{1}{\cos\theta} - \frac{e^{-\alpha/\cos\theta} - 1}{\alpha}\right]\left[\frac{e^{\alpha/\cos\theta} - 1}{\alpha}\right]\left[\frac{e^{-\alpha/\cos\theta} - e^{-2\alpha/\cos\theta}}{\alpha}\right] \qquad (7.41)$$

We can use (7.41) to get an idea of the variation of the correlation coefficient with θ. Suppose that when θ equals 0, ρ equals 0.9. This value is close to that obtained in typical ERTS imagery. We then find $e^{-\alpha}$ using numerical techniques to be 0.924.

Substituting a value for θ of 30° into (7.41) we obtain

$$\rho = 0.886 \tag{7.42}$$

Thus a variation in ρ of about 1.5% may be expected as one goes from θ equals 0° to θ equals 30°.

Thus for the two devices, we expect between 2 and 5% variation in correlation coefficient due to sensor phenomena. This results in a variation of less than half a bit/sample in the rate required to maintain a specific SNR.

7.3.2 Implementation Complexity for Compression Techniques

This section discusses the complexity of implementing the various compression techniques in terms of their storage requirements (number of bits) and computational requirements (number of adds, subtracts, multiples). For each candidate method, we indicate the approximate storage requirement as well as the number of computations needed as a function of the parameters of the compression techniques. Then we give a typical value for these parameters for each compression technique. These numbers are for the encoders in their most general and optimal form. In practice one can reduce the complexity of these systems significantly by designing them in a slightly suboptimal fashion. Experiments with similar bandwidth compression algorithms has shown that significant design simplification results when one uses slightly suboptimal procedures.

The results are described below and summarized in Table 7.5. Some detailed preliminary costing derivations are contained in Appendix B. Throughout this section it is assumed that the parameters of the technique will be chosen so that the various fast transforms will have a size which is a power of 2. The numbers identifying the compression techniques are those listed in Table 7.6.

Table 7.6. Computational and Storage Needs for Compression Techniques

COMPRESSION TECHNIQUES	COMPUTATIONAL NEEDS		STORAGE NEEDS (BITS)	
	ADDS (OR SUBTRACTS)/PIXEL	MULTIPLIES/PIXEL	RECORD STORAGE	MEMORY
	TYPICAL	TYPICAL	TYPICAL	TYPICAL
1. 3-Dimensional Fourier Transform and Block Quantization	$1.5\log_2 B^2S+2.5$	$\log_2 B^2S+2$	$16BSW$	$44B^2S+16B+8000$
	17.5	12	3,300,000	545,000
2. 3-Dimensional Hadamard Transform and Block Quantization	$\log_2 B^2S+T$	1	$16BSW$	$44B^2S+8000$
	11	0	3,300,000	54,000
3. 3-Dimensional Slant Transform and Block Quantization	$\log_2 B^2S+\frac{3}{2}-\frac{4}{B}-\frac{2}{S}+T$	$7-\frac{8}{B}-\frac{4}{S}$	$16BSW$	$44B^2S+64\log_2 B+8000$
	12	6	3,200,000	54,000
4. 3-Dimensional Cosine Transform and Block Quantization	$3\log_2(B-1)^{2(1-\frac{1}{B})(S-1)(1-\frac{1}{S})}$ $+7.5-\frac{5.5}{S}+\frac{1}{B}+T$	$2\log_2(B-1)^{2(1-\frac{1}{B})(S-1)(1-\frac{1}{S})}$ $+7-\frac{8}{B}-\frac{4}{S}$	$16BSW$	$76B^2S+32B+8000$
	34	24	4,300,000	119,000
5. Karhunen-Loeve Transform in the Spectral Domain followed by 2-Dimensional Fourier Transform on the spatial domain followed by Block Quantization	$1.5\log_2 B^2+S+T+1.5$	$\log_2 B^2+S+1$	$16BSW$	$32B^2+4B^2S$
	17.5	13	3,200,000	12,000
6. 2-Dimensional Hadamard Transform in the spatial domain followed by a DPCM encoder in the spectral domain	$\log_2 B^2+T+1$	1	$16BSW$	$108B^2+8000$
	10	1	3,300,000	36,000
7. 2-Dimensional Cosine Transform in the spatial domain followed by a DPCM encoder in the spectral domain	$3\log_2(B-1)^{2(1-\frac{1}{B})}+6+\frac{1}{B}+T$	$2\log_2(B-1)^{2(1-\frac{1}{B})}$ $+6-\frac{8}{B}$	$16BSW$	$140B^2-32B+8000$
	30	21	44,400000	28,000
8. 1-Dimensional Karhunen-Loeve Transform on the spectral domain followed by 2-Dimensional DPCM	$S+T+3$	$S+4$	$16SW$	$16S^2+148S+8000$
	8	8	200,000	9,000
10. Karhuner-Loeve Transform on the spectral domain followed by a Hadamand Transform in the scan direction (x-direction) with y-direction DPCM using block quantization.	$\log_2 B+S+T+1$	$S+2$	$32SW$	$84BS+32B+32S(S+1)+8000$
	14	6	400,000	15,000
11. Karhuner-Loeve Transform on the spectral domain followed by a Cosine Transform in the scan direction (x-direction) with y-direction DPCM using block quantization.	$3\log_2(B-1)^{(1-\frac{1}{B})}+S+T+3.5-\frac{1}{2B}$	$2\log_2(B-1)^{(1-\frac{1}{B})}+S+4-\frac{4}{B}$	$32SW$	$116BS+64B+32S(S-1)+8000$
	20	16	400,000	18,000

Three-Dimensional Transform Coding Techniques

Three-dimensional transform coding methods, listed as compression methods 1 through 4 in Table 7.6, differ in the type of the basis functions they use to transform the data. Slant and Hadamard transforms use basis matrices that are largely 1 and -1, thus the need for storing the basic matrices and the multipliers is eliminated. However, Cosine and Fourier transforms require storing the basic matrices and multipliers. Therefore the storage and the computational requirements for these methods are different.

A typical LANDSAT picture has 2400 x 3200 spatial points by four spectral bands, with 7 bits representing each sample in the first 3 and 6 samples on the 4^{th} band. We will compress the bandwidth of the picture to an average of T bits/pixel. First the picture is divided into blocks of size B x B x S. (B = 16 has previously been found reasonable.) We will consider a block size of 16 x 16 x 4 to be a typical block size. Let each block be identified by indices ℓ, m, i, j, and k where ℓ and m index the blocks in the vertical and horizontal directions respectively. i and j index the elements within each block in vertical and horizontal directions respectively. k indexes the spectral bands. Then the number of Fourier coefficients in each block is B^2S samples. These samples are referred to as $C_m(i,j,k)$ where $1 \leq I \leq B$, $1 \leq J \leq B$, $1 \leq K \leq S$. We could combine the I, J, K into one index IX so that we can think of the coefficients as a vector $C_{\ell,m}(IX)$; $IX = 1,\ldots,B^2S$. Leaving out the coefficients that are redundant because of symmetry, we end up with B^2S real coefficients. Now for $IX=1,\ldots,B^2S$, C(IX) is transmitted using a predetermined number R(IX) of binary digits. (R(IX) may be zero for some values of IX.) The numbers R(IX) have been chosen so that for an average bit rate "T", the expected distortion is minimized. The strategy is based on the fact that most of the transform coefficients tend to concentrate in a relatively small number of spectral coeffients to which most of the available binary digits are assigned.

Implementation. Collect and store (record, etc.) 16 scan lines of picture at 8 bits/pixel. After 16 lines, we start processing while simultaneously storing the next 16 lines.

Processing. For each block, compute the three-dimensional transform by taking three one-dimensional transforms in the horizontal, vertical, and spectral directions. When we transform real sequences, the result has conjugate symmetry and we need only calculate the transform for about half the spectrum. Using the symmetry, we find we can represent the results with B^2S real numbers $C_m(IX)$.

Accuracy. Note that $|C_{\ell m}(IX)|$ is less than or equal to

$$\sum_{i,j,k} |B_{\ell m}(i,j,k)|$$

$B_{\ell m}(i,j,k)$ refers to the gray level of pixel specified by indices ℓ,m,i,j,k, and could achieve this bound; furthermore, B^2S typically equals $16^2(4)$ $\approx$ 1000, so $|C_{\ell m}(IX)|$ could be as big as 1000 $\max|B_{\ell m}(i,j,k)|$, but more typical would be $\sqrt{1000}$ $\max|B_{\ell m}(i,j,k)|$. If we scale to avoid losing the most significant bits, then many of the coefficients will be a factor of 30 or more (= 5 bits worth) smaller than max. We want 8-bit reconstructed results, which experience has shown requires sending some coefficients with 10-bit accuracy; so we need a minimum of 16 bits computational accuracy.

After calculating the transform coefficients $C_{\ell m}(IX)$ for each block, we proceed with:

- Multiply each coefficient by prespecified scale factors SC(IX)
- Pass the result through some nonlinear function FQ implemented using a table look up algorithm (see Appendix B)
- Quantize each coefficient using a prespecified number of bits R(IX).

Storage Requirements. The storage requirements for a three-dimensional transform coder can be calculated by considering the storage requirements for three successive operations. These are storage requirements at the input prior to transformation, storage requirements for storing the transform coefficients, and the transform basis vectors (for Fourier and Cosine transforms), and finally the storage requirements for performing block quantization of the transform coefficients.

To store 2B lines of the original samples with an accuracy of 8 bits/pixel, we need 16BWS binary digits. This has to be done prior to any processing. A typical value for this expression is 3,300,000 bits or about 200K minicomputer words (for B = 16, S = 4, and W = 3200). This demands a rather large storage device. A disk or a drum must be utilized to store these samples. For an on-board processor, charge-coupled devices can be used to meet this storage requirement.

The storage requirement for storing the transform coefficients is approximately B^2S words of 32 bits/word for each block of B^2 samples. An additional B/2 words are also needed to store the transform basis vectors for Fourier and Cosine transform. This requires a total of $32B^2S+16B$ bits of storage to perform the transform and store the coefficients. A typical value for this expression is 33,000 words.

For block quantization, B^2S words are needed at 4 bits/word to store R(IX) numbers. Another B^2S words at 8 bits/word are needed to store scaling coefficients. 2^9 words at 16 bits/word are needed to store half of 2^{10} values of the function FQ^{-1} with 16 bits of accuracy. Since FQ is monotone, we evaluate it with a binary search on FQ^{-1}. It is also symmetric so we need only half the table. This makes the total equal to $12B^2S + 2^{13}$ bits. For a typical case (i.e., B = 16, S = 4) we need 20,000K bits of memory to perform operation of block quantization.

There will be additional storage requirements for the program and for storing the transform coefficients; however, this is relatively small. We will not attempt to estimate this factor.

Computational Complexity. See Appendix B for outline giving the transform processing cost. Our cost is the transform cost + (1 multiply/pixel and T adds/pixel) to do the block quantization.

Depending on the nature of the hardware, there will be additional costs associated with indexing, looping, fetching, and storing from the computer input/output bit manipulation operation. This computation and overhead will be highly dependent on the nature of the hardware and the degree to which it is specialized to the task at hand. We will not attempt to estimate it at this level of study.

The storage and the computational needs for the various three-dimensional transforms are listed in Table 7.6.

KL - Two-Dimentional Fourier Transform

Implementation. As the data comes in, we transform along the spectral coordinate by a predetermined transformation. For four spectral bands, each sample in multispectral imagery is multiplied by a given 4 x 4 matrix. Then, the resulting coefficients are stored for 16 scan lines before we process the blocks (as explained below) while the next 16 scan lines are being stored.

Processing. For each spectral band, the BxB sample array is Fourier transformed just as indicated in 3-dimensional transforms except there is no transformation over the S direction in this case. Then we get S sets of B^2 Fourier coefficients/block of data. For each block these B^2S coefficients are quantized with specified accuracy and are transmitted.

Storage Requirements. The storage requirements consist of storing the input, the transform coefficients, and the transform basis functions, and finally the storage needs for performing the block quantization.

These requirements are 8BWS bits for storing 2B lines of the imagery data, using 8 bits per sample (a typical value is 1,600,000 bits). Approximately $B^2+\frac{B}{2}$ words of 32 bits/word are required to store Fourier coefficients. This is equal to $32B^2+16B$ bits. The block quantizer employed with this technique is identical to the block quantizer used with technique 1. Thus, it requires $12B^2S+8,000$ bits of storage to perform the operation of block quantization.

Computational Complexity. The computational complexity of this method is calculated using a procedure identical to the one employed in technique 1. The results are shown in Table 7.6.

Two-Dimensional Hadamard/DPCM Encoder

As for technique 1 the imagery is divided into blocks of BxBxS samples. For each block a two-dimensional Hadamard transform is taken. Then an array of differential signals along the spectral direction is generated using the transformed components. These signals are quantized using a bank of quantizers and are transmitted. The system is an extension of the hybrid encoder.

Implementation. The processing begins by taking the two-dimensional Hadamard transform of blocks of B^2 samples. Using the transformed blocks of data a corresponding differential signal is generated. The elements of the transform domain along with the differential signals are quantized and transmitted. The quantization procedure is similar to that of technique 1.

Storage Requirements. The storage requirements for this technique are as follows:

(1) For storing 2B lines of picture 16BSW bits of memory are needed (a typical value of 3,300,000 bits).

(2) For the Hadamard transform B^2 words of memory at 32 bits/word are needed.

(3) For the block of DPCM encoders B^2 words at 32 bits/word are needed.

(4) For the block quantizer B^2 words at 4 bits/word are needed for storing the bit-assignment table, B^2 words at 8 bits/word for storing scaling coefficients, and B^2 words at 32 bits/word for storing DPCM gians and as in technique 1 about 8,000 bits for the table used with a nonlinear quantizer. This requires a total of $44B^2+8,000$ bits of storage. A typical value for this number is 20,000 bits.

Computational Complexity. This method requires $\log_2 B^2$ adds/pixel for the Hadamard transform + (1 add/pixel and 1 multiply/pixel) for the DPCM + (T adds/pixel and 1 multiply/pixel) for the block quantization. A summary of the number of computations needed for this technique is given in Table 7.6.

Two-Dimensional Cosine/DPCM Encoder

Implementation. Like technique 6, except that we use the Cosine transform instead of the Hadamard transform.

Storage Requirements. The storage requirements for this technique are as follows:

(1) For storing 2B lines of S bands at 8 bits per sample 16SW bits of memory are required. This gives a typical number of 3,300,000 bits for S = 4, W = 3200, and B = 16.

(2) The Cosine transform requires 2B(B-1) words of memory. Storage of Cosine basis vectors requires an additional (B-1) words of memory. Using 32 bits/word this requires a total of $64B^2-32B-32$ bits of memory.

(3) The DPCM encoders require B^2 words at 32 bits/words for storing a BxB block of sample from the previously processed band of the multispectral imagery.

(4) Similar to technique 6 a total of $44B^2+8000$ bits are required for the operation of block quantization.

Computational Complexity. This method requires $(1 - \frac{1}{B})\ [3\log_2(B-1)^2 + 5 + \frac{6}{B-1}\ ]$ adds and $(1 - \frac{1}{B})\ [2\log_2(B-1)^2 + 4 - \frac{4}{B-1}] + 1$ multiplies for two-dimensional cosine transform of a block of BxB samples. Each DPCM encoder requires 1 add and 1 multiply operation and the block quantizer requires (T adds and 1 multiply)/pixel. The total number of operations is shown in Table 7.6.

KL Transform — Two-Dimensional DPCM Encoder

Implementation. In this method the incoming data is first transformed in the spectral domain using a SxS KL matrix. The transformed coefficients are stored. One line of each transformed band needs to be stored before one can proceed with a two-dimensional DPCM coding of these bands.

Storage Requirements. The storage requirements for this technique are as follows:

(1) WS words of 16 bits/word for storing one line of each band. This is assuming that 16 bits/word are sufficient for the storage of the KL components. This requires a total of 16WS bits of digital memory.

(2) S^2 words of 16 bits/word are required for storing the KL transform matrix. S words of 16 bits/word are required to keep the KL transform before or after the transformation.

(3) 35 words are required for storing the coefficients used in the feedback loop of the DPCM encoder. This requires 16 bits/word accuracy.

(4) An additional S words at 4 bits/word are needed to store the bit assignment table (bits/pixel used). S words at 16 bits/word are needed for storing the scaling parameters and as in technique 1 about 8000 bits are required for storing the function FS.

Computational Complexity. The computational complexity for this technique consists of (S adds and S multiples)/pixel for the KL transform, (3 adds and 3 multiplies)/pixel for DPCM and (T adds and 1 multiply)/pixel for the quantization. The total number of required computations is shown in Table 7.6.

KL — Hadamard Transform/DPCM Encoder

The scan direction is divided into segments of length B samples for Hadamard transforming. The quantizers use a different number of quantization levels which varies with spectral band and position within the Hadamard transform results, but does not vary from line to line or from segment to segment.

Implementation. In this method the incoming data is first transformed in the spectral domain using an SxS KL matrix. Blocks of length B of the transformed components are then formed. Each block of B samples is Hadamard transformed. One line of the transformed data is required prior to DPCM processing. Note that a block of B DPCM systems are required for the encoder in its most general form.

Storage Requirements. The storage requirements for this technique are as follows:

(1) Storing incoming data requires BS words of memory at 8 bits/word.

(2) S^2 words of 16 bits/word are required for storing the KL transform matrix. S words of 16 bits/word are required to store the KL transform. Additional BS words at 32 bits/word are needed to store the BS elements of the segment being KL and Hadamard transformed.

(3) BS words at 32 bits/word are needed to store the previously transformed segments which are required for the DPCM encoder. We also need B words at 32 bits/word to store the starting value for the DPCM encoder.

(4) The block quantizer requires BS words at 4 bits/word to store the bit assignment rule, and BS words at 8 bits/word to store the scaling coefficients and an additional 8000 bits of memory to store the function FQ.

Computational Complexity

The number of computations required for this technique is summarized in Table 7.6.

KL — Cosine Transform/DPCM Encoder

Implementation. In this method the incoming data is first transformed in the spectral domain using a SxS KL matrix. Blocks of length B of the transformed components are then formed. Each block of B samples is Cosine

transformed. One line of the transformed data is required prior to DPCM processing. Note that a block of B DPCM systems is required for the encoder in its most general form.

Storage Requirements. The storage requirements for this technique are as follows:

(1) Storing incoming data requires BS words of memory at 8 bits/word.

(2) S^2 words of 16 bits/word are required for storing the KL transform matrix. S words of 16 bits/word are required to store the KL transform. An additional 2 BS words at 32 bits/word are needed to store the BS elements of the segment being KL and Cosine transformed. We also need (B-1) words at 32 bits/word to store Cosine basis vectors.

(3) BS words at 32 bits/word are needed to store the previously transformed segments which are required for the DPCM encoder. We also need B words at 32 bits/word to store the starting value for the DPCM encoder.

(4) The block quantizer requires BS words at 4 bits/word to store $R(i_x,k)$ and BS words at 8 bits/word to store the scaling coefficients $SC(i_x,k)$ and an additional 8000 bits of memory to store the function FQ.

Computational Complexity. The number of computations required for this technique is summarized in Table 7.6.

8. SELECTION OF THE RECOMMENDED TECHNIQUES

The performance of the candidate bandwidth compression techniques listed in Section 5.5 were evaluated and compared in Section 7 using analytical and simulation results, as well as system considerations. In this section we examine these techniques and utilize the results of Section 7 to recommend three bandwidth compression techniques.

8.1 THREE-DIMENSIONAL TRANSFORMS

Three-dimensional transforms and three-dimensional mixed transforms were not selected as recommended bandwidth compression techniques for the following reasons.

- The spectral correlation of the MSS data, in particular the LANDSAT data, is not exponential. In this sense it is different from the spatial correlation of this data. Thus, the unitary transforms which approximate the performance of the KL transform for data with exponential correlations do not perform as well in the spectral domain. For this reason the performance of the three-dimensional transform coding methods are not as good as other candidate methods.

- The mixed transform techniques that use the KL transform in the spectral domain do not have the above shortcoming. In this sense they perform better than the three-dimensional transform techniques. However, two candidate techniques listed in this category (KL-2D Fourier and KL-2D Hadamard) follow the spectral KL transform with two-dimensional Hadamard or Fourier transforms. The result is not as good as one would obtain if the spectral transformation is followed with a hybrid encoder (transform-DPCM). This point has been shown in Section 7 by both analytical and simulation results. In addition, the implementational complexity of the hybrid encoder (transform-DPCM) is significantly less than the corresponding two-dimensional transforms.

8.2 TWO-DIMENSIONAL TRANSFORM/DPCM SYSTEMS

Both methods in the category of two-dimensional spatial transforms with DPCM coding in the spectral domain were rejected for the following reasons:

- The spectral correlation of the MSS data is not exponential. Thus it cannot be encoded with DPCM systems very efficiently.

- The number of spectral bands in the MSS data is small. This does not allow the DPCM encoder to reach its steady state mode of operation. Also the performance of DPCM systems in the transition state is very inefficient. As a result, the performance of the techniques that use a combination of two-dimensional transform with DPCM encoders is not as good as the other candidate techniques. It is worth mentioning that other studies [146] have shown that this method surpasses the performance of the three-dimensional transform techniques for compressing the bandwidth of television data.

8.3 RECOMMENDED BANDWIDTH COMPRESSION TECHNIQUES

The following bandwidth compression techniques perform best and were selected as the recommended techniques of this study. These are:

- KL transform in the spectral domain followed by a Cosine transformation/DPCM
- KL transform in the spectral domain followed by a two-dimensional DPCM
- Cluster Coding technique using Swain-Fu measure for clustering MSS data.

These techniques are further analyzed and compared in Section 9.

9. COMPARISON OF THE RECOMMENDED TECHNIQUES

The selected bandwidth compression techniques were narrowed down to three candidate bandwidth compression methods as discussed in Section 5. In this section the three candidate methods are discussed based on various criteria of optimality such as mean square error, signal-to-noise ratio, recognition accuracy as well as the subjective quality of the reconstructed imagery. In addition the following discussion will answer a number of questions about the recommended bandwidth compression methods. These are:

- The reduction in the bit rate caused by concatenation of the bandwidth compression algorithms with the entropy coding methods such as a Huffman encoder.
- Most of the experimental results reported in this study relate to the 4-channel spectral data of LANDSAT imagery. The simulation studies are intended to evaluate the performance of the finally selected coding algorithms for multispectral data with a larger number of channels. Results relevant to 12-channel aircraft data are reported and are compared with the results obtained using LANDSAT imagery.

9.1 COMPARISON OF THE RECOMMENDED TECHNIQUES BASED ON MSE AND SIGNAL-TO-NOISE RATIO

Figure 9.1 shows the performance of the three-dimensional hybrid encoder using KL-Cosine transforms with the DPCM encoder in comparison with the other two recommended bandwidth compression systems using MSE as the criterion of optimality. One is the system that follows the Karhunen-Loeve Transform in the spectral domain with a two-dimensional DPCM encoder. The other is the cluster coding technique. The cluster coding system uses a fixed number of clusters in each block of 16 by 16 samples. In this sense it is a fixed bit-rate system. It is shown that the performance of the encoder using KL transformation followed by a two-dimensional DPCM encoder performs significantly worse than the hybrid encoder (KL-Cosine-DPCM) at low bit rates. However, their performance is rather similar at higher bit rates (about 2 bits per sample per band). The performance of the cluster coding algorithms is superior to that of the hybrid encoder at low bit rates. However, it gives inferior results at high bit rates. In this aspect, its performance is completely opposite to that of the KL-2 Dimensional DPCM encoder.

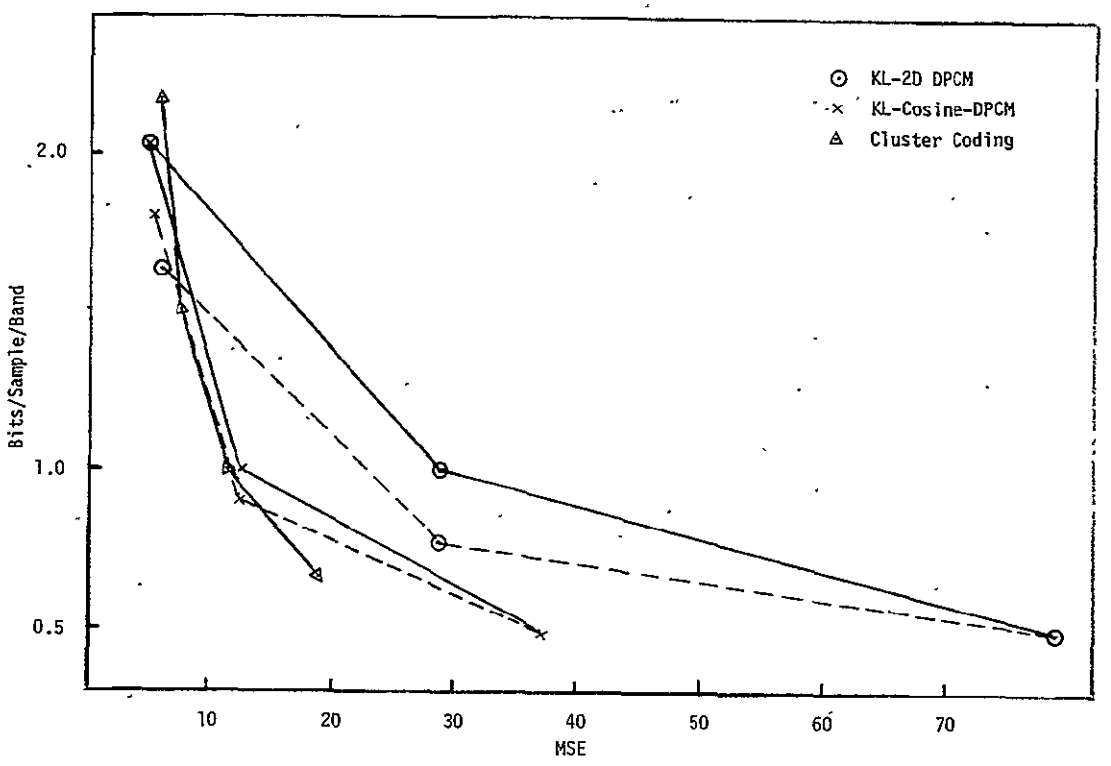

Figure 9.1. Bit Rate vs MSE for KL-2D DPCM, KL-Cosine-DPCM, and Cluster Coding Methods. Dashed lines refer to variable Bit Rate.

Figure 9-1 also shows the performance of the hybrid (KL-Cosine-DPCM) and KL-2 Dimensional DPCM encoders in concatenation with a variable rate encoder. The variable rate encoder is the Huffman encoder which reduces the output bit rate by assigning shorter-length words to more probable output levels and longer words to less probable output levels. Addition of the variable rate entropy coding systems reduces the bit rate for both bandwidth compression methods without affecting the coding degradation. The effect of entropy coding on the performance of the KL-Cosine-DPCM encoder is less than its effect on the performance of the KL-2 Dimensional DPCM System. The KL-Cosine-DPCM System uses a bank of DPCM modulators whereas the KL-2 Dimensional System uses a single DPCM modulator. Using a number of DPCM modulators increases the total number of output symbols, thus reducing the number of times each symbol occurs. This reduces the effectiveness of the variable-length encoder in reducing the output bit rate. As a result, the performance of the KL-2 Dimensional DPCM System improves an average of 25% while the performance of the KL-Cosine-DPCM System improves only about 10%.

The performance of the above two bandwidth compression systems does not change significantly by substituting the Haar transform for the KL transform for spectral transformation or by substituting the Hadamard or Slant transform for the Cosine transform for spatial transformation. The software delivered to NASA Ames Research Center and Marshall Space Flight Center has an option for making these substitutions in a variety of ways (see Appendix E).

Figure 9.2 shows the performance of the two systems using a peak-to-peak signal-to-noise ratio. As discussed in Section 9.2, this criterion is a normalized form for the MSE. Thus the comparative performance of the above systems using this criteria is exactly the same as it is using MSE. The only advantage of this criterion is that it includes a peak-to-peak signal value in addition to MSE. This value is widely used in evaluating television signal quality.

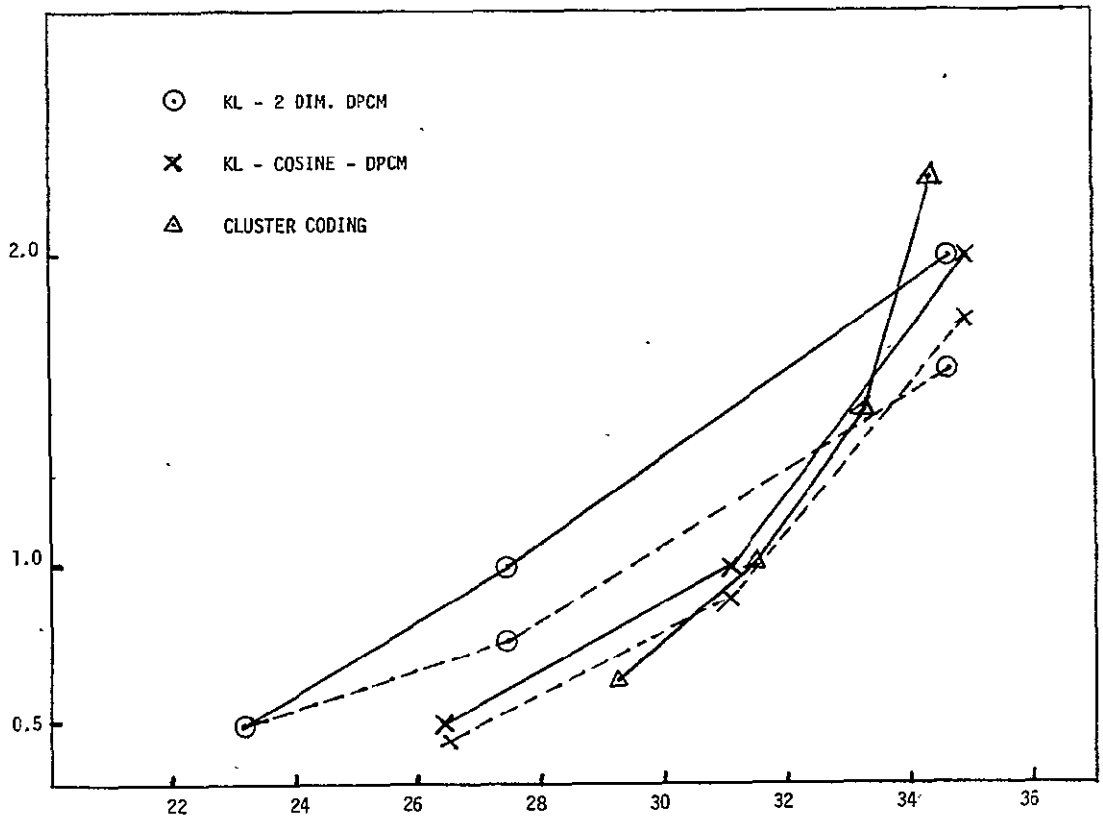

Figure 9.2. Bit Rate vs Signal-to-Noise Ratio for KL-2 Dim. DPCM, KL-Cosine-DPCM, and Cluster Coding

9.2 COMPARISON OF THE RECOMMENDED TECHNIQUES BASED ON RECOGNITION ACCURACY

Figure 9.3 shows the performance of the three recommended bandwidth compression methods using as the criterion of optimality "preserving the classification accuracy of the reconstructed multispectral LANDSAT imagery." Using this criterion, the comparative performance of the KL-2 Dimensional DPCM System and KL-Cosine-DPCM System is basically the same as it was for using signal-to-noise ratio as the criterion of optimality. This shows a strong correlation between the signal-to-noise ratio (or equivalently mean square error) and the classification accuracy. This is further illustrated in Figure 9.4. Figure 9.3 also shows the performance of the cluster coding algorithm measured in terms of classification inaccuracy. The classification accuracy actually decreases as a result of increasing the number of clusters in each block up to 16 clusters per block. Then the classification accuracy increases sharply when 32 clusters per block are allowed. This behavior is due to the fact that the cluster coding algorithm is using a classification procedure on blocks of 16 by 16 samples where classification accuracy is measured using a classification procedure on blocks of 256 by 256 samples. Actually a 64 by 64 sub-sample of 256 by 256 samples is used in the classification procedure. Of course, a classification accuracy of 100% results if the block size for measuring the classification accuracy and the block size in cluster coding methods are the same. The reason for keeping the block size in the cluster coding method small is the complexity of the clustering algorithms. The complexity of the system in terms of memory and the speed of processing increases rapidly for larger block sizes. A larger block size also requires allowing for a larger number of clusters for high fidelity. This further increases the complexity of the cluster coding algorithm. Considering the fact that the system is already complex* for small block sizes, it is inconceivable to envision cluster coding systems that use block sizes much larger than 16 by 16. The argument for using large block sizes in classifying multispectral data is not very solid. This depends very much on the users and applications of LANDSAT imagery. However, classifying LANDSAT imagery using large block sizes has many attractive

*The cluster coding system reported in this study requires about 20 minutes of a PDP-85 computer time for bandwidth compression of 4 channels of 256 by 256 LANDSAT imagery using a block size of 16 by 16.

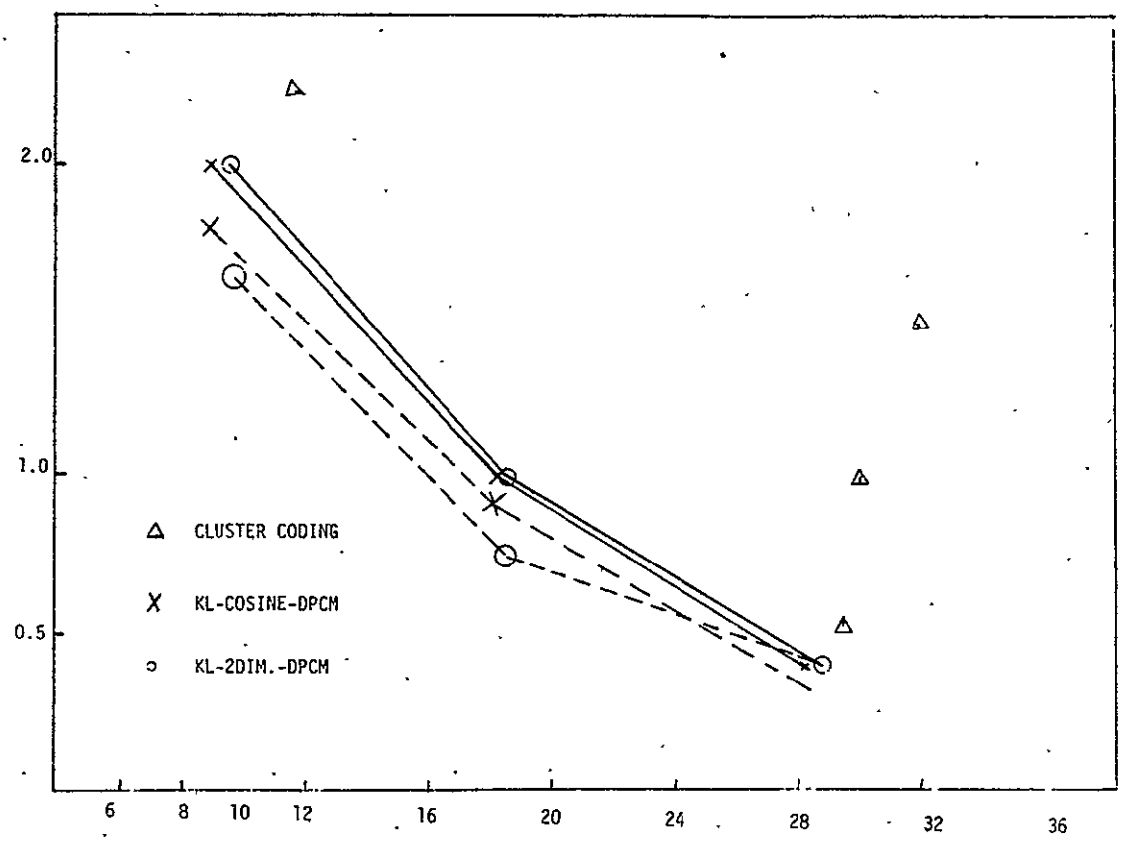

Figure 9.3. Bit Rate vs Classification Inaccuracy

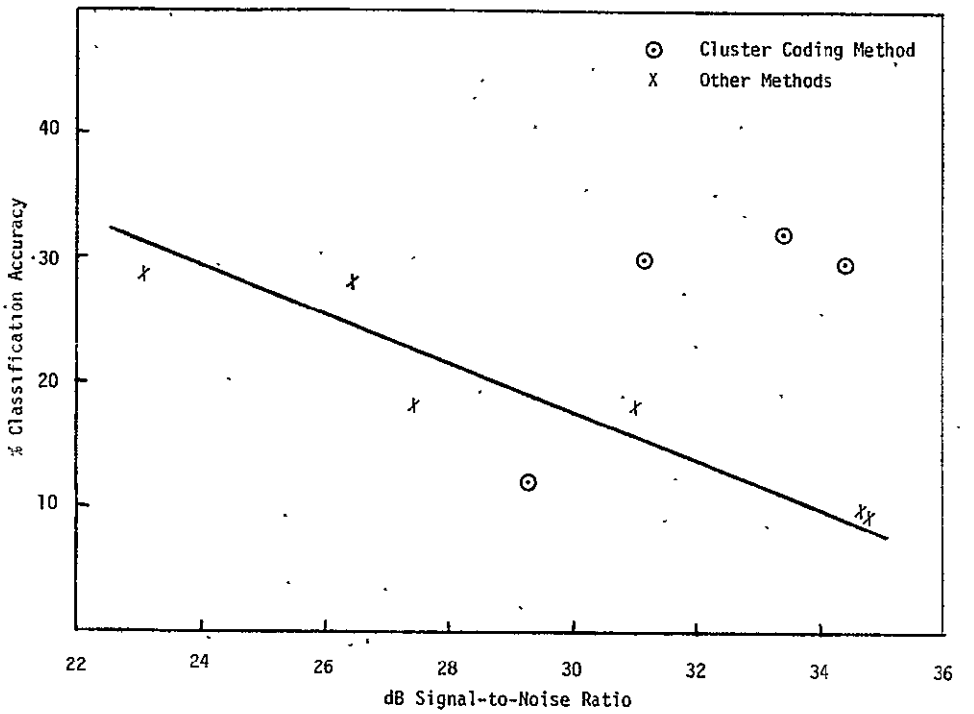

Figure 9.4. Signal-to-Noise Ratio vs Classification Accuracy for the Recommended Methods

features. Large block sizes are likely to be used in applications where one is only interested in a limited number of objects in the multispectral imagery such as in hydrology and urban planning where one is interested in classifying the imagery using a large segment of the imagery. For this application the imagery obtained using a cluster coding algorithm has a rather poor classification accuracy compared to the other two recommended bandwidth compression algorithms.

Figure 9.4 shows two criteria of signal-to-noise ratio and the classification accuracy for the three bandwidth compression methods discussed. A strong correlation between the two criteria is displayed for KL-2 Dimensional DPCM and KL-Cosine-DPCM methods. A much smaller correlation exists between the two criteria for the cluster coding method. This is shown by scattered points indicated by circles.

9.3 COMPARISON OF THE RECOMMENDED TECHNIQUES BASED ON SYSTEM COMPLEXITY

The implementational complexity of the selected bandwidth compression techniques is discussed in Section 7.3.2. For recommended systems using KL-Cosine-DPCM and KL-2 Dimensional DPCM systems, this is shown on Table 9.1 in terms of the number of computations and memory per picture element. This table also shows typical numbers for 4 channel data and the block sizes used in simulating the compression methods. A detailed analysis of the complexity of the cluster coding method is not performed. But based on the computer time required for compressing the bandwidth of the representative ERTS data using this system and comparing it with the computer time required in simulating the KL-2 Dimensional DPCM encoder, it was concluded that the cluster coding algorithm is about one order of magnitude more complicated than the Haar-2 Dimensional DPCM encoder.

9.4 COMPARISON OF THE RECOMMENDED TECHNIQUES BASED ON CHANNEL NOISE AND SENSOR EFFECT

Figure 9.5 shows the reduction in the signal-to-noise ratio and the classification accuracy which is caused by introduction of a noisy channel. The results refer to a binary symmetric channel with bit-error rates ranging from 10^{-4} to 10^{-2}. A bit-error rate of 10^{-4} reduces the signal-to-noise ratio by less than 0.25 dB for the KL-2 Dimensional DPCM and KL-Cosine-DPCM encoder. Both algorithms degrade significantly at higher

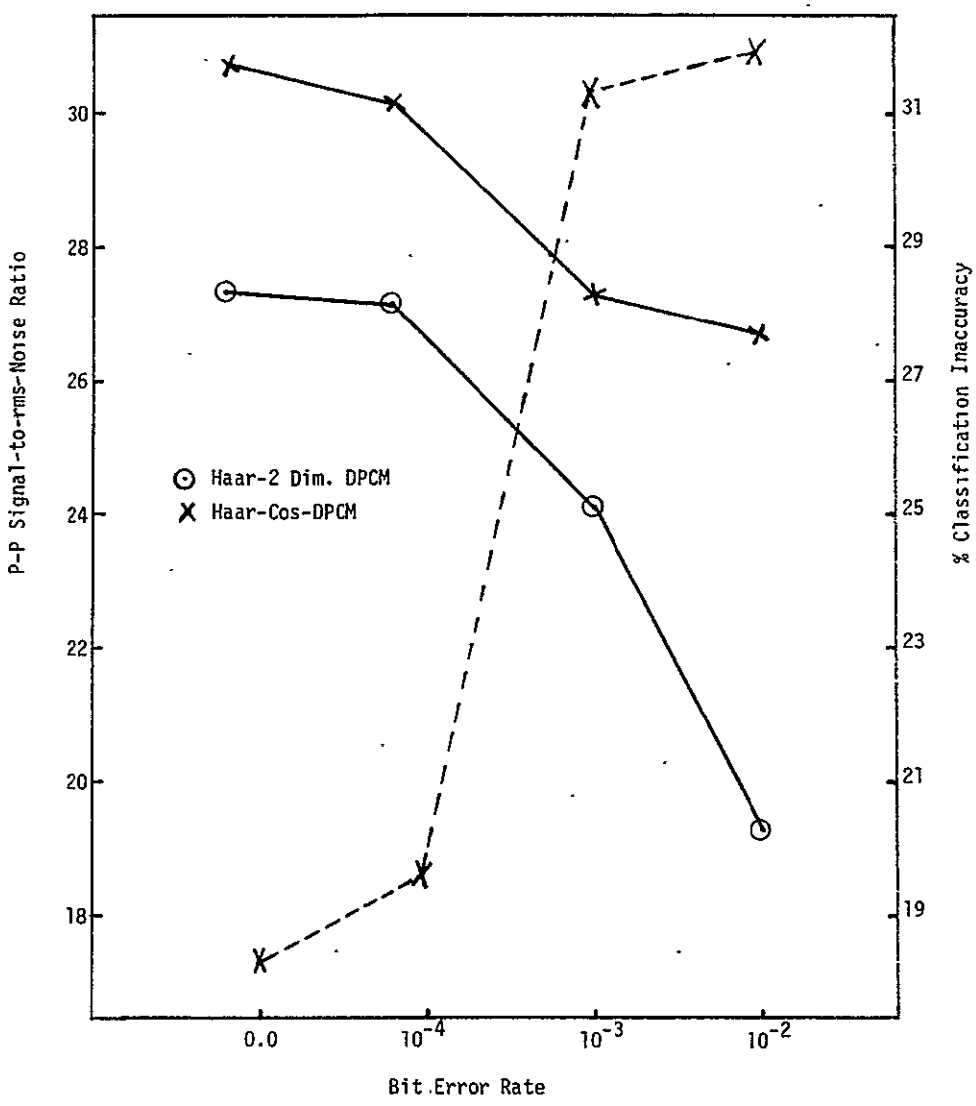

Figure 9.5. P-P Signal-to-Noise Ratio and Classification Inaccuracy (Dash Line) vs Bit Error Rate

Table 9.1. Summary of Computational and Storage Needs for 3D Hadamard, KL-2D DPCM, and KL-Hadamard-DPCM Methods

	COMPUTATIONAL NEEDS		STORAGE NEEDS (BITS	
	ADDS (OR SUBTRACTS)/ PIXEL	MULTIPLIES/ PIXEL	RECORD STORAGE	MEMORY
	TYPICAL	TYPICAL	TYPICAL	TYPICAL
2. 3-Dimensional Hadamard Transform and Block Quantization	Log_2B^2S+T	1	16BSW	$44B^2S+8000$
	11	1	3,300,000	54,000
8. 1-Dimensional Karhunen-Loeve Transform, on the spectral domain followed by 2-Dimensional DPCM	S+T+3	S+4	16SW	$16S^2+148S+8000$
	8	8	200,000	9,000
10. Karhuner-Loeve Transform on the spectral domain followed by a Hadamard Transform in the scan direction (x-direction) with y-direction DPCM using block quantization	$Log_2B+S+T+1$	S+2	32SW	84BS+32B+32S(S+1) +8000
	14	6	400,000	15,000

		TYPICAL
B,	Block size	B = 16
T,	Bits/pixel	T = 1
S;	Spectral Bands	S = 4
W;	Sample in each scan	W = 3200

bit-error rates. The system using the KL-2 Dimensional encoder degrades more significantly. Figure 9.6 shows the reconstructed form of band 3 of the ERTS data after bandwidth compression using the Haar-2 Dimensional DPCM encoder at bit error rates of 10^{-3} and 10^{-4}. The propagation of the channel error is clearly visible for a bit-error rate of 10^{-3}. However this is less significant than the effects of channel error for a simple two-dimensional DPCM system. This is because the recommended system using a Haar-2 Dimensional DPCM encoder utilizes the two-dimensional DPCM encoder in the spectral domain. The signal at the receiver of the two-dimensional DPCM system is then transformed by the inverse of the Haar transform to reconstruct the multispectral data. The total effect of the inverse Haar transform at the receiver is to distribute the channel error and its propagation among all spectral bands. Although this leaves the total error unchanged, it distributes the channel error among all spectral bands thus making it less objectionable to human vision.

BAND 3 - 1 BIT - HAAR - 2 DIM. DPCM

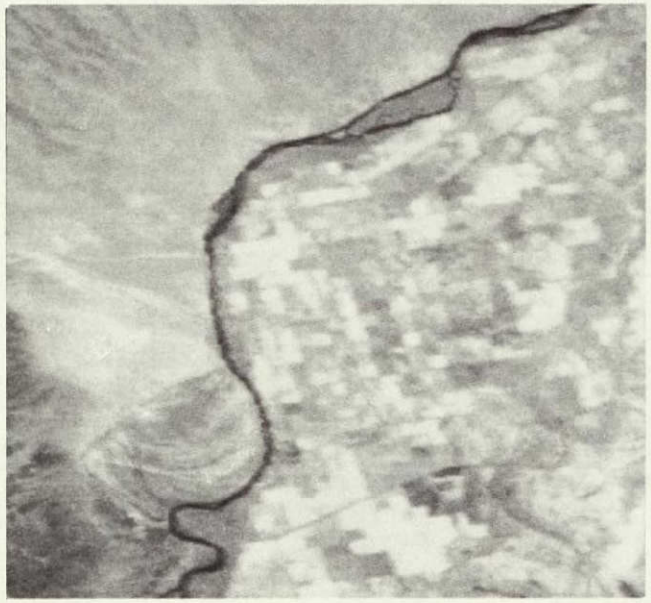

$P = 10^{-4}$

$P = 10^{-3}$

Figure 9.6

The sensor imperfections that affect the performance of bandwidth compression methods are discussed in Section 7.3.1. These imperfections affect the correlation of the data which in turn affects the performance of the candidate bandwidth compression techniques. The analytical results reported in Section 7.3.1 show that this effect is minimal and in general it favors the transform methods and the methods that rely less on an exact correlation of the data. For this reason it is expected that the sensor imperfections would have a smaller effect on the candidate method using a Haar-Cosine-DPCM encoder.

9.5 COMPARISON OF THE RECOMMENDED TECHNIQUES BASED ON SUBJECTIVE QUALITY OF RECONSTRUCTED IMAGERY

The simulation results reported in previous sections resulted in the reconstruction of a large number of images. The reconstructed images were displayed using a Dicomed color image recorder to generate hard copies. In addition, side by side comparison of reconstructed imagery was performed on a Comtal digital image displayer. These devices are discussed in Appendix D. Due to practical limiations, only a cross section of the reconstructed imagery is included in this report. A larger number of reconstructed images was supplied to NASA Ames Research Center as well as Marshall Space Flight Center and NASA Headquarters during the final briefing on the contract in the form of 35 mm slides. The color composite imagery was generated using a red, a green, and an infrared component of the multispectral imagery. Figures 9.7 and 9.8 show the reconstructed imagery using the recommended method that utilizes a KL-2 Dimensional DPCM encoder at bit rates of 1 and 2 bits/pixel. Figures 9.9 and 9.10 show the color composites and classified pictures obtained using the corresponding reconstructed multispectral imagery. Comparison of these images with the originals shows only a very small degradation at a bit rate of 2 bits/pixel. Of course this bit rate reduces to 1.5 bits/pixel as a result of adding a Huffman encoder to the system.

Figures 9.11 and 9.12 show similar pictures of the recommended technique that uses Haar-Cosine-DPCM encoder at 1 bit/pixel. Subjectively this is a closer approximation to the original imagery than the corresponding imagery shown on Figure 9.7. This is also true for the corresponding composite color imagery.

1 BIT KL - 2 DIM. DPCM

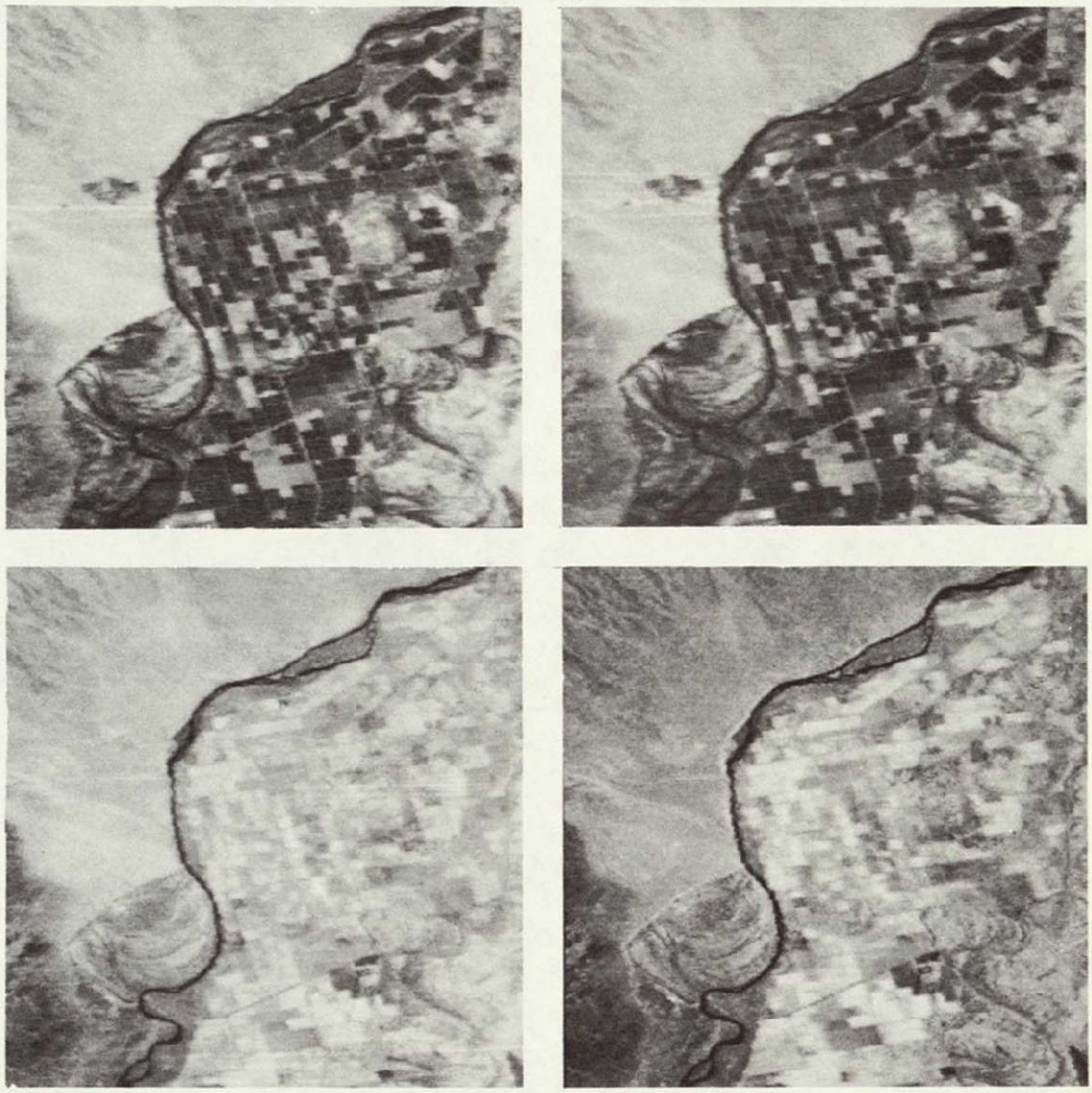

Figure 9.7

2 BIT KL - 2 DIM. DPCM

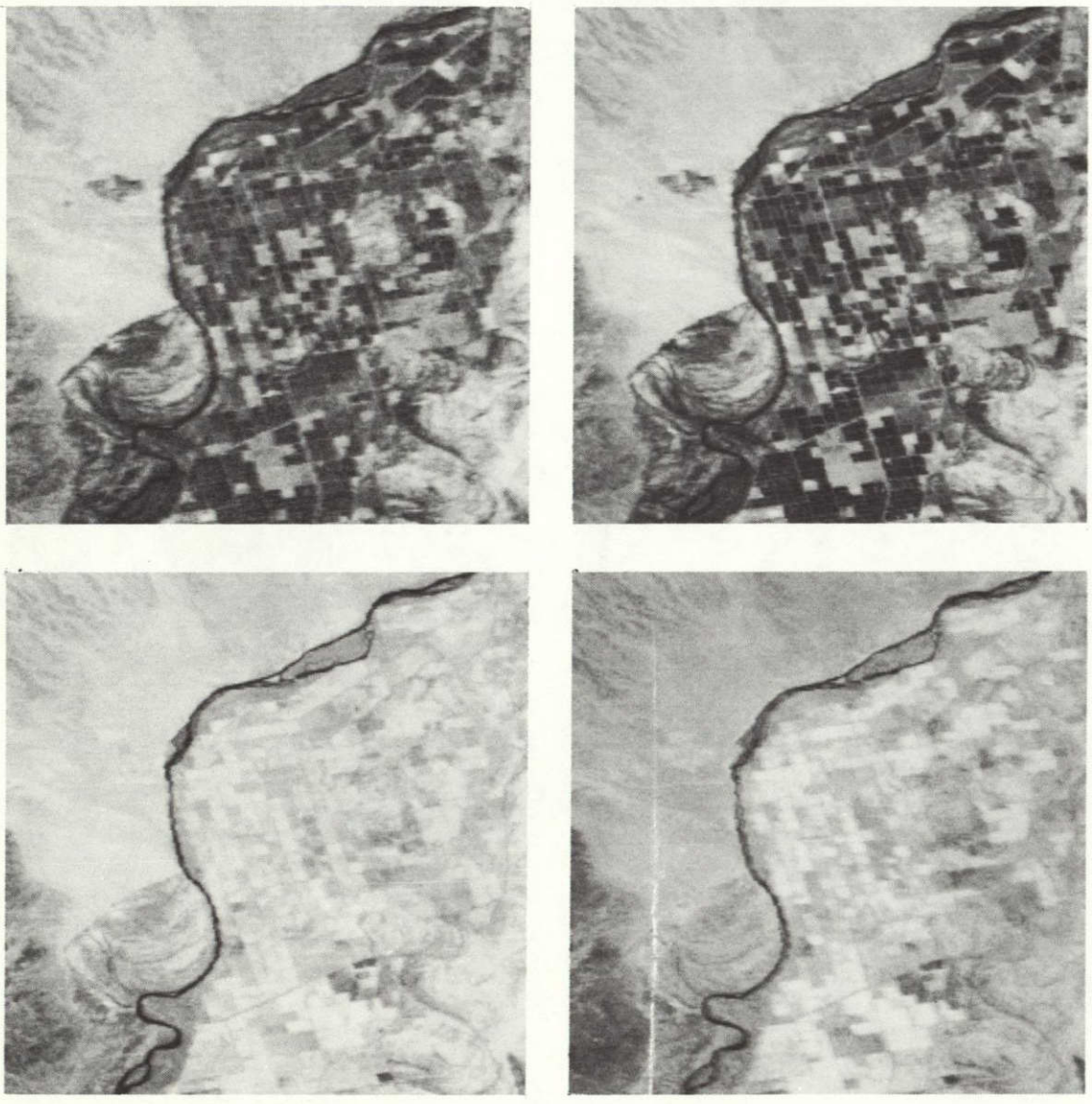

Figure 9.8

1 BIT KL - 2 DIM. DPCM

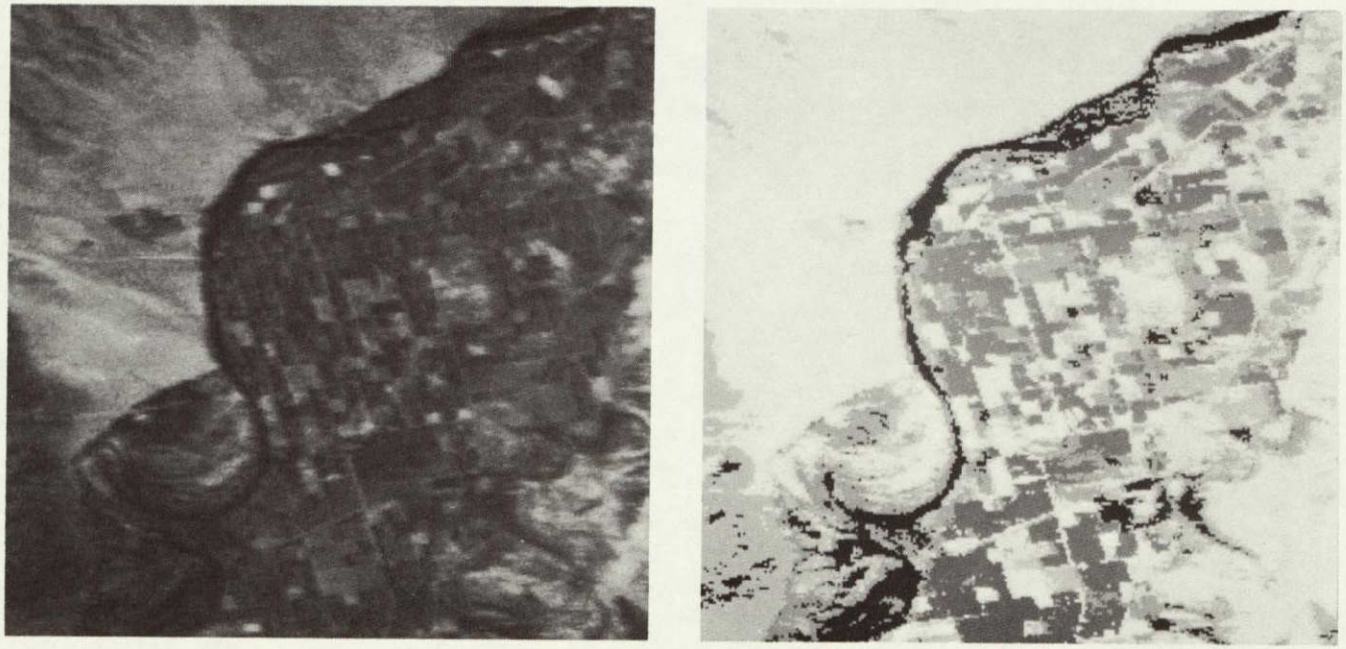

Figure 9.9

2 BIT KL - 2 DIM. DPCM

Figure 9.10

1 BIT HAAR - COSINE - DPCM

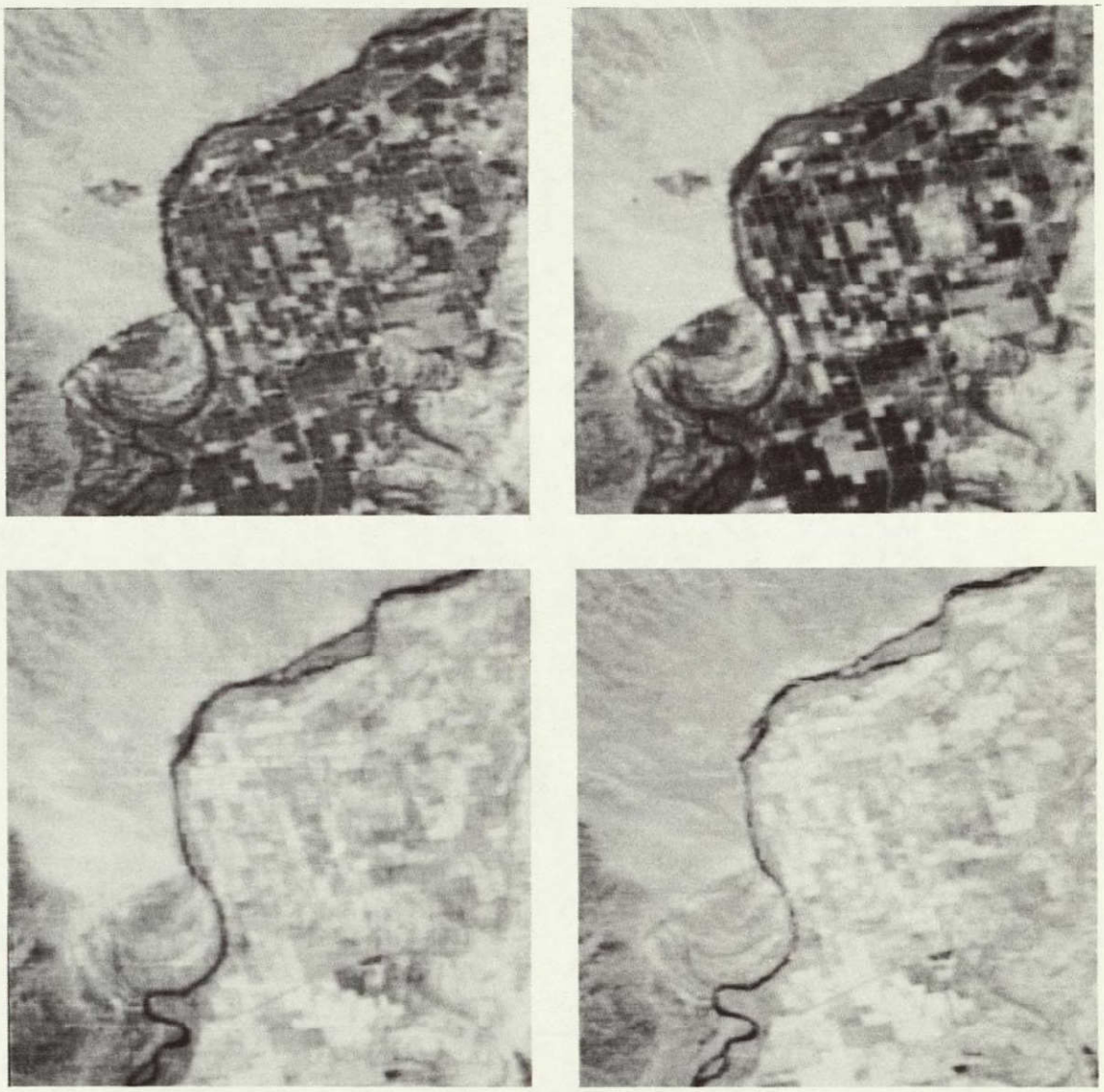

Figure 9.11

1 BIT HAAR - COSINE - DPCM

Figure 9.12

The individual bands as well as the color composite and classified imagery using the cluster coding method are shown on Figures 9.13 and 9.14. Comparison of the reconstructed imagery obtained using cluster coding with the corresponding imagery obtained using a Haar-Cosine-DPCM encoder shows the following:

- The subjective quality of the individual bands of imagery encoded using the cluster coding method is inferior to the subjective quality of the corresponding imagery using a Haar-Cosine-DPCM encoder. This is because individual clusters are visible in the individual bands and this makes an undesirable effect on a human observer. This effect becomes more significant if the reconstructed imagery is viewed on larger screens. It is worth nothing that the MSE of the cluster coded imagery at 1 bit/pixel is less than the MSE of the imagery encoded using a Haar-Cosine-DPCM encoder at the same bit rate.

- The subjective quality of the color composite imagery obtained using the cluster coding system is superior to that of a Haar-Cosine-DPCM encoder. This is because the individual clusters which degrade the subjective quality of the individual bands have a cancelling effect when they are used to form a color composite picture.

1 BIT CLUSTER CODING

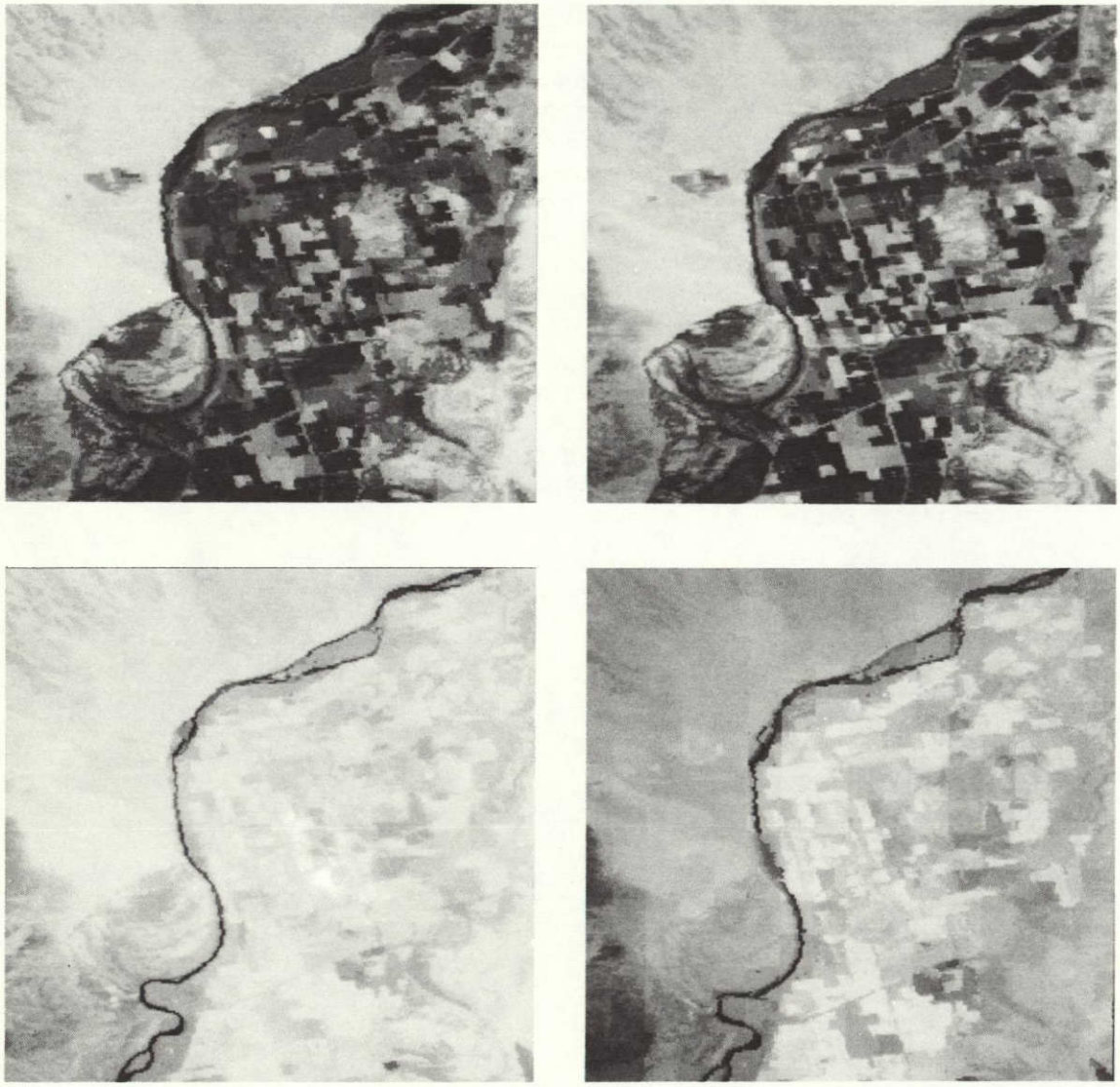

Figure 9.13

1 BIT CLUSTER CODING

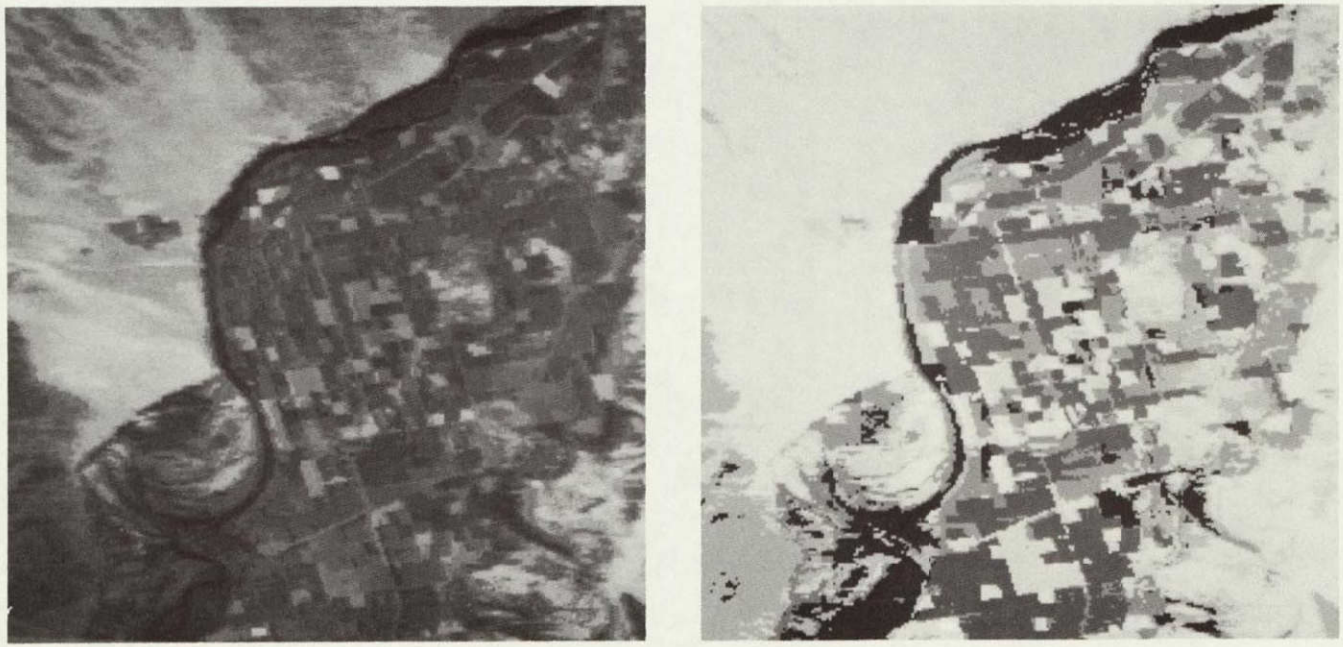

Figure 9.14

10. SUMMARY OF RESULTS

This section presents the key results of the study and summarizes the merits and deficiencies of the recommended techniques.

10.1 SIGNIFICANT RESULTS

(1) The bandwidth of the MSS data is reduced using either two-dimensional or three-dimensional bandwidth compression techniques. The simulated results show that, using non-adaptive coding methods, the performance of the three-dimensional methods gives about one decible more signal-to-noise ratio than the corresponding two-dimensional methods. This small improvement is partially due to the fact that an average value for the spectral correlation is used in the three-dimensional non-adaptive systems. Using an adaptive system utilizes different spectral correlation values for different regions of the imagery, thus the encoder matches the statistics of the MSS imagery more closely and this is expected to result in a larger improvement in the performance of the three-dimensional methods over their two-dimensional counterparts.

(2) The performance of the recommended methods does not change significantly when the Haar transform is substituted for the KL transform in the spectral domain. This is because of the present band allocation for earth imagery. For other multispectral data, a fixed transform matched to the sensors is also adequate for spectral processing

(3) The effects of noisy channels and sensor imperfections on the performance of the recommended methods are negligible. Channel noise corresponding to bit error rates in the order of 10^{-4} or lower does not affect the performance of the encoder. A higher channel error is very unlikely for the present communications system.

(4) The simulation results reported in the study show a very strong correlation between the mean square error and the classification accuracy of the encoded imagery. This is partially due to the fact that the classification algorithm is a recursive method that uses Euclidean distance in classifying the multispectral data to various clusters.

10.2 MERITS AND DEFICIENCIES OF THE RECOMMENDED SYSTEMS

(1) The KL-Cosine-DPCM method gives a better result than the KL-2 Dimensional DPCM system at fixed bit rates. However, addition of the Huffman encoder improves the performance of the latter by about a 25% reduction in the bit rate. It improves the performance of the former system by about a 10% reduction in the bit rate. This makes the performances of both systems at high bit rates about the same. The complexity of KL-2 Dimensional DPCM system is much less. Therefore, at equal performance levels (larger than 1.5 bits/sample) the KL-2 Dimensional DPCM system is recommended.

(2) The cluster coding technique shows good potential for coding multispectral imagery. The performance of this encoder as studied here is only preliminary and it could be improved by utilizing the spatial correlation of the clustered imagery and also inter-and intra-correlation of centroid vectors. The performance of this method is further improved by making the system adaptive. This will allow the number of clusters in each block to vary according to the amount of detailed information in that block.

The performance of the cluster coding method in comparison with the other two recommended techniques is summarized as follows:

- The cluster coding method gives a smaller MSE at low bit rates. At high bit rates it has a larger MSE.
- The reconstructed imagery using the cluster coding method has a poor subjective quality when each band of the MSS imagery is viewed individually. But when these bands are used to generate a color composite imagery the artifacts in various bands cancel and the composite color imagery has good subjective quality.
- Classification accuracy of the cluster coding method is rather poor. This is due to using different block sizes for bandwidth compression and for classifying the MSS data. This will affect the users who must use a large block size for classification of the MSS imagery.
- The biggest defect of the cluster coding technique is its implementational complexity. Its complexity is estimated to be about one order of magnitude higher than the complexity of the Haar-2 Dimensional DPCM system.

11. CONCLUSIONS AND RECOMMENDATIONS

This section discusses the major conclusions and recommendations of the study.

11.1 CONCLUSIONS

(1) Fixed rate encoders give excellent quality for the reconstructed imagery at a 4 to 1 compression ratio. This compression ratio is increased to 6 to 1 by making the system operate at a variable rate through the addition of a Huffman encoder. One such system is the recommended technique that uses a Haar-2 Dimensional DPCM system. At this compression ratio, it has a signal-to-noise ratio better than 35 dB, a classification accuracy better than 91%, and gives reconstructed imagery which is almost indistinguishable from the original.

(2) At a fixed bit rate and a compression ratios of 8 to 1, a Haar-Cosine-DPCM system gives acceptable results. This corresponds to a signal-to-noise ratio of better than 31 dB, a recognition accuracy of better than 82%, and slightly degraded imagery.

(3) Cluster coding methods can be used to obtain a compression ratio of 12 to 1 which corresponds to a signal-to-noise ratio of better than 29 dB, a recognition accuracy of better than 71%, and possibly acceptable reconstructed imagery. Compression ratios of 16 to 1 and higher correspond to noticeably degraded imagery which is only acceptable to some users.

(4) This study only considered non-adaptive bandwidth compression methods. Since adaptive methods result in a higher compression ratio, it is concluded that for higher compression ratios, adaptive methods should be considered.

(5) The effects of sensor imperfections on the performance of the candidate bandwidth compression methods are minimal. These imperfections have a minimal impact on the choice of recommended techniques.

(6) Channel error effects are minimal for transform and DPCM systems for bit error rates less than 10^{-4}.

11.2 RECOMMENDATIONS

11.2.1 Recommended Systems

The recommended systems are presented in Table 11.1. Three systems are recommended based on the desired bandwidth compression ratios.

Table 11.1 Recommended Multispectral Image Data Compression Systems

COMPRESSION RATIO	SYSTEM DESCRIPTION SPECTRAL	SPATIAL	COMPLEXITY	FIDELITY/ACCURACY
6 TO 1	FIXED TRANSFORM (HAAR)	TWO DIMENSIONAL DPCM	LOW	EXCELLENT FIDELITY RECOGNITION ACCURACY >91% SIGNAL/NOISE >35dB
8 TO 1	FIXED TRANSFORM (HAAR)	HYBRID COSINE-DPCM	MODERATE	MODERATE FIDELITY RECOGNITION ACCURACY >82% SIGNAL/NOISE >31dB
12 TO 1	CLUSTER CODING		VERY HIGH	RECOGNITION ACCURACY >71% SIGNAL/NOISE >29dB

11.2.2 Recommendations for Future Activities

We recommend the following for future activities in compressing the bandwidth of multispectral imagery.

(1) Build a prototype data compression unit around the Haar-2 Dimensional DPCM technique. We recommend integrating this data compression unit with an operational multispectral scanner, such as a thematic mapper, which could be tested in aircraft flight to demonstrate the following two points:

- 6 to 1 increase in data recorded per tape
- Realtime data link to ground for quick observation.

We also recommend providing this reconstructed data to users to evaluate and test their acceptance of the compressed data.

(2) Perform system application studies by using representative earth resources projects such as LANDSAT or EOS. One such study could be the application of image data compression to the EOS spacecraft. The block diagram of this system is shown in Figure 11.1. Data compression can be performed at a number of locations. A Haar-2 Dimensional DPCM system with a compression ratio of 6 to 1 will reduce the bit rate for this system from 120 Mbps to 20 Mbps. Then extrapolating the LANDSAT results to the 6-band thematic mapper, the bandwidth compression system gives a signal-to-noise ratio of about 32 dB with a classification accuracy of over 85%. The system benefits for this application for a 6 to 1 data compression ratio are:

- Full thematic mapper data to local users
- Reduced bandwidth compression
- Simpler tape recorder-extended storage
- Potential for increased sensor data on the 120 Mbps link.

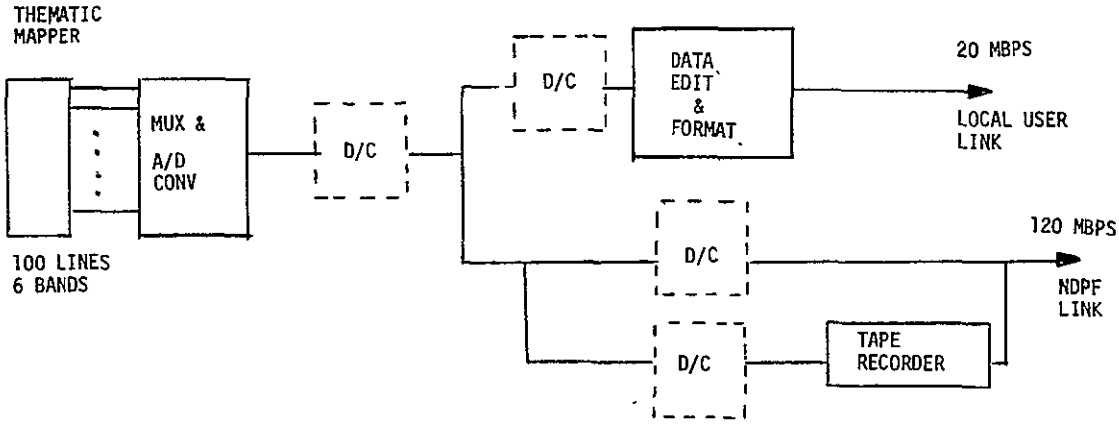

SYSTEM BENEFITS WITH 6:1 DATA COMPRESSION

- FULL THEMATIC MAPPER DATA TO LOCAL USERS
- REDUCED BANDWIDTH TRANSMISSION VIA TDRSS
- SIMPLER TAPE RECORDER - EXTENDED STORAGE
- POTENTIAL FOR INCREASED SENSOR DATA ON 120 MBPS LINK

Figure 11.1 Image Data Compression Applied to EOS Spacecraft

(3) Perform user acceptance studies. This is of major importance in the evaluation of bandwidth compression methods since at present it is not known just which reconstructed images are acceptable to which users. This can be performed by selecting current users of the multispectral data and verifying the effects of the bandwidth compressed data on their standard processing.

(4) Study use of adaptive techniques for greater compression ratios.

(5) A further study of the cluster coding method is recommended to determine its implementational feasibility.

12. GENERAL REFERENCES

[1] T. S. Huang, W. F. Schreiber, Oleh J. Tretiak, "Image Processing," Proceedings of the IEEE, vol 59, November 1971, pp 1586-1609.

[2] W. K. Pratt, Bibliography on Digital Image Processing and Related Topics, Electronic Sciences Laboratory, University of Southern California, USCEE Report 453, September 1, 1973.

[3] A. Rosenfeld, "Progress in Picture Processing: 1969-71," University of Maryland Computer Science Center, Technical Report TR-176, January 1972.

[4] USC Image Processing Laboratory, Bibliography on Digital Image Processing and Related Topics, ARPA Code No. 1706, February 1972, USCEE Report 410.

[5] V. Algazi, D. J. Sakrison, J. Schriebman, W. Dere, B. Romberger, A. Samulon, "Digital Handling and Processing of Remote Sensing Data," Chapter 8 of An Integrated Study of Earth Resources in the State of California, Annual Report for NASA Contract 5-21827, July 30, 1973.

[6] C. H. Chang, L. A. Young, "Remote Measurement of Water Temperature by Raman Scattering," Symposium of Remote Sensing of the Environment, Proceedings, vol 2, pp 1049-1068, October 1972.

[7] R. N. Colwell, Manual of Photographic Interpretation, American Society of Photogrammetry, 1960.

[8] L. W. Ham, "Remote Sensing of Water Pollution," Journal of the Water Pollution Control Federation, vol 40:10, October 1968, pp 1728-1738.

[9] R. A. Holmes, R. B. MacDonald, "The Physical Basis of System Design for Remote Sensing in Agriculture," Proceedings of the IEEE, vol 57, April 1969, pp 629-639.

[10] G. Nagy, "Digital Image-Processing Activities in Remote Sensing for Earth Resources," Proceedings of the IEEE, vol 60, October 1972, pp 1177-1200.

[11] NASA, Revised ERTS Data Users Handbook, Goddard Space Flight Center, Greenbelt, Maryland, August 25, 1972.

[12] S. S. Rifman, "Evaluation of Digitally Corrected ERTS Imagery," Symposium on Management and Utilization of Remote Sensing Data, Sioux Falls, South Dakota, October 1973, pp 206-221.

[13] H. Sievering, R. Mittra, "The Effect of Coherence on Laser Radar Air Pollution Measurements," Symposium on Remote Sensing of the Environment, Proceedings, vol 1, pp 751-757, May 1971.

[14] B. J. Wobber, "Orbital Photos Applied to the Environment," Photogrammetric Engineering, vol 36, August 1970, pp 852-864.

[15] J. E. Abate, "Linear and Adaptive Delta Modulation," Proceedings of the IEEE, vol 55, No. 3, March 1967, pp 298-308.

[16] V. K. Agarwal, "A New Approach to the Fast Hadamard Transform Algorithm," presented at the Hawaii International Conference on System Sciences, Honolulu, Hawaii, January 1971.

[17] V. K. Agarwal, T. J. Stephens, On-Board Processor (Picture Bandwidth Compression, TRW IRAD Report for Space Vehicles Division, February 1970.

[18] V. R. Algazi, "Adaptive Line by Line Encoder for Image Transmission," International Telemetering Conference Proceedings, 1972.

[19] G. B. Anderson, T. S. Huang, "Piecewise Fourier Transformation for Picture Bandwidth Compression," IEEE Transactions on Communication Technology, vol 19, April 1971, pp 133-140.

[20] J. B. Anderson, "A Stack Algorithm for Source Coding with a Fidelity Criterion," IEEE Transactions on Information Theory, vol 20, March 1974, pp 211-226.

[21] J. B. Anderson, F. Jelinek, "A 2-Cycle Algorithm for Source Coding with a Fidelity Criterion," IEEE Transactions on Information Theory, vol 19, January 1973, pp 77-92.

[22] C. A. Andrews, J. M. Davies, G. R. Schwartz, "Adaptive Data Compression," Proceedings of the IEEE, vol 55, No. 3, March 1967, pp 267-277.

[23] H. C. Andrews, Computer Techniques in Image Processing, Academic Press, 1970.

[24] H. C. Andrews, Fourier Coding of Images, University of Southern California, 1968.

[25] H. C. Andrews, W. K. Pratt, "Fourier Transform Coding of Images," 1969 International Conference on System Science, Honolulu, Hawaii, pp 677-679.

[26] R. J. Arguello, H. R. Sellner, J. A. Stuller, "The Effect of Channel Errors in the Differential Pulse Code Modulation Transmission of Sampled Imagery," IEEE Transactions on Communication Technology, vol 19, December 1971, pp 926-933.

[27] A. V. Balakrishnan, "An Adaptive Nonlinear Data Predictor," Proceedings of the National Telemetering Conference (Washington, D.C., May 23-25 1962), vol 2, Suppl. paper 6-5.

[28] T. Berger, "Optimum Quantizers and Permutation Codes," IEEE Transactions on Information Theory, vol IT-18, November 1972.

[29] T. Berger, Rate Distortion Theory, A Mathematical Basis for Data Compression, Prentice-Hall, 1971.

[30] T. Berger, F. Jelinek, J. K. Wolf, "Permutation Codes for Sources," IEEE Transactions on Information Theory, January 1972.

[31] W. T. Bisignani, G. P. Richards, J. W. Whelan, "The Improved Gray Scale and the Coarse-Fine Systems, Two New Digital TV Bandwidth Reduction Techniques," Proceedings of the IEEE, vol 54, No. 3, March 1966, pp 376-390.

[32] R. C. Brainard, J. C. Candy, "Direct Feedback Coders: Design and Performance with Television Signals," Proceedings of the IEEE, vol 57, May 1969, pp 776-786.

[33] Z. L. Budrikis, J. L. Hullett, D. Q. Phiet, "Transient Mode Buffer Stores for Nonuniform Code TV," IEEE Transactions on Communication Technology, vol 19, December 1971, pp 913-922.

[34] D. Chan, R. W. Donaldson, "Optimum Pre- and Post-filtering of Sampled Signals with Application to Pulse Modulation and Data Compression Systems," IEEE Transactions on Communication Technology, vol Com-19, No. 2, April 1971, pp 141-157.

[35] D. J. Connor, "Techniques for Reducing the Visibility of Transmission Errors in Digitally Encoded Video Signals," IEEE Transactions on Communications, Vol 21, June 1973, pp 695-706.

[36] D. J. Connor, R. C. Brainard, J. O. Limb, "Intraframe Coding for Picture Transmission," Proceedings of the IEEE, vol 60, No. 7, July 1972, pp 779-791.

[37] C. C. Cutler, "Delayed Encoding: Stabilizer for Adaptive Coders," IEEE Transactions on Communication Technology, vol. 19, No. 6, December 1971.

[38] L. D. Davisson, "An Approximate Theory of Prediction for Data Compression," IEEE Transactions on Information Theory, vol 13, April 1967, pp 274-278.

[39] L. D. Davisson, "Data Compression Using Straight Line Interpolation," IEEE Transactions on Information Theory, vol IT-14, No. 3, May 1968, pp 390-394.

[40] L. D. Davisson, "Rate-Distortion Theory and Application," Proceedings of the IEEE, July 1972, pp 800-808.

[41] L. D. Davisson, "The Theoretical Analysis of Data Compression Systems," Proceedings of the IEEE, vol 56, No. 2, February 1968, pp 176-187.

[42] L. D. Davisson, "Theory of Data Compression," USC Report No. 64-46, September 1964, pp 800-808.

[43] L. D. Davisson, "Universal Noiseless Coding," IEEE Transactions on Information Theory, vol 19, November 1973, pp 783-795.

[44] J. R. Duan, P. A. Wintz, "Error Free Coding," LARS Information Note 022073, Purdue University, 1973.

[45] L. Ehrman, "Analysis of Some Redundancy Removal Bandwidth Compression Techniques," Proceedings of the IEEE, vol 55, No. 3, March 1967, pp 278-287.

[46] D. J. Eigen, F. R. Framm, R. A. Northouse, "Cluster Analysis Based on Dimensional Information with Applications to Feature Selection and Classification," IEEE Transactions on Systems, Man, and Cybernetics, vol 4, May 1974, pp 284-294.

[47] J. E. Essman, P. A. Wintz, "The Effects of Channel Errors in DPCM Systems and Comparison with PCM Systems," IEEE Transactions on Communications, vol COM-21, No. 8, August 1973, pp 867-877.

[48] B. J. Fino, "Relations Between Haar and Walsh/Hadamard Transforms," Proceedings of the IEEE, May 1972, pp 647-648.

[49] L. E. Franks, "A Model for the Random Video Process," Bell System Technical Journal, April 1966, pp 609.

[50] A. Frei, H. Schindler, P. Vettiger, "An Adaptive Dual-Mode Coder/Decoder for Television Signals," IEEE Transactions on Communication Technology, vol 19, December 1971.

[51] T. Fukinuki, "Optimization of D-PCM for TV Signals with Consideration of Visual Property," IEEE Transactions of Communications, vol 22, June 1974, pp 821-826.

[52] T. Fukinuki, M. Miyata, "Intraframe Image Coding by Cascaded Hadamard Transforms," IEEE Transactions on Communications, vol 21, March 1973, pp 175-180.

[53] G. G. Furman, Removing the Noise from the Quantization Process by Dithering: Linearization, RM-3271-PR, The Rand Corporation, February 1963.

[54] R. G. Gallager, Information Theory and Reliable Communication, John Wiley and Sons, 1968.

[55] H. Gish, J. N. Pierce, Asymptotically Efficient Quantizing, IEEE Transactions on Information Theory, vol 14, September 1968, pp 676-683.

[56] T. J. Goblick, Jr., "Analog Source Digitization: A Comparison of Theory and Practice," IEEE Transactions on Information Theory, April 1967, pp 323-326.

[57] B. Gold, C. Rader, A. V. Oppenheim, T. G. Stockham, Jr., Digital Processing of Signals, McGraw-Hill, 1969.

[58] L. S. Golding, R. K. Garlow, "Frequency Interleaved Sampling of a Color Television Signal," IEEE Transactions on Communication Technology, vol 19, December 1971, pp 972-979.

[59] L. S. Golding, P. M. Schultheiss, "Study of an Adaptive Quantizer," Proceedings of the IEEE, vol 55, No. 3, March 1967, pp 293-297.

[60] D. J. Goodman, L. J. Greenstein, "Quantizing Noise of ΔM/PCM Encoders," Bell System Technical Journal, vol 52, No. 2, February 1973, pp 183-204.

[61] L. M. Goodman, "A Binary Linear Transformation for Redundancy Reduction," Proceedings of the IEEE, March 1967, pp 467-468.

[62] A. Habibi, "Comparison of n^{th} Order DPCM Encoder with Linear Transformations and Block Quantization Techniques," IEEE Transactions on Communication Technology, vol COM-19, No. 6, December 1971, pp 948-956.

[63] A. Habibi, "Delta Modulation and DPCM Coding of Color Signals," International Telemetering Conference Proceedings, 1972.

[64] A. Habibi, Performance of Zero-Memory Quantizers Using Rate-Distortion Criteria.

[65] A. Habibi, R. Hershel, "A Unified Representation of DPCM and Transform Coding."

[66] A. Habibi, P. A. Wintz, "Image Coding by Linear Transformation and Block Quantization," IEEE Transactions on Communication Technology, vol COM-19, No. 1, February 1971, pp 50-62.

[67] R. M. Haralick, I. Dinstein, "An Iterative Clustering Procedure," IEEE Transactions on Systems, Man, and Cybernetics, vol 1, July 1971, pp 275-289.

[68] R. M. Haralick, K. Shanmugam, "Comparative Study of a Discrete Linear Basis for Image Data Compression," IEEE Transactions on Systems, Man, and Cybernetics, vol 4, January 1974, pp 16-27.

[69] B. G. Haskell, "Computation and Bounding of Rate-Distortion Functions for Certain Message Sources and Distortion Criteria," Ph.D dissertation, University of California at Berkeley, June 1968, (Sep 531).

[70] H. Heffes, S. Horing, D. L. Jagermar, "On the Design and Analysis of a Class of PCM Systems," Bell System Technical Journal, vol 50, No. 3, March 1971, pp 917-918.

[71] D. Hockman, H. Katyman, D. R. Weber, "Application of Redundancy Reduction to Television Bandwidth Compression," Proceedings of the IEEE, vol 55, No. 3, March 1967, pp 263-266.

[72] J. J. Y. Huang, P. M. Schultheiss, "Block Quantization of Correlated Gaussian Variables," IEEE Transactions on Communication Systems, September 1963, pp 289-296.

[73] F. Jelinek, "Study of Sequential Decoding," Quarterly Progress Report to the National Aeronautics and Space Administration, NASA Contract NAS 2-5643, December 1969.

[74] F. Jelinek, K. S. Schneider, "On Variable-Length-to-Block Coding," IEEE Transactions on Information Theory, November 1972, pp 765-774.

[75] W. Kaminski, E. F. Brown, "An Edge-Adaptive Three-Bit Ten-Level Differential PCM Coder for Television," IEEE Transactions on Communication Technology, vol COM-19, No. 6, December 1971, pp 944-947.

[76] J. D. Kennedy, et al., Digital Imagery Data Compression Techniques, McDonnell Douglas Astronautics Co., MDC G0402, January 1970.

[77] C. M. Kortman, "Redundancy Reduction - A Practical Method of Data Compression," Proceedings of the IEEE, vol 55, No. 3, March 1967, pp 253-263.

[78] E. R. Kretzmer, "Statistics of Television Signals," Bell System Technical Journal, vol 31, July 1952, pp 751-763.

[79] R. L. Kuehn, E. R. Omberg, G. D. Forry, "Processing of Images Transmitted from Observation Satellites," Information Display, September/October 1971.

[80] T. Kummerow, "Statistics for Efficient Linear and Non-Linear Picture Coding," International Telemetering Conference Proceedings, 1972.

[81] R. L. Kuta, J. A. Sciulli, "The Performance of an Adaptive Image Compression System in the Presence of Noise," IEEE Transactions on Information Theory, vol IT-14, No. 2, March 1968, pp 273-279.

[82] H. J. Landau, D. Slepian, "Some Computer Experiments in Picture Processing for Bandwidth Reduction," Bell System Technical Journal, vol 50, No. 5, May-June 1971.

[83] M. Levine, "Feature Extraction: A Survey," Proceedings of the IEEE, vol 57, August 1969, pp 1391-1405.

[84] J. O. Limb, F. W. Mounts, "Digital Differential Quantizer for Television," Bell System Technical Journal, September 1969, pp 2583-2599.

[85] J. O. Limb, C. B. Rubinstein, "Plateau Coding of the Chrominance Component of Color Picture Signals," IEEE Transactions on Communications, vol 22, June 1974, pp 812-820.

[86] J. O. Limb, C. B. Rubinstein, K. A. Walsh, "Digital Coding of Color Picturephone Signals by Element-Differential Quantization, IEEE Transactions on Communications, vol 19, December 1971, pp 992-1006.

[87] J. O. Limb, I. G. Sutherland, "Run-Length Coding of Television Signals," Proceedings of the IEEE, February 1965, pp 169-170.

[88] J. L. Mannos, D. J. Sakrison, "The Effects of a Visual Fidelity Criterion on the Encoding of Images," IEEE Transactions on Information Theory, vol 20, July 1974, pp 525-536.

[89] J. Max, "Quantizing for Minimum Distortion," IEEE Transactions on Information Theory, March 1960, pp 7-12.

[90] C. L. May, D. J. Spencer, T. A. Zimmerman, "Data Compression Techniques," TRW IRAD Report 7132.44-04, August 1972.

[91] C. L. May, D. J. Spencer, ERTS Image Data Compression Technique Evaluation, Final Report for NASA Contract NAS5-21746, April 1974.

[92] J. B. Millard, H. I. Maunsell, "Digital Encoding of the Video Signal," Bell System Technical Journal, February 1971, pp 459-479.

[93] S. C. Noble, S. C. Knauer, J. I. Giem, "A Real-Time Hadamard Transform System for Spatial and Temporal Redundancy Reduction in Television," (unpublished), authors with Ames Research Center, Mt. View, California.

[94] J. B. O'Neal, "A Bound on Signal-to-Quantizing Noise Ratios for Digital Encoding Systems," Proceedings of the IEEE, vol 55, No. 3, March 1967, pp 287-292.

[95] J. B. O'Neal, "Delta Modulation Quantizing Noise Analytical and Computer Simulation Results for Gaussian and Television Input Signals," Bell System Technical Journal, January 1966, pp 117-141.

[96] J. B. O'Neal, "Entropy Coding in Speech and Television Differential PCM Systems," IEEE Transactions on Information Theory, November 1971, pp 758-761.

[97] J. T. Pinkston, "An Application of Rate-Distortion Theory to a Converse of the Coding Theorem," IEEE Transactions on Information Theory, vol 15, January 1969, pp 66-71.

[98] E. C. Posner, et al., "Epsilon Entropy of Stochastic Processes," The Annuals of Mathematical Statistics, vol 38, No. 4, August 1967, pp 1000-1020.

[99] W. K. Pratt, "A Bibliography on Television Bandwidth Reduction Studies," IEEE Transactions on Information Theory, vol IT-13, No. 1, January 1967, pp 114-115.

[100] W. K. Pratt, L. R. Welch, W. H. Chen, "Slant Transforms for Image Coding," Proceedings of the 1972 Application of Walsh Functions Symposium.

[101] W. K. Pratt, W. H. Chen, L. R. Welch, "Slant Transform Image Coding," IEEE Transactions on Communications, vol 22, August 1974, pp 1075-1093.

[102] W. K. Pratt, "Spatial Transform Coding of Color Images," IEEE Transactions on Communication Technology, vol 19, December 1971, pp 980-992.

[103] W. K. Pratt, J. Kane, H. C. Andrews, "Hadamard Image Coding," Proceedings of the IEEE, vol 57, January 1969, pp 58-68.

[104] P. J. Ready, P. A. Wintz, "Information Extraction, SNR Improvement and Data Compression in Multispectral Imagery," IEEE Transactions on Communications, vol 21, October 1973, pp 1123-1131.

[105] R. L. Remm, "Analysis and Implementation of a Delta Modulation Pictorial Encoding System," 1966 International Telemetering Conference Proceedings, pp 27-34.

[106] R. F. Rice, J. R. Plaunt, "Adaptive Variable-Length Coding for Efficient Compression of Spacecraft Television Data," IEEE Transactions on Communication Technology, vol COM-19, No. 6 December 1971, pp 889-897.

[107] R. F. Rice, "Channel Coding and Data Compression System Considerations for Efficient Communication of Planetary Imaging Data," Jet Propulsion Laboratory, Technical Memorandum 33-695.

[108] G. P. Richards, W. T. Bisignani, "Redundancy Reduction Applied to Coarse-Fine Encoded Video," Proceedings of the IEEE, vol 55, No. 10, December 1967.

[109] M. P. Ristenbatt, "Alternatives in Digital Communications," Proceedings of the IEEE, vol 61, No. 6, June 1973.

[110] G. S. Robinson, Orthogonal Transform Feasibility Study, COMSAT Technical Report No. CL-TR-5-71, NASA Contract NAS9-11240, November 1971.

[111] D. J. Sakrison, Communication Theory: Transmission of Waveforms and Digital Information, John Wiley & Sons, Inc., 1968.

[112] D. J. Sakrison, "Factors Involved in Applying Rate Distortion Theory to Image Processing," Proceedings of the UMR - Mervin J. Kelly Communications Conference, October 1970.

[113] D. J. Sakrison, "The Rate-Distortion Function for a Class of Random Processes," IEEE Transactions on Information Theory, vol 16, January 1970, pp 10-16.

[114] D. J. Sakrison, The Rate Distortion Function of a Gaussian Process with a Weighted Mean Square Error Criterion, (Corres.), IEEE Transactions on Information Theory, vol 19, May 1968, Addendum, vol 15, September 1969, pp 610-611.

[115] D. J. Sakrison, V. R. Algazi, "Comparison of Line-by-Line and Two-Dimensional Encoding of Random Images," IEEE Transactions on Information Theory, July 1971, pp 386-398.

[116] J. E. Savage, "The Complexity of Decoders - Part II: Computational Work and Decoding Time," IEEE Transaction on Information Theory, vol IT-17, No. 1, January 1971, pp 77-85.

[117] W. F. Schreiber, "Picture Coding," Proceedings of the IEEE, vol 55, No. 3, March 1967, pp 320-330.

[118] J. W. Schwartz, "Bit-Plane Encoding: A Technique for Source Encoding," IEEE Transactions on Aerospace and Electronic Systems, vol AES-2, No. 4, July 1966, pp 385-392.

[119] L. F. Shaefer, A. Macovski, "Encoding and Decoding of Color Information Using Two-Dimensional Spatial Filtering," IEEE Transactions on Computers, vol 21, July 1972, pp 642-647.

[120] K. Sharmugam, R. M. Haralick, "A Computationally Simple Procedure for Imagery Data Compression by Karhunen-Loève Method," IEEE Transactions on Systems, Man, and Cybernetics, vol 3, March 1973, pp 202-204.

[121] C. E. Shannon, "Coding: Theorems for a Discrete Source with a Fidelity Criterion," in Information and Decision Processes, edited by Robert E. Macchol; New York, McGraw-Hill Book Co., Inc., 1960, pp 93-126.

[122] D. Slepian, "Permutation Modulation," Proceedings of the IEEE, March 1965, pp 228-236.

[123] D. J. Spencer, "Data Compression of Spacecraft Imagery."

[124] M. Tasto, P. A. Wintz, "A Bound on the Rate-Distortion Function and Application to Images," IEEE Transactions on Information Theory, vol 18, January 1972, pp 150-159.

[125] M. Tasto, P. A. Wintz, "Image Coding by Adaptive Block Quantization," Transactions on Communication Technology, vol COM-19, No. 6, December 1971, pp 957-972.

[126] A. J. Viterbi, J. K. Omura, Convolutional Encoding of Memoryless Discrete-Time Sources.

[127] W. C. Wilder, Subjectively Relevant Error Criteria for Pictorial Data Processing, Purdue University, Report TR-EE 72-34, December 1972.

[128] P. A. Wintz, "Transform Picture Coding," Proceedings of the IEEE, vol 60, No. 7, July 1972, pp 809-820.

[129] R. C. Wood, On Optimum Quantization, IEEE Transactions on Information Theory, vol 15, March 1969, pp 248-252.

[130] H. C. Andrews, Introduction to Mathematical Techniques in Pattern Recognition, John Wiley & Sons, 1972.

[131] P. E. Anuta, "Digital Registration of Multispectral Video Imagery," Journal of the Society of Photo-Optical Instrumentation Engineers, vol 7, September 1969, pp 168-175.

[132] P. E. Anuta, "Spatial Registration of Multispectral and Multitemporal Digital Imagery Using Fast Fourier Transform Techniques," IEEE Transactions on Geoscience Electronics, vol 8, October 1970.

[133] R. O. Duda, P. E. Hart, Pattern Classification and Scene Analysis, Artifical Intelligence Group, Stanford Research Institute, Menlo Park, California, 1970.

[134] K. S. Fu, "On the Application of Pattern Recognition Techniques to Remote Sensing Problems," Purdue University School of Electrical Engineering Report No. TR-EE 71-13, June 1971.

[135] K. S. Fu, D. A. Landgrebe, T. L. Phillips, "Information Processing of Remotely Sensed Agricultural Data," Processing of the IEEE, vol 57, April 1969, pp 639-653.

[136] A. S. Gliniewicz, H. M. Lachowski, W. H. Pace, P. Salvato, ASTEP Users' Guide and Software Documentation, TRW Note No. 74-FMT-939, Document No. 25990-H028-R0-00.

[137] R. M. Haralick, D. E. Anderson, "Texture-Tone Study with Application to Digitized Imagery," The University of Kansas Center for Research, Inc., Technical Report 182-2, November 1971.

[138] G. G. Lendaris, G. L. Stanley, "Diffraction Pattern Sampling for Automatic Pattern Recognition," Proceedings of the IEEE, vol 58, February 1970, pp 198-216.

[139] K. Preston, Jr., "A Comparison of Analog and Digital Techniques for Pattern Recognition," Proceedings of the IEEE, vol 60, October 1972, pp 1216-1231.

[140] N. Ahmed, T. Natarajan, and K. R. Rad, "On Image Processing and a Discrete Cosing Transform," IEEE Trans. on Computers, C-23, January 1974, pp. 90-93.

[141] H. J. Whitehouse, J. M. Speiser, and R. W. Means, "High Speed Aerial Access Linear Transform Implementation," Symp. All Applications Digital Computer, Orlando, Florida.

[142] Definition of the Total Earth Resources System for the Shuttle Era, General Electric Space Division, Contract No. NAS9-13401, NASA Lyndon B. Johnson Space Center, Houston, Texas 77058.

[143] Multispectral Scanner Data Redundance Study, Final Report, May 15, 1971, Philco-Ford, Contract No. NAS5-21162, NASA/Goddard Space Field Center, Greenbelt, Maryland.

[144] A. Habibi, "Hybrid Coding of Pictorial Data," IEEE Trans., on Communications, Vol. COM-22, No. 5, May 1974, pp. 614-624.

[145] B. Smith, "Instantaneous Companding of Quantized Signals," BSTJ, Vol. 36, January 1951, pp. 44-48.

[146] J. A. Roese, W. K. Pratt, G. S. Robinson, and A. Habibi, "Interframe Transform Coding and Predictive Coding Methods," Conference Record of International Conference on Communications, June 1975, pp. 23 (17-21).

[147] J. N. Gupta and P.A. Wintz, "A Boundary Finding Algorithm and its Applications," IEEE Transactions on Circuits and Systems, Vol. CAS-22, No. 4, April 1975, pp. 351-362.

[148] E. E. Hilbert, Joint Classification and Data Compression of Multi-dimensional Information Source Applications to ERTS, Converence Record Vol. II, International Conference on Communications, June 1975, pp. 27(1-6).

[149] L. C. Wilkins and P. A. Wintz, "A Contour Tracing Algorithm for Data Compression for Two-Dimensional Data," School of Elect. Engr., Purdue University, W. Lafayette, Indiana, Tech. Rep. TR-EE 69-14, 1969.

[150] "Tradeoff Analysis of Modes of Data Handling for Earth Resources," Study Final Report, Prepared for NASA Goddard Space Flight Center, by TRW Systems Group, TRW Report No. 22591-6001-RV-00, March 1975.

A

APPENDIX A

OPTIMUM BIT ALLOCATION USING VITERBI ALGORITHM

A.1 INTRODUCTION

Rate allocation is a classical isoperimetric problem. A fixed resource, the channel capacity, must be distributed among several signals of unequal power such that the distortion is minimized. This problem can be solved by variational calculus if rate is a continuous variable (block coding). Integer solutions, suitable for computer evaluation, are obtained by dynamic programming methods. The classical analytical solution gives intuitive insight.

The function to be minimized has the general form

$$\int_{\Omega} f[\phi(x)]dx \tag{1}$$

and is subject to the constraint

$$C \leq \int_{\Omega} \alpha(x)\ \phi(x)dx \tag{2}$$

where $\phi(x)$ is the distribution of resources and $\alpha(x)$ is a positive weighting function. The summation over a set of measure, Ω, includes the multidimensional case.

Form the Lagrangian

$$L = \int_{\Omega} f[\phi(x)]dx + \lambda\left[C - \int_{\Omega} \alpha(x)\ \phi(x)dx\right] \tag{3}$$

Stationary values of L occur when $\phi(x)$ satisfies the equations

$$\frac{\delta L}{\delta \phi} = \int_{\Omega} \left[\frac{\delta f[\phi(x)]}{\delta \phi(x)} - \lambda\alpha(x)\right] dx = 0 \tag{4}$$

and

$$\frac{\delta L}{\delta \lambda} = C - \int_{\Omega} \alpha(x)\ \phi(x)\ dx = 0 \tag{5}$$

Thus, $\phi(x)$ satisfies the optimizing relation

$$\frac{1}{\alpha(x)}\ \frac{\delta f[\phi(x)]}{\delta \phi(x)} = \lambda,\ \alpha\ 11_X \in \Omega \tag{6}$$

This analytical relation applies to allocation problems in coding, quantization, rate distortion theory, search theory, thermodynamics, and the economic theory of production.

For an example, assume N Gaussian variables $\{X_1, X_2, \ldots, X_N\}$ with zero-mean and variances $\{\sigma_1^2, \sigma_2^2, \ldots, \sigma_N^2\}$. Shannon showed that the ideal quantizing relation between rate, R_i, and distortion, D_i, for a zero mean, variance σ_i^2, normal random process is

$$D_i = \sigma_i^2\ 2^{-2R_i} \tag{7}$$

From equation (6), the distortion D_i satisfies

$$D_i = -\frac{\lambda}{2\ \ell_n 2}\ , \tag{8}$$

for $1 \leq i \leq N$, provided that $D_i < \sigma_i^2$.

If $D = \Sigma D_i$ is sufficiently small, (rate sufficiently large) the distortion is uniformly distributed.

$$D_i = D/N\ ;\quad 1 \leq i \leq N \tag{9}$$

The rates R_i obey the recurrence relation

$$R_i = R_j + \frac{1}{2} \log_2 \left(\frac{\sigma_i^2}{\sigma_j^2}\right) \tag{10}$$

As the rate is reduced, some truncation is necessary. The best way to do this is as follows. Arrange the σ_i^2 in monotonic order, such that

$$R_i \geq R_k \text{ , if } k \geq i. \tag{11}$$

Then

$$R = \sum_{i=1}^{L} R_i = LR_j + \frac{1}{2} \sum_{i=1}^{L} \log_2 \frac{\sigma_i^2}{\sigma_j^2} \tag{12}$$

or

$$R_j = \frac{1}{L} \left[R - \frac{1}{2} \sum_{i=1}^{L} \log_2 \frac{\sigma_i^2}{\sigma_j^2} \right] \tag{13}$$

where L is the largest integer such that

$$R \geq \frac{1}{2} \sum_{i=1}^{L} \log_2 \frac{\sigma_i^2}{\sigma_j^2} \tag{14}$$

Then, the sampling error, due to truncation, is

$$D_{\text{sampling}} = \sum_{i=L+1}^{N} \sigma_i^2 \text{ , } \tag{15}$$

the quantization error is

$$D_{\text{quantization}} = L \left(\prod_{i=1}^{N} (\sigma_i^2)^{\frac{1}{L}} \right) 2^{-R/L} \text{ , } \tag{16}$$

and the total distortion, which is minimized, is

$$D = D_{\text{quantization}} + D_{\text{sampling}}. \tag{17}$$

By arranging the variances in monotonic order, the sampling error is minimized for a given total rate, R, and the allocation rule (13) minimizes the quantization distortion.

The optimum allocation rule produces a uniform distribution of distortion for large rates. As the rate is reduced, some truncation is necessary, resulting in sampling error. To minimize the sampling error, the variances are arranged in monotonically decreasing order so that the sampling error is as small as possible.

A.2 INTEGER SOLUTION OF THE RATE ALLOCATION PROBLEM

In the previous discussion of the rate allocation problem, analytical solutions were presented, to give intuitive insight. But the analytical solution has its shortcomings. It is necessary to assume continuity of rates, and the Lagrange multiplier method cannot handle inequality (one-sided) constraints. Without block coding, however, only integer rates can be assigned, and the rates must be positive.

An integer solution by dynamic programming is easily implemented by an application of the Viterbi algorithm. The total number of bits is B_{max}/block, with N samples/block. After transformation these bits are to be allocated in N stages, so as to minimize the quantizing distortion for the block. To formulate the problem for dynamic programming solution, let the state variables, B_k, be the total number of bits used as of the $k^{\underline{th}}$ stage. Form a trellis as shown in Figure 1.

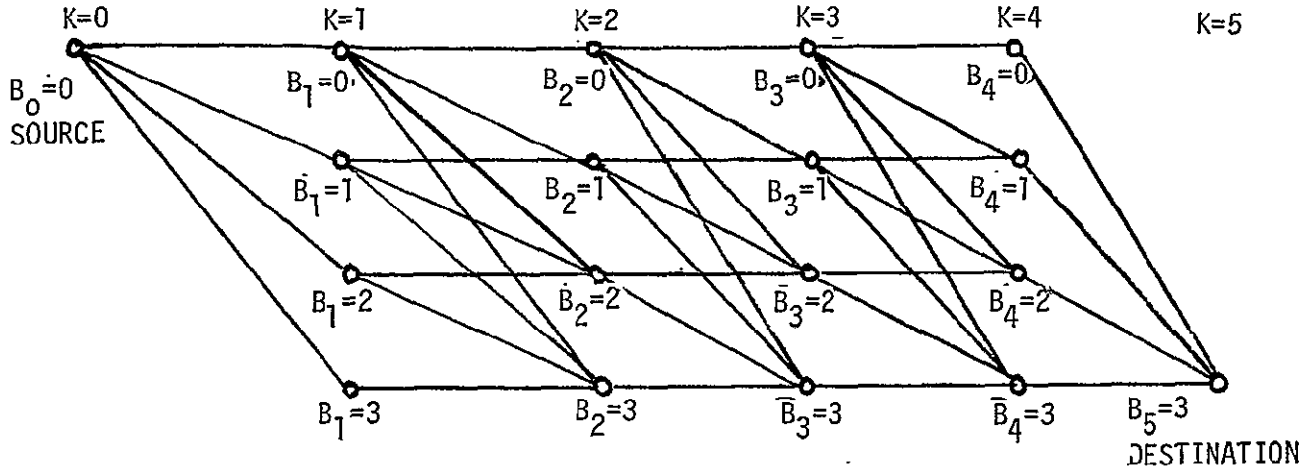

Figure 1. Trellis Diagram

Let the branch length be labelled with the distortion resulting from a transition between nodes in adjacent stages. The optimum solution corresponds to the shortest path through the network from k=0 to k=N, where the initial node corresponds to B_0=0 and the final node corresponds to $B_N = B_{max}$.

For a computer solution, the following storage is required.

Storage:

k	index of stage
$\hat{\underline{B}}_k$, $B_{k-1} \leq B_k \leq B_{max}$	survivor sequences terminating in B_k.
$D_k(B_k)$, $B_{k-1} \leq B_k \leq B_{max}$	survivor lengths

The states are initialized as

$$B_0 = 0 \tag{18}$$

$$D_0(B_0) = 0 \tag{19}$$

The succeeding are computed by the recursion:

$$D(B_{k+1}) \triangleq D(B_k) + \min d\,[B_{k+1}, B_k]\; B_k \leq B_{k+1} \leq B_{max} \tag{20}$$

At each node, only the transition branch corresponding to the shortest total path entering the node from the previous stage is retained.

The simple form of the trellis makes it easy to calculate the complexity of the algorithm as a function of block length and bit rate. For N stages and M+1 states an exhaustive search of the trellis requires a search of

$$S(M,N) = (N-1)\,\frac{M(M+1)}{2} + 2M. \tag{21}$$

This relation is evaluated and the results are shown in Table 1.

If the special case M=N is considered, the number of branches is seen to grow proportionally to the cube of the block length.

Table 1. Number of Trellis Branches

M \ N	1	2	4	8	16	32	64
8	9	25	78	268			
16	17	49	158	556	2072		
32	33	97	318	1132	4248	16432	
64	65	193	638	2284	8600	66592	131168

If the special case M = N is considered, the number of branches is seen to grow proportionally to the cube of the block length.

Actually, the number of branches searched is much less than this because the algorithm only requires that the minimum path length be found at each node. Typically, about two branches per node is searched before finding the minimum is found, averaged over the block. In a 64 x 64 trellis, 6.6% were searched, in a typical run on voice source data. There were 4096 nodes in a 64 x 64 trellis. This means that the average depth of search was 2.13 branches/node. If one branch could be searched in a microsecond, it would take 8.721 milliseconds to complete the bit allocation for 64 samples.

At 8000 samples/second in blocks of 64 samples, there were 125 μsecs between samples or 8 milliseconds/frame. By averaging over 5 frames, quantizers could be allocated every 0.04 secs. Over 20 frames, the quantizer is allocated every 0.16 sec. Over 64 frames, quantizing is allocated every 0.512 seconds.

The memory requirements are presented in Table 2, below.

Table 2. Algorithm Storage Requirements

M X N	8 x 8	16 x 16	32 x 32	64 x 64
Distortion Table	72	272	1056	4160
Path Map	72	272	1056	4160
Path Costs	18	34	66	138
Total	162_{10}	578_{10}	2178_{10}	8450_{10}

B

APPENDIX B

DETAILS OF PROCESSING COST

B.1 PRELIMINARIES

In this section the number of adds-multiples to perform a particular transformation is referred to as the cost of the particular transformation. For instance cost of N point complex FFT is $3N \log_2 N$ adds and $2N \log_2 N$ multiples.

Now for N real points, referred to by function F(n) we form add and even functions $g_o(n)$ and $g_e(n)$ such that

$$g_e(n) = F(2n) \qquad n = 0, \cdots, \frac{N}{2} - 1$$

$$g_o(n) = F(2n + 1)$$

Referring to $\frac{N}{2}$ point FFt of the complex sequences g_e and g_o by G_e and G_o respectively,we have

$$G_e = F(g_e) = \frac{g(k) + \bar{G}(-k)}{2}$$

$$G_o = F(g_o) = \frac{G(k) - \bar{G}(-k)}{2_y}$$

when F is used to denote Fourier transform and the overbar to denote conjugate now

$$f(k) = \sum_{n=0}^{N-1} F_n W_N^{-nk} = \sum_{n=0}^{\frac{N}{2}-1} g_o(n) W^{-2kn} + g_o(n) W^{-2kn-k}$$

$$= G_e(k \bmod \tfrac{N}{2}) + G_o(k \bmod \tfrac{N}{2}) W^{-k}$$

since F is real F(k) = F(-k), k=0, $\frac{N}{2}$. Note that F(0) and F($\frac{N}{2}$) are real. Now, given G_e and G_o, we can get F(k);-k=0,$\cdots$, $\frac{N}{2}$ with ($\frac{N}{2}$ -1)(cmul*+cadd*) + 2 adds.

---

* cmul and cadd are notations for complex add and complex multiples.

We need $G_e(k)$, $G_o(k)$ for $k=0, \frac{N}{2}-1$, but g_e, g_o, are real, so these values are only needed for $k=0, \frac{N}{4}$ which requires a total of N adds. Thus, the total cost of taking the fourier transform of N points is (2N-4) multiples and (3N-2 adds. If we wish to calculate the fourier transform of only real arrays then the cost of getting G_e is $(\frac{N}{4}+1)$ adds and the cost of getting G_o is $\frac{N}{2}$ adds, where calculating F( ) from G_e and G_o requires $(\frac{N}{2}+2)$ adds and (N-2) multiples. This gives a total of $(\frac{5}{4}N+3)$ adds and (N-2) multiples.

Hadamard transform of an array of N points requires only $N \log_2 N$ adds, using fast Hadamard transform [103].

The cost of Slant transform is $(N\log_2 N + (\frac{N}{2}) - 2)$ adds and (2N-4) multiples using fast slant transform [101].

B.2 COST OF PERFORMING MULTIDIMENSIONAL TRANSFORMS

To perform a multidimensional transformation one has to follow the following procedure;

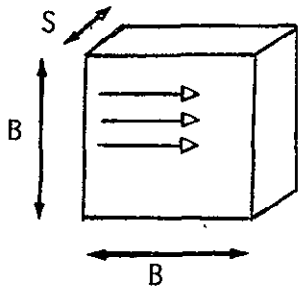

Figure 1

(1) First transform in the X direction. (See Figure 1) This is a real transform.

$$\text{X direction transform cost} = SB\left[\begin{array}{l}\frac{3}{2}B\log_2\frac{B}{2}\text{ adds} + 3B\text{ adds} - 2\text{ adds} \\ B\log_2\frac{B}{2}\text{ muls} + 2B\text{ muls} - 4\text{ muls}\end{array}\right]$$

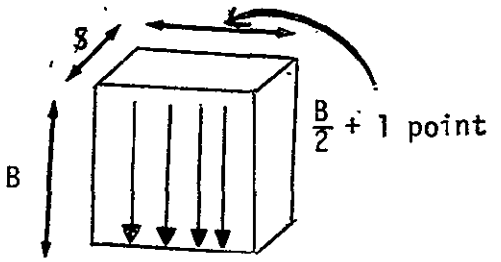

(2) For the y direction transform we have the following situation. (See Figure 2)

First and the last points are real, the rest of the points are complex.

The cost of performing 2S real transforms is

$$2S\begin{bmatrix}(\frac{3}{2}\,B\,\log_2 B + \frac{3}{2}\,B\text{-}2)\ \text{adds}\\(B\,\log_2 B + B\text{-}4)\ \text{muls}\end{bmatrix}$$

and the cost of $(\frac{B}{2}-1)S$ complex is

$$(\frac{B}{2}-1)S\begin{bmatrix}3B\,\log_2 B\ \text{adds}\\2B\,\log_2 B\ \text{muls}\end{bmatrix}$$

y direction transforms has a total cost of $B^2S\ [(\frac{3}{2}\log_2 B + \frac{3}{B} - \frac{4}{2})]$ adds and $B^2S\ [(\log_2 B + \frac{2}{B} - \frac{8}{B^2})]$ multiples.

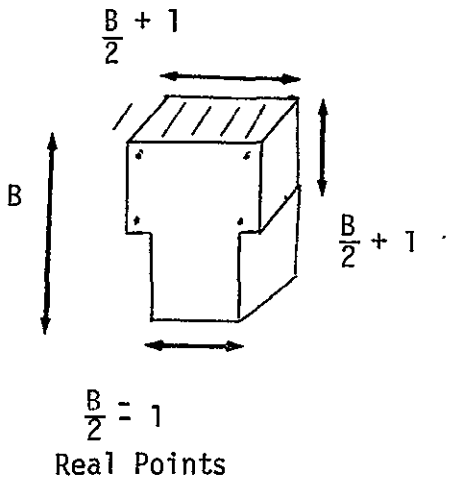

(3) For the S direction transform we have the diagram shown on Figure 3. We need to perform S real and $[(B(\frac{B}{2} - 1) + S(\frac{B}{2} - 1))]$ complex S point transforms. This costs $4\,[(\frac{3}{2} S \log_2 S + \frac{3}{2} S - 2)]$ adds and $4\,[(S \log_2 S + S - 4) + \frac{1}{2}(B^2-4)]$ multiples.

The total cost of S direction transforms is $B^2S\,[(\frac{3}{2}\log_2 S + \frac{6}{B^2} - \frac{8}{B^2S})]$ adds and $B^2S\,[(\log_2 S + \frac{4}{B^2} - \frac{16}{B^2S})]$ multiples

B.3 COST OF VARIOUS TRANSFORMATIONS

B.3.1 Three-Dimensional Fourier Transform

Cost of three-dimensional fourier transform per sample is the total cost divided by B^2S. This is equal to $(\frac{3}{2}\log_2 B^2S + \frac{3}{2} + \frac{1}{B} + \frac{2}{B^2} - \frac{8}{B^2S})$ add and $(\log B^2S + 1 - \frac{2}{B} - \frac{4}{B^2S} - \frac{16}{B^2S})$ multiples. Typical values for B=16, S=4, are 16.5 adds and 11 multiples.

B.3.2 Two-Dimensional Fourier Transform

The cost per sample for two-dimensional fourier transform is $(\frac{3}{2}\log_2 B^2 + \frac{3}{2} + \frac{1}{B} - \frac{4}{B^2})$ adds $(\log_2 B^2 + 1 - \frac{2}{B} - \frac{8}{B^2})$ multiples. Typical values for B=16, S=4 are 14.5 adds and 9 multiples.

B.3.3 Three-Dimensional Cosine Tranform

The cost for the cosine transform is calculated by going through the same procedure. Let C(B) refer to cost per sample of a 8-point cosine transform. Then for a three-dimensional cosine transform the cost per sample is 2C(B) + C(S). To perform an N point cosine transform we form a 2(N-1) real sequence and, as before, calculate the fourier transform of this real sequence by means of an intermediate N-1 point

complex transforms. Cost of (N-1) point complex transform is $3(N-1)\log_2(N-1)$ adds and $2(N-1)\log_2(N-1)$ multiples.

To obtaine the cosine transform we want, we modify our complex transform as indicated in section B.1 This requires a total of $(3\log_2(N-1) + \frac{5}{2} + \frac{3}{N-1})$ adds and $(2\log_2(N-1) + 2 - \frac{2}{N-1})$ multiples for an N point cosine transform. Then the cost of cosine transform cost/pixel is $(1-\frac{1}{B}[3\log_2(B-1)^2 + 5 + \frac{6}{B-1}] + (1-\frac{1}{S})[3\log_2(S-1) + \frac{5}{2} - \frac{3}{S-1}]$ adds/sample and $(1-\frac{1}{B})[2\log_2(B-1)^2 + 4 - \frac{4}{B-1}] + (1-\frac{1}{S})[2\log_2(S-1) + 2 - \frac{2}{S-1}$ multiples/pixel. This gives typical values of 34 adds/pixel and 24 multiples/pixel for B=17, S=5.

B.3.4 Two-Dimensional Cosine Transform

For the two-dimensional cosine transform one must drop the second term (one's with S's) form the above expressions. This gives typical values of 28 adds/pixel and 19 multiples/pixel for B=16, S=4.

B.3.5 Three-Dimensional Hadamard Transform

Cost of three-dimensional Hadamard transform is $BS[B\log_2 B]$ adds for X and Y direction transforms and $B^2[S\log_2 S]$ adds for the S direction. This gives a total cost of $\log_2(B^2S)$ adds/pixel for the three-dimensional Hadamard transform. This gives a typical value of 10 adds/pixel for B=16, S=4.

B.3.6 Two-Dimensional Hadamard Transform

For two-dimensional Hadamard transform one needs $\log_2(B^2)$ a-d/pixel which gives a typical value of 8 adds/pixel for B=16.

B.3.7 Three-Dimensional Slant Transform

Cost of a three-dimensional slant transform is calculated using the same procedure this gives $(\log_2 B^2S + \frac{3}{2} - \frac{4}{B} - \frac{2}{S})$ add/pixel and $(6 - \frac{8}{B} - \frac{4}{S})$ multiple/pixel. Typical values are 10.75 add/pixel and 4.5 multiples/pixel for B=16, S=4.

B.3.8 Two-Dimensional Slant Transform

For two-dimensional slant transform the cost is $(\log_2 B^2 \pm 1 - \frac{4}{B})$ adds/pixel and + $(4 - \frac{8}{B})$ multiples/pixel. Typical values are 9 adds/pixel and 3.5 multiples/pixel for B=16, S=4.

APPENDIX C

GENERAL REFERENCES

[1] T. S. Huang, W. F. Schreiber, Oleh J. Tretiak, "Image Processing," Proceedings of the IEEE, vol 59, Nov 1971, pp 1586-1609.

Keywords:
1. image enhancement
2. picture coding
3. image digitization
4. redundancy reduction
5. psychovisual coding
6. contour coding
7. transformational coding
8. Hadamard transform coding
9. optical image processing
10. distortion measure

A survey article of image processing, including coding. The article has an excellent list of references.

[2] W. K. Pratt, Bibliography on Digital Image Processing and Related Topics, Electronic Sciences Laboratory, University of Southern California, USCEE Report 453, September 1, 1973.

Keywords:
1. image coding
2. pulse code modulation
3. quantization reduction coding
4. run length coding
5. differential pulse code modulation
6. interpolative coding
7. contour coding
8. transform coding
9. color image coding
10. frame to frame coding

This report is a large bibliography organized by subject, author, and year of publication.

[3] A. Rosenfeld, "Progress in Picture Processing: 1969-71," University of Maryland Computer Science Center, Technical Report TR-176, January 1972.

Keywords:
1. picture compression
2. coding
3. quantization and sampling
4. transform and contour coding
5. image enhancement
6. pattern recognition

This report is a survey of the literature between 1969 and 1971. A large bibliography is included.

[4] USC Image Processing Laboratory, Bibliography on Digital Image Processing and Related Topics, ARPA Code No. 1706, February 1972, USCEE Report 410.

Keywords: 1. digital image processing
2. bibliography

REMOTE SENSING

[5] V. Algazi, D. J. Sakrison, J. Schriebman, W. Dere, B. Romberger, A. Samulon, "Digital Handling and Processing of Remote Sensing Data," Chapter 8 of An Integrated Study of Earth Resources in the State of California, Annual Report for NASA contract 5-21827, July 30 1973.

Keywords: 1. ERTS
2. sensor equalization

This progress report covers techniques for equalizing sensor response of the ERTS multi-spectral scanner on the imagery after it is received on the ground. Consideration is also given to ways of combining pictures for display and enhancing certain image contents.

[6] C. H. Chang, L. A. Young, "Remote Measurement of Water Temperature by Raman Scattering," Symposium of Remote Sensing of the Environment, Proceedings, vol 2, pp 1049-1068, October 1972.

Keywords: 1. remote sensing
2. water temperature
3. Raman Scattering
4. spectroscopy

A technique for remotely measuring water temperature is discussed.

[7] R. N. Colwell, Manual of Photographic Interpretation, American Society of Photogrammetry, 1960.

Keywords: 1. multispectral imagery
2. photo interpretation
3. earth resources

The book covers the application of photointerpretation to various disciplines.

[8] L. W. Ham, "Remote Sensing of Water Pollution," Journal of the Water Pollution Control Federation, vol 40:10, October 1968, pp 1728-1738.

Keywords: 1. remote sensing
2. multispectral imagery
3. spectral signature

Discussion of the use of multispectral imagery for detection of water pollution.

[9] R. A. Holmes, R. B. MacDonald, "The Physical Basis of System Design for Remote Sensing in Agriculture," Proceedings of the IEEE, vol 57, April 1969, pp 629-639.

Keywords: 1. remote sensing
2. agriculture
3. system design
4. spectral radiance
5. multispectral scanner

This discussion is a survey of the factors involved in multispectral remote sensing of agricultural areas.

[10] G. Nagy, "Digital Image-Processing Activities in Remote Sensing for Earth Resources," Proceedings of the IEEE, vol 60, October 1972, pp 1177-1200.

Keywords: 1. remote sensing
2. earth resources
3. multispectral scanner
4. classification techniques
5. spectral signature
6. shape detection

Survey article describing the sources and uses of high altitude imagery, particularly in relation to earth resources. It has an excellent bibliography.

[11] NASA, Revised ERTS Data Users Handbook, Goddard Space Flight Center, Greenbelt, Maryland, August 25, 1972.

Keywords: 1. ERTS
2. multispectral scanner
3. return beam vidicon
4. radiometric accuracy
5. cartographic accuracy

Describes the ERTS multispectral scanner and return beam vidicon systems, both their methods of operation and their accuracy.

[12] S. S. Rifman, "Evaluation of Digitally Corrected ERTS Imagery," Symposium on Management and Utilization of Remote Sensing Data, Sioux Falls, South Dakota, October 1973, pp 206-221.

Keywords: 1. ERTS
2. geometric correction

Precision geometric correction of ERTS imagery is accomplished by using a low order piecewise approximation to image distortion, incorporating spacecraft attitude refinement from ground control points, and using special interpolation techniques.

[13] H. Sievering, R. Mittra, "The Effect of Coherence on Laser Radar Air Pollution Measurements," Symposium on Remote Sensing of the Environment, Proceedings, vol 1, pp 751-757, May 1971.

Keywords: 1. remote sensing
2. air pollution
3. laser radar

A technique for measuring the amount of air pollution using scattering of laser radiation is discussed.

[14] B. J. Wobber, "Orbital Photos Applied to the Environment," Photogrammetric Engineering, vol 36, August 1970, pp 852-864.

Keywords: 1. orbital photography
2. environmental quality
3. air pollution
4. water quality
5. residential quality

Discussion of the application of orbital photography to assessment of environmental quality.

DATA COMPRESSION

[15] J. E. Abate, "Linear and Adaptive Delta Modulation," Proceedings of the IEEE, vol 55, No. 3, March 1967, pp 298-308.

Keywords: 1. adaptive data compression
2. adaptive delta modulation
3. PCM
4. comparison

Adaptive ΔM provides a companding capability, offers a bit rate reduction over PCM, is better suited to TV and speech than fixed ΔM, gets same maximum S/N performance as fixed ΔM.

The S/N performance is the same for both Gaussian and exponential densities.

[16] V. K. Agarwal, "A New Approach to the Fast Hadamard Transform Algorithm," presented at the Hawaii International Conference on System Sciences, Honolulu, Hawaii, January 1971.

Keywords: 1. Hadamard transform
2. fast algorithm
3. ordering

A fast algorithm is described which is simple to implement, because of the repetition of identical operations. Sequences are ordered by a permutation procedure.

[17] V. K. Agarwal, T. J. Stephens, On-Board Processor (Picture Bandwidth Compression), TRW IRAD Report for Space Vehicles Division, February 1970.

Keywords: 1. fast Hadamard transform
2. quantization
3. sampling
4. hardware study

Theory, computer simulations and hardware study.

[18] V. R. Algazi, "Adaptive Line by Line Encoder for Image Transmission," International Telemetering Conference Proceedings, 1972.

Keywords: 1. adaptive
2. line by line encoder
3. Hadamard transform
4. Fourier transform
5. Gibb's effect

An adaptive line by line encoder which subtracts the signals' linear contribution to avoid the Gibb's effect.

[19] G. B. Anderson, T. S. Huang, "Piecewise Fourier Transformation for Picture Bandwidth Compression," IEEE Transactions on Communication Technology, vol 19, April 1971, pp 133-140.

Keywords: 1. Fourier transformation
2. bandwidth compression

Image is divided into blocks. In each block the Fourier transform of the logarithm of the data is obtained. Quantization is done according to statistics of the transform values in each block. High quality reconstructe monochrome images obtained with 1.25 bits per picture point.

[20] J. B. Anderson, "A Stack Algorithm for Source Coding with a Fidelity Criterion," IEEE Transactions on Information Theory, vol 20, March 1974, pp 211-226.

Keywords: 1. tree coding
2. stack algorithm
3. fidelity criterion
4. binary memoryless source
5. Hamming distortion measure

Analysis of a new scheme for source coding with a fidelity criterion by tree codes.

[21] J. B. Anderson, F. Jelinek, "A 2-Cycle Algorithm for Source Coding with a Fidelity Criterion," IEEE Transactions on Information Theory, vol 19, January 1973, pp 77-92.

Keywords: 1. tree coding
2. source coding
3. fidelity criterion

Discusses the application of convolutional coding to source coding with a fidelity criterion.

[22] C. A. Andrews, J. M. Davies, G. R. Schwartz, "Adaptive Data Compression," Proceedings of the IEEE, vol 55, No. 3, March 1967, pp 267-277.

Keywords: 1. adaptive data compression
2. polynomial predictor
3. interpolation compressor
4. transformation compressor
5. Karhunen-Loève compression
6. reconstruction interpolation

A number of compression techniques are discussed. Comparison is made of zero order predictors, first order interpolators, linear predictor difference coding, variable sample coding, Karhunen-Loève coding, and Fourier transform coding. All data is one dimensional. Results favor zero order perdictor and first order interpolator.

[23] H. C. Andrews, Computer Techniques in Image Processing, Academic Press, 1970.

Keywords: 1. orthogonal transformations
2. fast transformations
3. Fourier transform
4. Hadamard transform
5. image coding
6. quantization
7. bandwidth reduction
8. transform sampling
9. checkerboard sampling
10. random sampling
11. zonal sampling
12. threshold sampling
13. channel noise effects

A survey book on computer techniques in image processing, with several chapters on transform techniques and coding.

[24] H. C. Andrews, Fourier Coding of Images, University of Southern California, 1968.

Keywords: 1. transform processing
2. sampling
3. quantization

Ph.D. dissertation.

[25] H. C. Andrews, W. K. Pratt, "Fourier Transform Coding of Images," 1969 International Conference on System Science, Honolulu, Hawaii, pp.677-679.

Keywords: 1. Fourier transform coding

Study of frequency domain bandwidth compression using the Fourier transform of entire pictures.

[26] R. J. Arguello, H. R. Sellner, J. A. Stuller, "The Effect of Channel Errors in the Differential Pulse Code Modulation Transmission of Sampled Imagery," IEEE Transactions on Communication Technology, vol 19, December 1971, pp 926-933.

Keywords: 1. channel error
2. differential pulse code modulation

The effect of channel errors in channels having various bit error probabilities is shown for sampled imagery.

[27] A. V. Balakrishnan, "An Adaptive Nonlinear Data Predictor," Proceedings of the National Telemetering Conference (Washington, D.C., May 23-25 1962), vol 2, Suppl. paper 6-5.

Keywords: 1. Adaptive data compression
2. prediction algorithms
3. analysis
4. comparison

Three prediction algorithms are presented and results are illustrated with radar velocity data.

[28] T. Berger, "Optimum Quantizers and Permutation Codes," IEEE Transactions on Information Theory, vol IT-18, November 1972.

Keywords: 1. source coding
2. permutation codes
3. quantizers
4. comparison
5. variable length codes
6. analysis

Shows the equivalence of amplitude quantization and permutation coding. Permutation codes offer a readily implementable alternative to buffer-instrumented variable-length codes.

[29] T. Berger, Rate Distortion Theory, A Mathematical Basis for Data Compression, Prentice-Hall, 1971.

Keywords: 1. rate distortion theory
2. data compression
3. source coding
4. quantization
5. optimum modulation
6. complexity
7. instrumentability
8. analysis
9. prediction

A book which describes the application of rate distortion theory to data compression.

[30] T. Berger, F. Jelinek, J.K. Wolf, "Permutation Codes for Sources," IEEE Transactions on Information Theory, January 1972.

Keywords: 1. source coding
2. entropy coding
3. permutation coding
4. algorithms
5. rate distortion theory
6. comparison
7. analysis

Computer algorithms and simulation results.

[31] W. T. Bisignani, G. P. Richards, J. W. Whelan, "The Improved Gray Scale and the Coarse-Fine Systems, Two New Digital TV Bandwidth Reduction Techniques," Proceedings of the IEEE, vol 54, No. 3, March 1966, pp 376-390.

Keywords: 1. pulse code modulation
2. coarse-fine PCM
3. contouring
4. bandwidth reduction

Only the n most significant bits are transmitted. However, the least significant bits are used to alter the subsequent significant bits. Contouring is eliminated and the average signal value over small areas is correct.

[32] R. C. Brainard, J. C. Candy, "Direct Feedback Coders: Design and Performance with Television Signals," Proceedings of the IEEE, vol 57, May 1969, pp 776-786.

Keywords: 1. direct feedback coding
2. television signals

Comparison is made between direct feedback (of the decoded signal) coders and differential coders.

[33] Z. L. Budrikis, J. L. Hullett, D. Q. Phiet, "Transient Mode Buffer Stores for Nonuniform Code TV," IEEE Transactions on Communication Technology, vol 19, December 1971, pp 913-922.

Keywords: 1. buffer store
2. differential pulse code modulation
3. simulation
4. small-capacity stores

Deterministic constraints on sending and receiving stores are established, and store sizes are related to bit transmission rate and storage delay. Sending store's random behavior is modeled as a Markov chain with an absorbing state (overflow). Simulation of small capacity buffer stores to study overflow incidence is reported as well.

[34] D. Chan, R. W. Donaldson, "Optimum Pre- and Post-filtering of Sampled Signals with Application to Pulse Modulation and Data Compression Systems," IEEE Transactions on Communication Technology, vol Com-19, No. 2, April 1971, pp 141-157.

Keywords: 1. sampling
2. pre-emphasis
3. pulse modulation systems
4. PCM
5. PAM
6. DPCM

Joint optimization of pre-emphasis and post-emphasis filters (minimum mean square error criterion).

[35] D. J. Connor, "Techniques for Reducing the Visibility of Transmission Errors in Digitally Encoded Video Signals," IEEE Transactions on Communications, Vol 21, June 1973, pp 695-706.

Keywords: 1. transmission errors
2. differential pulse code modulation

Prediction techniques which minimize propagation of errors are discussed.

[36] D. J. Connor, R.C. Brainard, J.O. Limb, "Intraframe Coding for Picture Transmission," Proceedings of the IEEE, vol 60, No. 7, July 1972, pp 779-791.

Keywords: 1. survey article
2. DPCM
3. ΔM
4. source-receiver encoding
5. adaptive
6. reversible encoding

Main approaches are (1) noise frequency weighting, (2) source-receiver (psychovisual) coding, and (3) M-ary reversible coding.

[37] C. C. Cutler, "Delayed Encoding: Stabilizer for Adaptive Coders," IEEE Transactions on Communication Technology, vol. 19, No. 6, December 1971.

Keywords: 1. adaptive coding
2. 1 bit delta modulation
3. predictive encoder

Code is positive pulse if signal is increasing, negative if signal is decreasing. Size of step implied by pulse depends on number of pulses in a row of the same sign. Sampling done at 3 times the Nyquist frequency.

[38] L. D. Davisson, "An Approximate Theory of Prediction for Data Compression," IEEE Transactions on Information Theory, vol. 13, April 1967, pp 274-278.

Keywords: 1. prediction
2. data compression
3. stationary Gaussian time series
4. open-loop predictor
5. closed-loop predictor
6. polynomial approximation
7. simulation

Simulation confirms theoretical results implying closed-loop prediction is significantly better than open-loop prediction for a stationary Gaussian time series.

[39] L. D. Davisson, "Data Compression Using Straight Line Interpolation," IEEE Transactions on Information Theory, vol. IT-14, No. 3, May 1968, pp 390-394.

Keywords: 1. Interpolation
2. analysis
3. fan interpolation

Analysis and computer results show sensitivity to source statistics.

[40] L. D. Davisson, "Rate-Distortion Theory and Application," Proceedings of the IEEE, July 1972, pp 800-808.

Keywords: 1. analysis
2. comparison
3. transform coding
4. K-L
5. Fourier
6. Hadamard
7. DPCM
8. entropy coding
9. universal coding
10. optimum line coder
11. optimum area coder

Basic summary of rate distortion approach to evaluation of performance.

[41] L. D. Davisson, "The Theoretical Analysis of Data Compression Systems," Proc. of the IEEE, vol. 56, No. 2, February 1968, pp 176-187.

Keywords: 1. analysis
2. prediction
3. interpolation
4. Markov
5. figures of merit
6. comparison
7. channel errors

Considerations in the analysis of data compression systems are discussed together with some of the exact and approximate results which have been obtained.

[42] L. D. Davisson, "Theory of Data Compression," USC Report No. 64-46, September, 1964, pp 800-808.

Keywords: 1. data compression
2. analysis
3. predictive coding

Ph.D. Dissertation.

[43] L. D. Davisson, "Universal Noiseless Coding," IEEE Transactions on Information Theory, vol. 19, November 1973, pp 783-795.

Keywords: 1. universal coding
2. Rice coding

Discussion of blockwise memoryless coding where a performance measure is attained arbitrarily closely as block length approaches ∞.

[44] J. R. Duan, P. A. Wintz, "Error Free Coding," LARS Information Note 022073, Purdue University, 1973.

Keywords: 1. error free coding
2. DPCM
3. adaptive transform coding
4. quantization level expansion
5. ERTS
6. Karhunen Loève Transform

Transform coding is followed by DPCM where the difference is taken between the original and the reconstructed transformed data. An average reduction of 2:1 can be achieved for ERTS data with no error.

[45] L. Ehrman, "Analysis of Some Redundancy Removal Bandwidth Compression Techniques," Proceedings of the IEEE, vol. 55, No. 3, March 1967, pp 278-287.

Keywords: 1. bandwidth compression
2. redundancy removal
3. floating aperture prediction
4. zero-order interpolator
5. fan interpolator

The mean square error resulting from use of floating aperture prediction, zero order interpolation, and fan interpolation are compared for a signal which is a sample function of a first-order Gaussian Markov process. Conclusion is that fan interpolator is best.

[46] D. J. Eigen, F. R. Framm, R. A. Northouse, "Cluster Analysis Based on Dimensional Information with Applications to Feature Selection and Classification," IEEE Transactions on Systems, Man, and Cybernetics, vol. 4, May 1974, pp 284-294.

Keywords: 1. ERTS
2. multispectral scanner
3. cluster analysis

A method for clustering multidimensional data such as multispectral

scanner data is discussed. Clustering is done dimension by dimension and the results are combined.

[47] J. E. Essman, P. A. Wintz, "The Effects of Channel Errors in DPCM Systems and Comparison with PCM Systems," IEEE Transactions on Communications, vol. COM-21, No. 8, August 1973, pp 867-877.

Keywords: 1. channel errors
2. DPCM
3. PCM
4. sampling
5. quantization
6. comparison

Optimum prediction coefficient depends on the channel noise. Simulation results are shown.

[48] B. J. Fino, "Relations Between Haar and Walsh/Hadamard Transforms," Proceedings of the IEEE, May 1972, pp 647-648.

Keywords: 1. unitary transforms
2. Haar transform
3. Hadamard transform
4. Walsh transform
5. fast algorithms
6. comparison

For some applications, the Haar transform performs as well as, and faster than, the Walsh/Hadamard transform. Computations for a vector of order 2^n requires $2(2^n-1)$ operations for Haar and $n2^n$ for Walsh/Hadamard.

[49] L. E. Franks, "A Model for the Random Video Process," Bell System Technical Journal, April 1966, pp 609.

Keywords: 1. Gaussian/Markov
2. correlations
3. optimum linear filters

Continuous part of power spectral density if characterized as a product of three factors based on effects of point-to-point, line-to-line, and frame-to-frame correlation.

[50] A. Frei, H. Schindler, P. Vettiger, "An Adaptive Dual-Mode Coder/Decoder for Television Signals," IEEE Transactions on Communication Technology, Vol. 19, December 1971.

Keywords: 1. adaptive coder
2. delta modulation
3. differential pulse code modulation

[51] T. Fukinuki, "Optimization of D-PCM for TV Signals with Consideration of Visual Property," IEEE Transactions on Communications, vol. 22, June 1974, pp 821-826.

Keywords: 1. differential pulse code modulation
2. nonlinear quantization
3. properties of vision

Optimal quantization for DPCM is derived based on statistical properties of the signal and properties of human vision.

An adaptive coder is developed which uses delta modulation in slowly varying areas and DPCM in areas of larger variation. A bit rate of 1.5 bps was achieved using this method.

[52] T. Fukinuki, M. Miyata, "Intraframe Image Coding by Cascaded Hadamard Transforms," IEEE Transactions on Communications, vol. 21, March 1973, pp 175-180.

Keywords: 1. Hadamard transform
2. differential pulse code modulation
3. redundancy reduction

Implementation of Hadamard transform for real time videophone transmission. Three bits per sample are required for good picture quality in the case of a two-dimensional (4x2) transform.

[53] G. G. Furman, Removing the Noise from the Quantization Process by Dithering: Linearization, RM-3271-PR, The Rand Corporation, February 1963.

Keywords: 1. quantization
2. dithering
3. contouring
4. analysis

Sawtooth dithering linearizes the quantizer and reduces the contouring effects.

[54] R. G. Gallager, Information Theory and Reliable Communication, John Wiley and Sons, 1968.

Keywords: 1. information theory
2. distortion measure
3. source coding
4. Huffman code
5. data reduction
6. bandwidth compression

This book covers information theory and coding.

[55] H. Gish, J. N. Pierce, Asymptotically Efficient Quantizing, IEEE Transactions on Information Theory, vol. 14, September 1968, pp 676-683.

Keywords: 1. sampled data systems
2. quantizing
3. asymptotic efficiency

It is shown, under weak assumptions on the density function of a random variable and under weak assumptions on the error criterion, that uniform quantizing yields an output entropy which asymptotically is smaller than that for any other quantizer, independent of the density function or the error criterion. The asymptotic behavior of the rate distortion function is determined for the class of νth low loss functions, and the entropy of the uniform quantizer is compared with the rate distortion function for this class of loss functions. The extension of these results to the quantizing of sequences is also given. It is shown that the discrepancy between the entropy of the uniform quantizer and the rate distortion function apparently is a consequence of the inability of the optimal quantizing shapes to cover large dimensional spaces without overlap. A comparison of the uniform quantizer and of the minimum-alphabet quantizer is also given.

[56] T. J. Goblick, Jr., "Analog Source Digitization: A Comparison of Theory and Practice," IEEE Transactions on Information Theory, April 1967, pp 323-326.

Keywords: 1. quantization
2. symbol coding
3. block coding
4. entropy coding
5. Max quantizer
6. uniform quantizing
7. Gauss-Markov sources
8. comparison

Gives performance bounds and comparisons of quantizers.

[57] B. Gold, C. Rader, A. V. Oppenheim, T. G. Stockham, Jr., Digital Processing of Signals, McGraw-Hill, 1969.

Keywords: 1. digital signals
2. quantization
3. sampling
4. Fast Fourier Transform

Discussion includes effects of quantization and sampling in filtering and derivation of the Fast Fourier Transform.

[58] L. S. Golding, R. K. Garlow, "Frequency Interleaved Sampling of a Color Television Signal," IEEE Transactions on Communication Technology, vol. 19, December 1971, pp 972-979.

Keywords: 1. sampling
2. comb filtering

A color television signal is separated into luminance and chrominance signals, then sampled below the Nyquist rate. Since most energy in signals is at harmonics of the line and frame rate, proper choice of sampling rate results in interleaving of aliased energy in the gaps. NTSC quality color television can be transmitted using a sampling rate of 8.7 MHz.

[59] L. S. Golding, P. M. Schultheiss, "Study of an Adaptive Quantizer," Proceedings of the IEEE, vol. 55, No. 3, March 1967, pp 293-297.

Keywords: 1. quantization
2. adaptive systems
3. uniform quantizing
4. adaptive algorithms

Shows how a reduction in quantization error can be achieved by allowing the quantization scheme to depend on measurements of the short-term range of the signal. Reductions of up to one bit per sample obtained.

[60] D. J. Goodman, L. J. Greenstein, "Quantizing Noise of ΔM/PCM Encoders," Bell System Technical Journal, vol. 52, No. 2, February 1973, pp 183-204.

Keywords: 1. delta modulation
2. quantizing noise
3. Gaussian random process
4. digital filters
5. analysis
6. PCM

Delta modulator for A/D, followed by fixed length PCM coder and digital filter. Curves relate S/N to filter order, ΔM sampling rate, and PCM word length.

[61] L. M. Goodman, "A Binary Linear Transformation for Redundancy Reduction," Proceedings of the IEEE, March 1967, pp 467-468.

Keywords: 1. linear transformation
2. block quantization
3. Hadamard transform
4. bit allocations
5. comparison

Comparison of K-L and Hadamard transforms on Gauss-Markov data on the basis of a defined efficiency.

[62] A. Habibi, "Comparison of n^{th} Order DPCM Encoder with Linear Transformations and Block Quantization Techniques," IEEE Transactions on Communication Technology, vol. COM-19, No. 6, December 1971, pp 948-956.

Keywords: 1. DPCM
2. unitary transform
3. Hadamard
4. Fourier
5. Karhunen-Loève
6. picture coding
7. data compression comparison

The performance of the DPCM system improves by using higher-order predictors even though the change in the variance is not significant past the third-order predictor.

The performance in terms of output signal to noise ratio of a DPCM system with a third or higher order predictor is superior to all 2-dimensional transform techniques when the system is optimized for the particular picture. However, for the more realistic case of unmatched statistics, the performance of the transforms is superior. Other considerations favor DPCM.

[63] A. Habibi, "Delta Modulation and DPCM Coding of Color Signals," International Telemetering Conference Proceedings, 1972.

Keywords: 1. delta modulation
2. differential pulse code modulation
3. color signals
4. adaptive
5. simulation

Various DPCM and delta modulation schemes are simulated using luminance and chromaticity components of color video signals. The results are compared at various rates.

[64] A. Habibi, Performance of Zero-Memory Quantizers Using Rate-Distortion Criteria.

Keywords: 1. quantizing
2. comparison

The performance of uniform, Max, and instantaneous companding quantizers in coding single variates of Gaussian and two-sided exponential probability density functions are studied. The uniform quantizer with entropy coding is superior to the other quantizers used with symbol coding when the results are compared with the rate-distortion function.

[65] A. Habibi, R. Hershel, "A Unified Representation of DPCM and Transform Coding,"

Keywords: 1. differential pulse code modulation
2. transform coding

A method of coding is described in which blocks of data are transmitted. The first element in the block is transmitted. The n^{th} transmitted message is a linear combination of the first n elements of the block. For a Markov source this coder reduces to DPCM.

[66] A. Habibi, P. A. Wintz, "Image Coding by Linear Transformation and Block Quantization," IEEE Transactions on Communication Technology, vol. COM-19, No. 1, February 1971, pp 50-62.

Keywords: 1. linear transformations
2. block quantization
3. K-L
4. Fourier
5. Hadamard
6. Gauss-Markov data
7. theory
8. comparison

Comparison of transform performance, discussion of complexity.

[67] R. M. Haralick, I. Dinstein, "An Iterative Clustering Procedure," IEEE Transactions on Systems, Man, and Cybernetics, vol. 1, July 1971, pp 275-289.

Keywords: 1. clustering
2. remote sensing
3. multispectral imagery
4. principal components

Multispectral data is clustered into several groups based on spectral signature. Only a value indicating which cluster an element belongs to is transmitted.

[68] R. M. Haralick, K. Shanmugam, "Comparative Study of a Discrete Linear Basis for Image Data Compression," IEEE Transactions on Systems, Man, Cybernetics, vol. 4, January 1974, pp 16-27.

Keywords: 1. image data compression
2. Hadamard transform
3. Karhunen Loève transform
4. comparison
5. DPCM

6. slant transforms
7. discrete linear basis transform

Discussion concerns use of the discrete linear basis transform for image data compression. Authors say results are, in simplicity and accuracy, between Hadamard and K-L.

[69] B. G. Haskell, "Computation and Bounding of Rate-Distortion Functions for Certain Message Sources and Distortion Criteria," Ph.D. dissertation, University of Berkeley, June 1968, (Sep 531).

Keywords: 1. rate distortion functions
2. computation and bounding for certain memoryless message sources.

Methods are given for the numerical computation of Shannon's rate distortion function, R(D), for certain memoryless message sources. It is assumed first that U, the set of possible message-source outputs, and V, the set of possible destination symbols, are countable. The computation of R(D) for this case is reduced to a minimization problem in which the variables are the destination-symbol probabilities.

For arbitrary U and V, upper and lower bounds on R(D) are derived by partitioning U and V each into a countable collection of disjoint subsets and employing the results derived previously for the case of countable U and V. Conditions are then discussed under which these bounds can be made arbitrarily close to each other by choosing sufficiently fine partitions of U and V. Two examples are included to illustrate the results in detail.

[70] H. Heffes, S. Horing, D. L. Jagermar, "On the Design and Analysis of a Class of PCM Systems," Bell System Technical Journal, vol. 50, No. 3, March 1971, pp 917-918.

Keywords: 1. noiseless coding
2. PCM
3. sampling rate
4. quantizer
5. reconstruction filter
6. analysis

Design for peak error criterion. Tradeoffs between sampling rate, quantizer and reconstruction filter.

[71] D. Hockman, H. Katyman, D. R. Weber, "Application of Redundancy Reduction to Television Bandwidth Compression," Proceedings of the IEEE, Vol. 55, No. 3, March 1967, pp 263-266.

Keywords: 1. bandwidth compression
2. redundancy reduction

3. interpolator
4. predictor

Encoding using one-dimensional first order predictors is discussed.. TV bandwidth compression ratios of up to 4 are obtained.

[72] J. J. Y. Huang, P. M. Schultheiss, "Block Quantization of Correlated Gaussian Variables," IEEE Transactions on Communication Systems, September 1963, pp 289-296.

Keywords: 1. transforms
2. quantization
3. bit allocation

An approximate expression is obtained for the manner in which the available binary digits should be assigned to the quantized variables.

[73] F. Jelinek, "Study of Sequential Decoding," Quarterly Progress Report to the National Aeronautics and Space Administration, NASA Contract NAS 2-5643, December 1969.

Keywords: 1. convolutional code
2. fidelity criterion
3. Hamming distance
4. binary source
5. constraint length
6. discrete memoryless source

Gives the mean Hamming distortion attained by certain convolutional codes as a function of constraint length. Theoretical optimum is 0.11 for a rate ½ code.

[74] F. Jelinek, K. S. Schneider, "On Variable-Length-to-Block Coding," IEEE Transactions on Information Theory, November 1972, pp 765-774.

Keywords: 1. source coding
2. variable-length coding
3. block coding
4. run length coding
5. buffer overflow
6. complexity

Obtains codes that minimize probability of buffer overflow for a given rate and buffer length and presents asymptotically optimum coding algorithms whose complexity grows linearly with length.

[75] W. Kaminski, E. F. Brown, "An Edge-Adaptive Three-Bit Ten-Level Differential PCM Coder for Television," IEEE Transactions on Communication Technology, vol. COM-19, no. 6, December 1971, pp 944-947.

Keywords: 1. adaptive data compression
2. edge adaptive DPCM
3. psychovisual coding
4. direct feedback coding

Psychovisual tolerance to brightness errors in the neighborhood of brightness boundaries permits restricting coding accuracy near boundaries. Effective rate (DPCM) of 3-bit picture increased to 3-1/3 bits/pel (DPCM) by edge-adaptive coding.

[76] J. D. Kennedy, et al., Digital Imagery Data Compression Techniques, McDonnell Douglas Astronautics Co., MDC G0402, January 1970.

Keywords: 1. transform image processing
2. Hadamard transform
3. K-L transform
4. comparison

Comparison of fast Hadamard and Karhunen-Loève, with reductions of 5:1.

[77] C. M. Kortman, "Redundancy Reduction - A Practical Method of Data Compression," Proceedings of the IEEE, vol. 55, no. 3, March 1967, pp 253-263.

Keywords: 1. data compression
2. redundancy reduction
3. predictor
4. interpolator

One-dimensional predictive and interpolative encoding are discussed. For imagery, bandwidth compression ratios of 6 are obtained.

[78] E. R. Kretzmer, "Statistics of Television Signals," Bell System Technical Journal, vol. 31, July 1952, pp 751-763.

Keywords: 1. statistics
2. correlation
3. imagery

The correlation function of the process of which an image is a sample function is estimated experimentally for several different images.

[79] R. L. Kuehn, E. R. Omberg, G. D. Forry, "Processing of Images Transmitted from Observation Satellites," Information Display, September/October 1971.

Keywords: 1. border following
2. spectral signature
3. classification
4. maximum likelihood detection

A method for finding borders of areas separating different classes is demonstrated. Each class is defined by a spectral signature. Boundaries are tracked, once one boundary point is found, using maximum likelihood estimation.

[80] T. Kummerow, "Statistics for Efficient Linear and Non-Linear Picture Coding," International Telemetering Conference Proceedings, 1972.

Keywords: 1. differential pulse code modulation
2. video signals
3. fixed code word length
4. synchronous bit rate
5. adaptive
6. one-dimensional prediction
7. two-dimensional prediction

Spacing between quantization levels is done adaptively for DPCM. The number of levels is fixed.

[81] R. L. Kuta, J. A. Sciulli, "The Performance of an Adaptive Image Compression System in the Presence of Noise," IEEE Transactions on Information Theory, vol. IT-14, no. 2, March 1968, pp 273-279.

Keywords: 1. adaptive data compression
2. predictive coding
3. channel errors
4. comparison of adaptive prediction techniques

Average bit compression ratios between 2.5 and 3.5 can be attained with zero-order hold predictor and run-length coding. Such a system can perform satisfactorily with 10^{-4} channel error rate. Synchronization errors unknown.

[82] H. J. Landau, D. Slepian, "Some Computer Experiments in Picture Processing for Bandwidth Reduction," Bell System Technical Journal, vol. 50, No. 5, May-June 1971.

Keywords: 1. 2-D Hadamard transform
2. quantizing
3. bit allocations

Computer experiments in processing with 2-D Hadamard transform. Good quality pictures obtained at 2 bits/pel. Some general comments on the encoding of pictures are included.

[83] M. Levine, "Feature Extraction: A Survey," Proceedings of the IEEE, vol. 57, August 1969, pp 1391-1405.

Keywords: 1. Feature extraction

Discussion of various features which can be defined and how they can be extracted from imagery.

[84] J. O. Limb, F. W. Mounts, "Digital Differential Quantizer for Television," Bell System Technical Journal, September 1969, pp 2583-2599.

Keywords:
1. predictive coding
2. digital integrator time constant tracking
3. quantizing
4. dithered quantizing
5. transmission error protection

Report on construction and testing of 3-bit DPCM system with digital integrator. Dithered quantizing used to reduce contouring.

[85] J. O. Limb, C. B. Rubinstein, "Plateau Coding of the Chrominance Component of Color Picture Signals," IEEE Transactions on Communications, vol. 22, June 1974, pp 812-820

Keywords:
1. chrominance
2. plateau coding

Chrominance is coded by transmitting only the average chrominance value between two large changes in luminence. The address of the area having the particular chrominance value need not be transmitted since the luminence information reveals the address. The technique relies on the fact that generally chrominance changes imply luminence changes.

[86] J. O. Limb, C. B. Rubinstein, K. A. Walsh, "Digital Coding of Color Picturephone Signals by Element-Differential Quantization, IEEE Transactions on Communications, Vol. 19. December, 1971. pp 992-1006.

Keywords:
1. color signal
2. element differential quantizer
3. real time

Coding of all the chrominance information with one bit per picture element leads to a high quality color display. A rate of 6.3M bits/sec for video is adequate. Only one chrominance component is transmitted each line, and the missing component is obtained by line averaging.

[87] J. O. Limb, I. G. Sutherland, "Run-Length Coding of Television Signals," Proceedings of the IEEE, February 1965, pp 169-170.

Keywords: 1. source coding
2. run-length coding
3. effects of video noise on channel saving from simple run-length coding

Only marginal results are obtained from attempts to exploit statistical redundancy of the video signal. Elimination of irrelevant information by psychovisual coding is required.

[88] J. L. Mannos, D. J. Sakrison, "The Effects of a Visual Fidelity Criterion on the Encoding of Images," IEEE Transactions on Information Theory, vol. 20, July 1974, pp 525-536.

Keywords: 1. rate distortion
2. visual fidelity criterion
3. simulation
4. frequency weighting

A visual fidelity criterion is developed experimentally by simulating the optimum coding at a fixed rate for a variety of criteria and letting various subjects view the resulting images. The observers order the images in order of subjective quality.

[89] J. Max, "Quantizing for Minimum Distortion," IRE Transactions on Information Theory, March 1960, pp 7-12.

Keywords: 1. quantizing
2. minimum mean square error
3. entropy
4. optimum quantizing
5. quantizer recursion relations

Contains tables for the design of optimum (minimum mean square error) quantizers and for optimum uniform quantizers.

[90] C. L. May, D. J. Spencer, T. A. Zimmerman, "Data Compression Techniques," TRW IRAD Report 7132.44-04, August 1972.

Keywords: 1. data compression
2. multi-spectral imagery
3. spectral-spatial-delta interleave
4. shell coding
5. implementation considerations
6. Rice algorithm
7. hardware implementation
8. rate distortion function
9. differential pulse code modulation

A study and comparison of various data compression techniques as they apply to multispectral imagery.

[91] C. L. May, D. J. Spencer, ERTS Image Data Compression Technique Evaluation, Final Report for NASA Contract NAS5-21746., April, 1974.

Keywords: 1. data compression
2. multispectral imagery
3. Huffman code
4. Rice coding

The application of various information preserving techniques to ERTS imagery is investigated. A number of new techniques are included. Bit rates averaged over all scenes of as low as 2.67 bits/sample were obtained. (Each picture element consists of one sample in each of four spectral bands.)

[92] J. B. Millard. H. I. Maunsell, "Digital Encoding of the Video Signal," Bell System Technical Journal, February 1971, pp 459-479.

Keywords: 1. analysis
2. DPCM
3. predictive quantizing
4. signal impairments
5. channel noise

Theory and implementation of picturephone DPCM system.

[93] S. C. Noble, S. C. Knauer, J. I. Giem, "A Real-Time Hadamard Transform System for Spatial and Temporal Redundancy Reduction in Television," (unpublished), authors with Ames Research Center, Mt. View, Calif.

Keywords: 1. real-time Hadamard transform
2. spatial redundancy reduction
3. temporal redundancy reduction

Three dimensional Hadamard transform is implemented in real-time on 4x4x4 cubes of data where 2 dimensions represent spatial information and the third represents temporal information. The application is data compression for transmission of television signals. A compression ratio of 11.6 to 1.0 has been obtained.

[94] J. B. O'Neal, "A Bound on Signal-to-Quantizing Noise Ratios for Digital Encoding Systems," Proceedings of the IEEE, vol. 55, no. 3, March 1967, pp 287-292

Keywords: 1. analysis
2. comparison
3. DPCM
4. PCM
5. ΔM
6. Entropy coding

Bounds on the S/N performance of data compression systems.

[95] J. B. O'Neal, "Delta Modulation Quantizing Noise Analytical and Computer Simulation Results for Gaussian and Television Input Signals," Bell System Technical Journal, January 1966, pp 117-141.

Keywords: 1. delta modulation
2. quantizing
3. analysis
4. computer simulations
5. granular noise
6. slope overload

Slope overload formulas derived for Gaussian signals are shown to apply quite well to video signals for picturephone data.

Delta mod quantizing noise is subjectively less annoying than the same amount of additive noise.

[96] J. B. O'Neal, "Entropy Coding in Speech and Television Differential PCM Systems," IEEE Transactions on Information Theory, November 1971. pp 758-761.

Keywords: 1. entropy coding
2. DPCM
3. Huffman coding
4. Shannon/Fano coding

Much of the redundancy in a speech or television signal is eliminated when it is encoded by DPCM. Additional coding using entropy coding techniques can result in a further increase of 5.6 dB in signal-to-quantizing noise ratio without increasing the transmission rate.

[97] J. T. Pinkston, "An Application of Rate-Distortion Theory to a Converse of the Coding Theorem," IEEE Transactions on Information Theory Vol. 15 January 1969. pp 66-71.

Keywords: 1. rate-distortion theory

Application to coding theorem converse; discrete memoryless sources.

[98] E. C. Posner, et al, "Epsilon Entropy of Stochastic Processes," The Annals of Mathematical Statistics, Vol. 38, No. 4, August 1967, pp 1000-1020.

Keywords: 1. data compression
2. fidelity criterion
3. rate distortion theory

Basic rate distortion theorems.

[99] W. K. Pratt, "A Bibliography on Television Bandwidth Reduction Studies," IEEE Transactions on Information Theory, vol. IT-13, no. 1, January 1967, pp 114-115.

Keywords:
1. television bandwidth reduction
2. bibliography
3. physiological aspects of viewing
4. statistical picture properties
5. information theoretic aspects of television images

English-language books, journals, and periodicals containing studies of television bandwidth reduction.

[100] W. K. Pratt, L. R. Welch, W. H. Chen, "Slant Transforms for Image Coding," Proceedings of the 1972 Application of Walsh Functions Symposium.

Keywords:
1. slant transform
2. image coding

Use of sawtooth basis functions for transform data compression.

[101] W. K. Pratt, W. H. Chen, L. R. Welch, "Slant Transform Image Coding," IEEE Transactions on Communications, vol. 22, August 1974, pp 1075-1093.

Keywords:
1. slant transform
2. image coding
3. sawtooth basis vector
4. unitary transform
5. fast computational algorithm
6. monochrome imagery
7. color imagery
8. zonal sampling
9. two dimensional transform

Good quality imagery with 1 to 2 bits/pixel for monochrome imagery and 2 to 3 bits/pixel for color imagery by transmitting only values in the transform domain which exceed some threshold.

[102] W. K. Pratt, "Spatial Transform Coding of Color Images," IEEE Transactions on Communication Technology, vol. 19, December 1971, pp 980-992.

Keywords:
1. transform coding
2. Hadamard transform coding
3. Fourier transform coding
4. Karhunen-Loève transform coding
5. luminence
6. chrominance

Tristimulus color signals are transformed into various sets of three orthogonal pictures (e.g., luminance, and two chrominance images). These new sets are encoded using various techniques such as the K-L transform and Hadamard transform. Bit rates as low as 1.75 bits/pixel are obtained.

[103] W. K. Pratt, J. Kane, H. C. Andrews, "Hadamard Image Coding," "Proceedings of the IEEE , Vol. 57, January 1969, pp 58-68.

Keywords: 1. transform coding
2. Hadamard transform
3. fast algorithm
4. quantization

Good tutorial article on the fast Hadamard transform. Computational sequences produce ordered sequencies in the transform, but result in a more complex algorithm.

[104] P. J. Ready, P. A. Wintz, "Information Extraction, SNR Improvement, and Data Compression in Multispectral Imagery," IEEE Transactions on Communications, vol. 21, October 1973, pp 1123-1131.

Keywords: 1. Karhunen-Loève transform
2. principal components
3. data compression
4. multispectral imagery
5. information extraction
6. signal to noise ratio improvement
7. classification accuracy

Discussion of the application of the principal components or Karhunen-Loève transformation to data compression, feature extraction, signal to noise ratio improvement, and classification accuracy.

[105] R. L. Remm, "Analysis and Implementation of a Delta Modulation Pictorial Encoding System," 1966 International Telemetering Conference Proceedings, pp 27-34.

Keywords: 1. delta modulation
2. DPCM
3. System design and implementation

A 2 to 3:1 reduction in bit rate is achieved without appreciable information loss, using 2 bit DPCM. Error rates of 0.01 and 0.004 for PCM and DPCM, respectively, yield comparable quality.

[106] R. F. Rice, J. R. Plaunt, "Adaptive Variable-Length Coding for Efficient Compression of Spacecraft Television Data," IEEE Transactions on Communication Technology, vol. COM-19, no. 6, December 1971, pp 889-897.

Keywords: 1. adaptive data compression
2. variable-length coding
3. entropy coding
4. source coding
5. M-ary reversible coding

Using sample-to-sample prediction, the coding system produces output rates 0.25 bit/pel from the one-dimensional difference entropy between 0 and 8 bits/pel. Performance improvements of 0.5 bit/pel can be simply achieved by previous line correlation.

Adaptation, using concatenated codes, selects one of three codes to use for a block.

[107] R. F. Rice, "Channel Coding and Data Compression System Considerations for Efficient Communication of Planetary Imaging Data," Jet Propulsion Laboratory, Technical Memorandum 33-695.

Keywords: 1. data compression
2. imaging data
3. system considerations
4. channel coding
5. pulse code modulation
6. rate
7. quality

A general overview of the factors which must be considered in channel and source coding.

[108] G. P. Richards, W. T. Bisignani, "Redundancy Reduction Applied to Coarse-Fine Encoded Video," Proceedings of the IEEE, vol. 55, no. 10, December, 1967.

Keywords: 1. adaptive data compression
2. coarse-fine PCM systems
3. statistical time-buffering techniques

High activity data is coarsely quantized. Redundant data is finely quantized, coarse levels are extrapolated from previous elements. Compression ratio of 4.5:1 to 6.3:1 are obtained for good quality reproductions, relative to 6-bit PCM.

[109] M. P. Ristenbatt, "Alternatives in Digital Communications," Proceedings of the IEEE, vol. 61, no. 6, June 1973.

Keywords: 1. source encoding
2. channel encoding
3. transmission
4. receiver

Good survey article for basic concepts.

[110] G. S. Robinson, Orthogonal Transform Feasibility Study, COMSAT Technical Report No. CL-TR-5-71, NASA Contract NAS9-11240, November 1971.

Keywords: 1. rate distortion criteria
2. Fourier
3. Walsh-Hadamard
4. Haar transform
5. Karhunen-Loève
6. Speech processing
7. two-dimensional transform
8. image transform processing
9. bibliography
10. quantizing
11. bit allocation

Final report on transform study for NASA-MSC.

[111] D. J. Sakrison, Communication Theory: Transmission of Waveforms and Digital Information, John Wiley & Sons, Inc., 1968.

Keywords: 1. sampling theorem

The sampling theorem is one of many topics in communication theory covered by this book.

[112] D. J. Sakrison, "Factors Involved in Applying Rate Distortion Theory to Image Processing," Proceedings of the UMR - Mervin J. Kelly Communications Conference, October 1970.

Keywords: 1. rate distortion

A distortion criterion is proposed which consists of the mean square error between some transformation of the signal and the same transformation applied to the source coded signal.

[113] D. J. Sakrison, "The Rate-Distortion Function for a Class of Random Processes," IEEE Transactions on Information Theory, vol. 16, January 1970, pp 10-16.

Keywords: 1. rate distortion functions
2. distortion measure

The distortion function which applies to an entire class of sources, A, is derived.

[114] D. J. Sakrison, The Rate Distortion Function of a Gaussian Process with a Weighted Mean Square Error Criterion, (Corres.), IEEE Transactions on Information Theory, Vol. 19, May, 1968. Addendum, Vol. 15, September 1969 pp 610-611.

Keywords: 1. Gaussian processes

2. mean-square error distortion measure

Parametric expressions for the rate distortion function of a Gaussian process under a weighted mean-square error criterion is derived. The addendum corrects two shortcomings: one, of a physical orientation, was that transient effects were ignored; the second relates to analytical tractability in applying the results.

[115] D. J. Sakrison, V. R. Algazi, "Comparison of Line-by-Line and Two-Dimensional Encoding of Random Images," IEEE Transactions on Information Theory, July 1971, pp 386-398.

Keywords:
1. distortion measure
2. rate-distortion function
3. line by line encoding
4. two-dimensional encoding

Using a mean square error distortion measure, a comparison is made of the rate required to encode an image using line by line encoding and using two dimensional encoding.

[116] J. E. Savage, "The Complexity of Decoders - Part II: Computational Work and Decoding Time," IEEE Transaction on Information Theory, vol. IT-17, no. 1, January 1971, pp 77-85.

Keywords:
1. computational work
2. decoding time
3. complexity
4. decoders
5. Ziv iterative coding
6. Forney's concatenated coding
7. sequential decoding

The computational work and the time required to decode with reliability E at code rate R on noisy channels are defined, and bounds on the size of these measures are developed. A number of ad hoc decoding procedures are ranked on the basis of the computational work they require.

[117] W. F. Schreiber, "Picture Coding," Proceedings of the IEEE, vol. 55, no. 3, March 1967, pp 320-330.

Keywords:
1. survey
2. DPCM
3. PCM Pre- and Post-Quantizing filters
4. two-dimensional
5. dual-mode

6. psychophysical coding
7. subjective evaluation

After survey, a subjective optimization based on the point of marginal improvement is suggested.

[118] J. W. Schwartz, "Bit-Plane Encoding: A Technique for Source Encoding," IEEE Transactions on Aerospace and Electronic Systems, vol AES-2, no. 4, July 1966, pp 385-392.

Keywords: 1. M-ary reversible source coding
2. information preserving
3. information destroying
4. run length coding
5. Explorer XVII

Bit-plane encoding divides a group of bits into subgroups so that some of the groups can be summarily described.

[119] L. F. Shaefer, A. Macovski, "Encoding and Decoding of Color Information Using Two-Dimensional Spatial Filtering," IEEE Transactions on Computers, vol. 21, July 1972, pp 642-647.

Keywords: 1. transform coding
2. color imagery
3. Fourier transform

Color images modulate carriers of different spatial frequencies for combining three color signals on one frequency domain image. Carriers are implemented using gratings.

[120] K. Sharmugam, R. M. Haralick, "A Computationally Simple Procedure for Imagery Data Compression by Karhunen-Loève Method," IEEE Transactions on Systems, Man, and Cybernetics, vol. 3, March 1973, pp 202-204.

Keywords: 1. image data compression
2. Karhunen-Loève transform
3. computationally short procedure

Computations required to obtain the eigenvectors and eigenvalues of a covariance matrix are reduced by a factor of 4.

[121] C. E. Shannon, "Coding: Theorems for a Discrete Source with a Fidelity Criterion," in Information and Decision Processes, edited by Robert E. Macchol; New York, McGraw-Hill Book Co. Inc., 1960, pp 93-126.

Keywords: 1. binary source coding
2. rate distortion theory
3. error correcting codes

Source paper for theory on (n, k) algebraic codes (rate > 1).

[122] D. Slepian, "Permutation Modulation," Proceedings of the IEEE, March 1965, pp 228-236.

Keywords: 1. source coding
2. block coding
3. variable distortion coding
4. entropy coding
5. algebraic coding
6. analysis

Original article on permutation coding.

[123] D. J. Spencer, "Data Compression of Spacecraft Imagery,"

Keywords: 1. data compression
2. spacecraft imagery
3. earth resources satellite
4. source encoding
5. compression ratio
6. information rate
7. entropy codes

A survey of approaches to data compression of spacecraft imagery.

[124] M. Tasto, P. A. Wintz, "A Bound on the Rate-Distortion Function and Application to Images," IEEE Transactions on Information Theory, vol. 18, January 1972, pp 150-159.

Keywords: 1. rate distortion function
2. discrete ergodic sources with memory
3. bound
4. mean square error

An upper bound on the rate distortion function for discrete ergodic sources with memory is found.

[125] M. Tasto, P. A. Wintz, "Image Coding by Adaptive Block Quantization," Transactions on Communication Technology, vol. COM-19, no. 6, December 1971, pp 957-972.

Keywords:
1. adaptive block quantization
2. image coding
3. K-L transformation
4. bit allocation
5. Max's quantizers
6. subjective optimization
7. eigenvalue transformations

Use adaptive eigenvalue transformation on small blocks of data.

[126] A. J. Viterbi, J. K. Omura, Convolutional Encoding of Memoryless Discrete-Time Sources.

Keywords:
1. source coding
2. convolutional coding
3. rate distortion theory
4. M-ary reversible coding

Derives a bound on the average per letter distortion achievable by a time-varying convolutional source code of fixed constraint length.

[127] W. C. Wilder, Subjectively Relevant Error Criteria for Pictorial Data Processing, Purdue University, Report TR-EE 72-34, December 1972.

Keywords:
1. image processing
2. subjective evaluation
3. comparison
4. criteria

Ph.D. dissertation.

[128] P. A. Wintz, "Transform Picture Coding," Proceedings of the IEEE, vol. 60, no. 7, July 1972, pp 809-820.

Keywords:
1. linear transformations
2. quantizing
3. transform parameters
4. adaptive techniques
5. comparisons
6. survey

A survey article. Concludes that adaptive transform techniques are required to approach 1 bit/pel.

[129] R. C. Wood, On Optimum Quantization, IEEE Transactions on Information Theory, Vol. 15, March, 1969 pp 248-252

Keywords: 1. quantization error minimization
2. sampling of stochastic signals

The problem of minimizing mean-square quantization error is considered and simple closed form approximations based on the work of Max and Roe are derived for the quantization error and entropy of signals quantized by the optimum fixed-N quantizer. These approximations are then used to show that, when N is moderately large, it is better to use equi-internal quantizing than the optimum fixed-N quantizer if the signal is to be subsequently buffered and transmitted at a fixed bit rate. Finally, the problem of optimum quantizing in the presence of buffering is examined, and the numerical results presented for Gaussian signals indicate that equilevel quantizing yields nearly optimum results.

PATTERN CLASSIFICATION

[130] H. C. Andrews, Introduction to Mathematical Techniques in Pattern Recognition, John Wiley & Sons, 1972.

Keywords: 1. feature selection
2. classification

Discussion of feature selection and pattern classification.

[131] P. E. Anuta, "Digital Registration of Multispectral Video Imagery," Journal of the Society of Photo-Optical Instrumentation Engineers, Vol. 7, September 1969, pp 168-175.

Keywords: 1. multispectral imagery
2. registration
3. adaptive

Measure of difficulty of registration is defined and algorithm is changed depending on this measure.

[132] P. E. Anuta, "Spatial Registration of Multispectral and Multitemporal Digital Imagery Using Fast Fourier Transform Techniques," IEEE Transactions on Geoscience Electronics, vol 8, October 1970.

Keywords: 1. enhancement
2. correlation
3. overlay
4. registration
5. multispectral imagery
6. multitemporal imagery

Description of a method for registration of multispectral or multitemporal imagery where the correlation step is implemented using the Fast Fourier Transform.

[133] R. O. Duda, P. E. Hart, Pattern Classification and Scene Analysis, Artificial Intelligence Group, Stanford Research Institute, Menlo Park, California, 1970.

Keywords: 1. pattern classification
2. clustering

The theory of pattern classification is discussed.

[134] K. S. Fu, "On the Application of Pattern Recognition Techniques to Remote Sensing Problems," Purdue University School of Electrical Engineering Report No. TR-EE 71-13. June 1971.

Keywords: 1. remote sensing
2. pattern recognition
3. spectral signature
4. crop classification

Discussion of the application of various classification procedures to earth resources problems using multispectral imagery.

[135] K. S. Fu, D. A. Landgrebe, T. L. Phillips, "Information Processing of Remotely Sensed Agricultural Data," Proceedings of the IEEE, vol 57, April 1969, pp 639-653.

Keywords: 1. remote sensing
2. crop classification
3. feature selection
4. classification accuracy
5. spectral signature

Discussion of the application of pattern recognition techniques to classification of crop type using multispectral imagery.

[136] A. S. Gliniewicz, H. M. Lachowski, W. H. Pace, P. Salvato, ASTEP Users' Guide and Software Documentation, TRW Note No. 74-FMT-939, Document No. 25990-H028-R0-00.

Keywords: 1. clustering
2. factor analysis
3. feature selection
4. transform
5. maximum likelihood
6. multispectral imagery

Descriptions of programs for doing clustering and classification of multispectral imagery.

[137] R. M. Haralick, D. E. Anderson, "Texture-Tone Study with Application to Digitized Imagery," The University of Kansas Center for Research, Inc., Technical Report 182-2, November 1971.

Keywords: 1. texture analysis
2. pattern classification
3. remotely sensed imagery

Texture features are defined and measurement of these features is used for land use classification.

[138] G. G. Lendaris, G. L. Stanley, "Diffraction Pattern Sampling for Automatic Pattern Recognition," Proceedings of the IEEE, vol 58, February 1970, pp 198-216.

Keywords: 1. Fourier transform
2. pattern recognition

Spatial Fourier Transform used as basis for land use classification in imagery.

[139] K. Preston, Jr., "A Comparison of Analog and Digital Techniques for Pattern Recognition," Proceedings of the IEEE, vol 60, October 1972, pp 1216-1231.

Keywords: 1. earth resources analysis
2. land use analysis
3. pattern recognition
4. analog techniques
5. digital techniques

It is shown that the analog computer offers workers using low-precision high-speed linear-discriminant analysis a significant advantage in hardware performance in certain important areas.

APPENDIX D
TRW IMAGE CODING FACILITIES

A block diagram of TRW image coding facilities is shown in Figure 1. This includes an Interdata 85 IBM computer, a Dicomed color image recorder, and an 8000 COMTAL digital image displayer. Both the Dicomed and Comtal systems are interfaced with the Interdata computer. The Interdata computer is used for simulating and processing simple algorithms; TRW's time sharing system is used for simulating and processing more complicated algorithms.

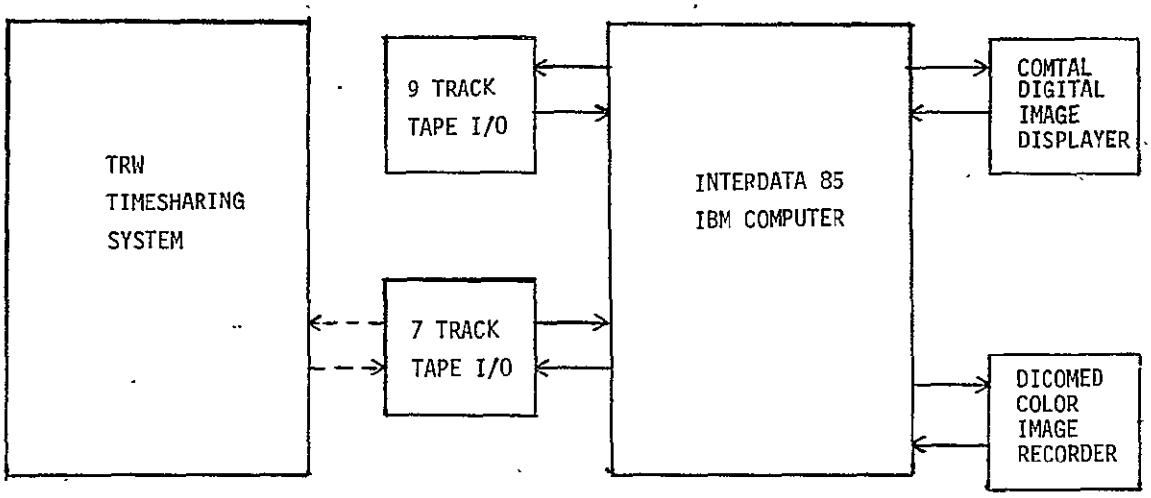

Figure 1. TRW's System Engineering Laboratory Image Coding Facilities

D.1 COMTAL DIGITAL IMAGE DISPLAYER

The COMTAL 8000 Series digital image displayer produces a high spatial resolution video image presentation over the full range of brightness levels in shades of gray, pseudo color, or full color. The displayer is completely self-contained, including the display monitor, digital refresh storage, the associated electronics, power supplies, and complete off-line diagnostic capabilities. Installation of a system requires only the application of the digital input information and 110 Vac power.

Operationally, this unit performs in a manner similar to other computer peripheral devices. It is unique only in the type of data processed and the resulting display presentation. It is designed to provide simple, inexpensive interfacing with all common sources of digital data. The entire display unit may be controlled either locally or from a remote source, using the same data structure for both commands and data. Local control of a

display unit is achieved with the control panel which provides the capability of generating all the required display commands. This control panel is connected into the basic interface structure in the same manner as an external device. The control panel also provides a logically oriented data pattern generator. Off-line diagnostic operations are performed using the facilities of the control panel.

D.2 DICOMED COLOR IMAGE RECORDER

The DICOMED color image recorder is a high performance cathode ray tube (CRT) film recorder capable of producing photographs in black and white or color from digitally encoded pictorial data. This data may be achieved from an on-line computer system or from an off-line Dicomed image digitizer or magnetic tape unit. The data is converted into exposure energy levels with values up to 256, which make up the picture elements (pixels) and is recorded at resolutions of 512, 1024, 2048, or 4096 pixels per axis. Three resolutions are selectable on a unit: 512, 1024, 2048, or 1024, 2048, 4096.

The recorder has an automatic color filter advance which may be controlled from the operator panel or from an externally connected unit. The three primary color filters selectable are blue, green, and red, with a neutral selectable for black and white.

The image recorder constructs either single or multiple images by using a full raster scan or a random position format. A command and status structure is provided in the logic which allows the image recorder to be operated manually or under program control. The recorder utilizes a parallel 8-bit digital interface.

APPENDIX E

DOCUMENTATION OF THE BANDWIDTH COMPRESSION SOFTWARE

INTRODUCTION

TRW has developed a number of bandwidth compression algorithms for multispectral ERTS data. These bandwidth compression algorithms are simulated on a digital computer using the following software package. The software includes the following coding algorithms.

1. Three-dimensional coding algorithms using a block size of 4x16x16 with a block quantizer. The system has the option of utilizing three-dimensional Hadamard, Cosine or Slant Transformations. The system uses a fixed block quantizer for all three options.

2. A hybrid coding algorithm using an option of Karhunen-Loeve or Haar transformation followed by a two-dimensional Differential Pulse Code Modulator (DPCM). The transformation is in spectral domain and the two-dimensional DPCM encoder uses a third-order predictor. The eigenvectors of the Karhunen-Loeve transform and the weightings in the two-dimensional DPCM encoder are fixed. They are based on the statistics of a typical data. They could be varied by simply reading a set of new values in the program.

3. A hybrid coding algorithm which uses an option of Karhunen-Loeve or Haar transform in the spectral domain followed by an option of Cosine, Slant, or Hadamard transform in the horizontal and a block of DPCM encoders in the vertical direction. The block size of the spectral transformation is four, and the block size of the transformation in the horizontal direction is 16. The system uses a fixed set of DPCM encoders for all preceding transformations.

   All three coding methods discussed above have a fixed bit rate. They encode the multispectral data at bit rates of 0.5, 1, 2 bits per picture element. The average bit rate can be varied easily by changing the data card in the program.

   The above coding algorithms have the option of using a binary symmetric channel at bit error rates of 10^{-2}, 10^{-3}, and 10^{-4}. This can also be varied to any optional value by changing the input data.

Main Programs

I - SPXT;

Definition - It performs spectral transformation (and the Inverse) on the 4 bands of ERTS multispectral data.

Specifications;

1. Transformation is one of the following:

   ITYPE = 1 Haar
   = 2 Cosine
   = 3 Hadamard
   = 4 Slant
   = 5 Karhunen-Loeve

2. 256x256 real data for each band at input and output.
3. Input; on Units 1, 2, 3, 4
   Output; on Units 11, 12, 13, 14
4. The output of SPXT is saturated to levels bounded by 0.0 and 255.

Inputs; on Unit 5.

1. ITYPE, IFR; Format (2I2)
   ITYPE specifies type of transformations.
   IFR = 1 forward transform.
   = -1 inverse transform.
2. AA(4,4); Format (10F8.3)
   AA is the matrix of spectral correlation of the original 4 bands. Note only upper triangular form is read in.

Subroutines;

1. KLMAT (AA,Z)
   AA; 4x4 covariance matrix.
   Z; matrix of eigenvectors of AA.
2. Haar (C,D,SQ,IFR); Haar transform of size 4.
   C(4) Input-Real
   D(4) Output-Real
   IFR=1 Forward
   IFR=-1 Inverse
   SQ = $\sqrt{2}$.

3. HAD4(C,D,IFR); Hadamard transform of size 4.
   C(4) Input-Real
   D(4) Output-Real
   IFR=1 Forward
   IFR=-1 Inverse
4. COS4 (C,4,IFR); Cosine transform of size 4.
   C(4) Input/Output - Real
   IFR=1 Forward
   IFR=-1 Inverse.
5. SLNT4 (C,D,SQ5,IFR); Slant transform of size 4.
   C(4) Input-Real
   D(4) Output-Real
   IFR=1 Forward
   IFR=-1 Inverse
   SQ5 = $\sqrt{5}$.
6. KLT (C,D,Z,IFR); Karhunen-Loeve transform of size 4.
   C(4) Input-Real
   D(4) Output-Real
   Z(4,4) Matrix of Eigenvectors - Real
   IFR=1 Forward
   IFR=-1 Inverse

II - DPCMCH

Definition - It encodes and reconstructs up to 4 bands of 256 by 256 real imagery data. Original or spectrally transformed data can be used as input. The system performs the following tasks as shown on Figure 1. Starting values II=1, JJ=11

1. Find mean and variance of data (256x256) on Unit JJ.
2. Normalize data on Unit JJ and put it on Unit 7.
3. Find horizontal, vertical and diagonal correlation of data on Unit 7.
4. Encode data on Unit 7 and renormalize and write it on Unit II.
5. Repeat above for II=2, .., IBAND and JJ=12,...

Specifications; 1. Input on Units 11, 12, 13, 14.
Output on Units 1, 2, 3, 4.

Inputs; on Unit 5

1. IBAND, IRATE, IREP (Format 3I2)

IBAND is the no. of bands which needs to be coded/dec. This depends on no. of bits/pixel allowed. For 0.5 and 1 bit/pixel only 2 bands are coded for 2 bits/pixel all 4 bands are coded.

IRATE specifies bit-error rate in the channel. Values of 0, 1, 2, 3, 4 correspond to bit error rates of 0.0, 0.1, 0.01, 0.001, 0.0001 respectively.

IREP IREP=0 is the normal mode for the program IREP=1 is a feature used to avoid measuring the statistics of a data repeatedly. For this mode weightings of predictor, correlation of data and mean, standard deviation of the signal, and the variance of the differential signal are read in.

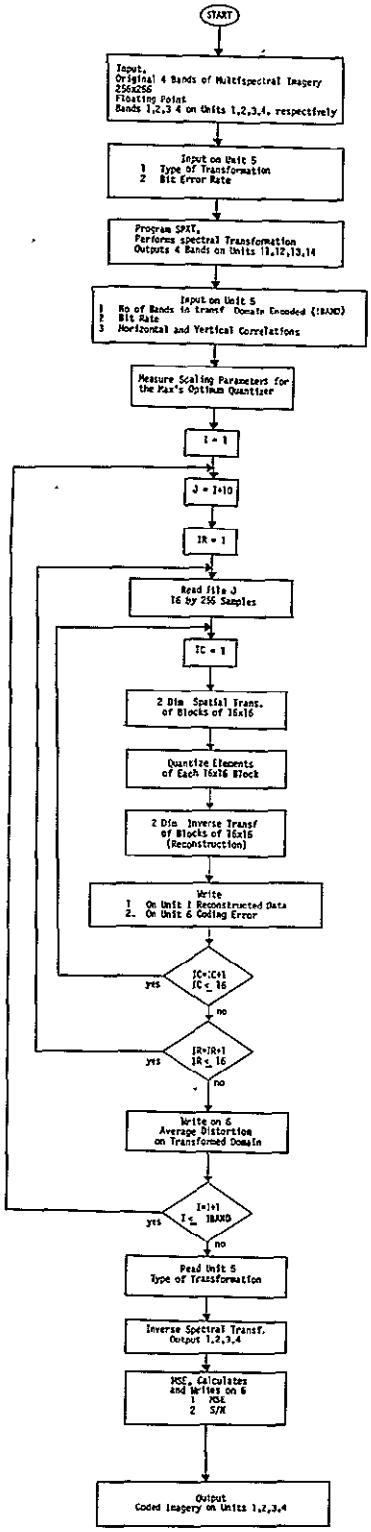

Figure 1. Flow-Chart Corresponding to the Program that Performs a Spectral Transformation (KL, Haar, Cosine, Hadamard, Slant) followed by a 2-Dimensional DPCM Encoding

2. IALI; (Format I2)
   IALI specifies the number of bits/sample in spectrally transformed domain that one desires to use for coding each band, i.e.,for an average of 0.5 bit/pixel values for IALI are 1, 1, 0, 0.For 2 bits/pixel values for IALI are 3, 3, 1, 1. Note; one value for IALI is read for each band.

Subroutines;

1. QUAN (E,EQ,JJ,II,IZ)
   Quantizes the differential signal non-linearly.
   E; differential signal-real.
   EQ; quantized value of differential signal-real
   IZ; Magnitude of quantized level - integer
   II; sign of quantized level - integer
   JJ; combined sign and magnitude of quantized level - integer.

2. EROR (ER,X,Y)
   Calculates mse for one line of imagery
   X(256); one line of original data-real
   Y(256); one line of encoded data-real
   ER; MSE between X and Y-real

3. STAT (B,S,V)
   Calculates first and 2nd moments of one line of imagery
   B(256); one line of data-real
   S; mean value of B(256)-real
   V; second moment of B(256)-real

4. CORL (R,V,D)
   Calculates horizontal, vertical and diagonal correlation of normalized imagery on Unit 7.
   R; Horizontal correlation of normalized real data on Unit 7 - real

   V; Vertical correlation of normalized. Real data on Unit 7 - real

   D; Diagonal correlation of normalized, real data on Unit 7 - real.

5. COEF (R,V,D,A)
   Finds optimum weightings for 3rd order predictor
   R; Horizontal correlation of an imagery data.
   V; Vertical correlation of an imagery data.
   D; Diagonal correlation of an imagery data.
   A(3); Optimum weightings of a 3rd order predictor for a 2 dim. DPCM encoder.

6. LEQT2F; TRW/TSS Document attached

7. CNLER (IZ,IZO,IIX,IBIT,II)
   Simulates a binary symmetric channel.
   IZ; Magnitude of quantized level as input to noise channel.
   IZØ; Magnitude of quantized level as output of noisy channel.
   II; Sign of quantized level (at input/output) of noisy channel.
   IIX; Seed for generating a normal random variable.
   IBIT; Bits/sample allowed for encoding.

8. RECHN (II,IZ,IIX,EQ,IBIT)
   Uses output of channel to generate a quantized value
   II; Sign of quantized level
   IZ; Magnitude of quantized level at input of noisy channel
   IIX; Seed for generating a normal random variable.
   EQ; Quantized value of the differential signal at the output of the noisy channel.
   IBIT; Bits/sample allowed for encoding.

III - TRB3D;

Definition - It performs two-dimensional transformation and a block quantization for up to 4 bands of 256x256 samples imagery (or spectrally transformed forms). The system operates as follows: Initial value for II=1 and JJ=10+II. (See Fig. 2).

1. Horizontal and vertical correlation of the imagery data is used to find the variance of the elements in the transform. domain. The elements in transformed domain are ordered according to the size of their variances.

2. Imagery data is divided into blocks of 16x16 and 2 dim. transform of each block is obtained.

3. Each block is quantized using Max's optimum quantizer using the variances in the transform domain, then the inverse 2 dim. transform of quantized components is performed.

4. The image is put in proper format and is written on Unit II.

5. Above operation is repeated for II=2,...,IBAN.

Specifications - Transformation is one of the following:

ITYPE=1	Hadamard
=2	Cosine
=3	Slant

Inputs; on Unit 5.

1. IBAND,ITYPE,IRATE (Format 3I2)

IBAND is the no. of bands which needs to be coded/dec. This depends on no. of bits/pixel allowed. For 0.5 and 1 bit/pixel only 2 bands are coded/decoded. For 2 bits/pixel all 4 bands are coded.

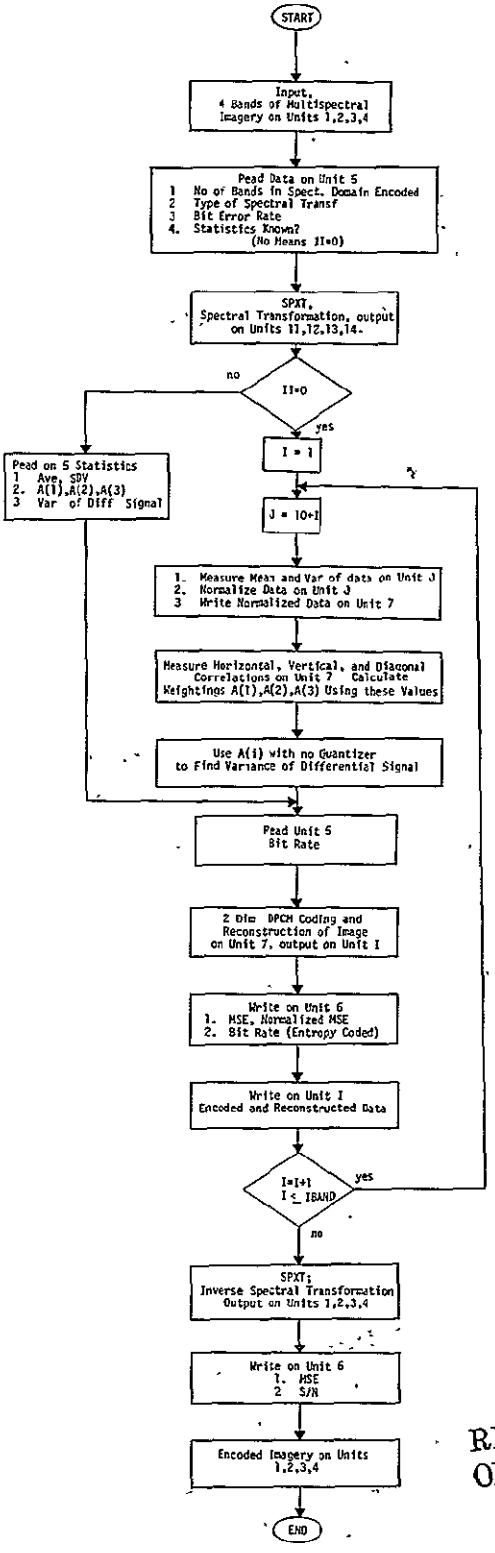

Figure 2: Flow Chart of the Program that Performs 3-Dimensional Transformation (Hadamard, Slant, Cosine) and Block Quantization

ITYPE Specifies type of the 2 dim. transform.

ITYPE=1	Hadamard
=2	Cosine
=3	Slant

IRATE Specifies bit error-rate (BER)

IRATE=1	BER=0.1
=2	=0.01
=3	=0.001
=4	=0.0001
=0	=0.0

2. (MFI(I),I=1,9) Format (9I8)
   MFI(I) indicates that I bits are used in coding ordered samples in transform domain indexed from MS(I) to MF(I). Where MS(I)=MF(I)+1 for I=2,...,9. MS(1)=1.

3. CORH,CORV - (Format 2F6.3)
   CORH; Horizontal correlation of imagery data on Unit JJ
   CORV; Vertical correlation of imagery data on Unit JJ.

Subroutines;

1. Channel (K,R,VALUE,VMAX,IEROR,IX)
   Simulates a binary symmetric channel.

K	No of bits.
R	Parameter in Max's optimum quantizer.
VALUE	Output of the noisy channel.
VMAX	Specifies bit error rate. It's related to IRATE in TRB3D.
IEROR	No of times error happens.
IX	Seed for generating a normal random variable.

2. FNRN (IX,V); TRW/TSS Subroutine
   generates a normal random variable n(0,1)
   IX; seed for generating a random number. Should be
   specified the first time FNRN is used only - integer
   V; random variable (zero mean, unit variance) - real

3. COVTRS (C,D,A,ITYPE)
   Finds the covariance of transformed data from the covariance
   of the original data.
   C(16x16) Covariance of original data - real.
   A(16) Diagonal elements of D - real.
   ITYPE =1 Hadamard
   =2 Cosine
   =3 Slant.

4. GTRSF(A,ITYPE,IFR)
   Performs one-dimensional transformation for block size=16.
   A(16) Input/output - real
   ITYPE =1 Hadamard
   =2 Cosine
   =3 Slant
   IFR=1 Forward, IFR=-1 Inverse

5. Subroutine HADD (A,B)
   One-dimensional fast Hadamard transform for a block size of 16.
   A(16) Input - real
   B(16) Output - real
   Both forward and reverse. For reverse divide by 16.

6. Subroutine COST (A,ISIZE,IFR)
   One-dimensional fast cosine transform for a block size of 16.
   Simple to modify for larger length up to 512.
   A(16) Input/output - real
   ISIZE = 16
   IFR = 1 forward, IFR=-1 Inverse

7. Slant (A,M,IFR)

   One-dimensional fast Slant transform for block size 8 to 512.

   A(16) Input/output - real

   M Block size = 2^M

   IFR=1 forward, IFR=-1 Inverse.

IV - HYBCH

Definition - It encodes and reconstructs (using one-dimensional transform/ DPCM systems) up to 4 bands of 256x256 real imagery data. Original or spectrally transformed data is used as input. The system performs the following tasks as shown on Fig. 3. Starting for II=1 and JJ=10+II.

1. Finds one-dimensional transform (block=16) of 16x256 samples of data on Unit JJ.

2. Finds correlation of transformed data for maximum of 16 rows and uses these for designing up to 16 DPCM system.

3. Reconstructs the data at the receiver of DPCM decoders and finds the inverse transform.

4. The above is performed for all 16x256 blocks then the reconstructed imagery is put on Unit II.

5. Above is repeated for II=1,...,IBAND.

Specifications; 1. Input on Units 11, 12, 13, 14.
Output on Units 1, 2, 3, 4.

Input on Unit 5; 1. ITYPE,IBAND,IRATE (Format 3I2)
ITYPE specifies type of transform
ITYPE=1 Hadamard
=2 Cosine
=3 Slant.
IBAND is the no. of bands which needs to be coded/dec. This depends on no. of bits/pixel allowed. For 0.5 and 1 bit/pixel only 2 bands are coded/decoded, for 2 bits/pixel all 4 bands are coded.

IRATE specifies bit-error rate in the channel. Values of 0, 1, 2, 3, 4 correspond to bit error rates of 0.0, 0.1, 0.01, 0.001, 0.0001 respectively.

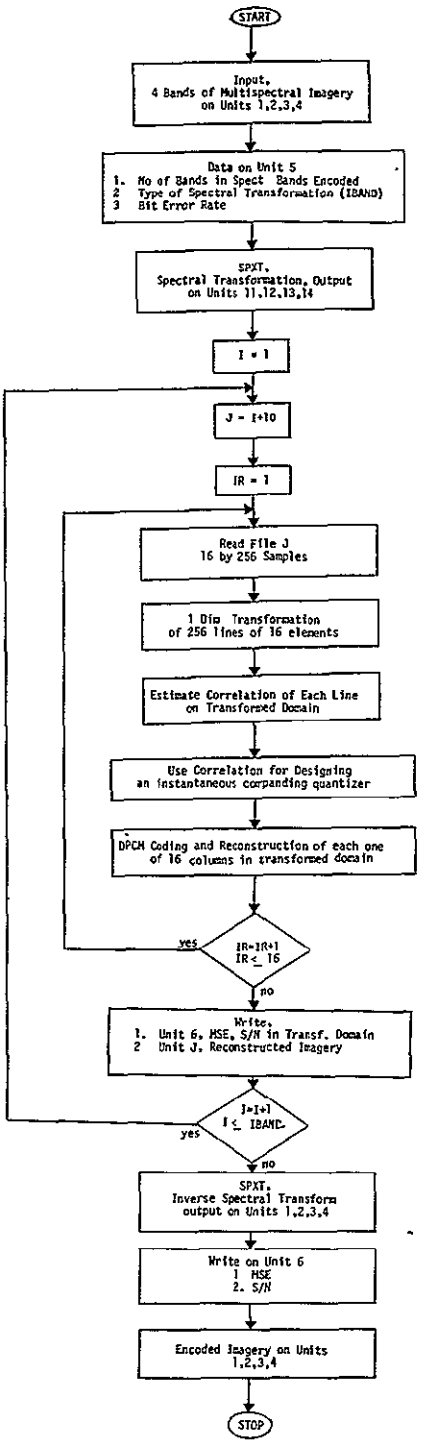

Figure 3. Flow Chart Corresponding to the Program that Performs a Spectral Transformation (KL, Haar, Cosine, Hadamard, Slant) followed by a Horizontal Transformation (Slant, Cosine, Hadamard) and a DPCM Encoding

2. K; (Format I2)
   K== no of coefficients to be encoded $1 \leq K \leq 16$.
   i.e. for 2 bits/pixel K=16
   for 1 bit/pixel K=8

3. (BIT(I),I=1,K); Format (16F3.0)
   BIT(I) is the number of bits allocated to the Ith row in the transform domain.

Subroutines;

1. HADD (A,B)
2. COST (A,16,IFR)
3. SLANT (A,M,IFR)

HADD, COST and SLANT are documented in Section III (TRB3D)

4. QUAN (E,II,IBIT,EM,EMAX,EXPM,LEVEL,EQ,IZ)
5. RECHN (II,IZ,IIX,LEVEL,EXPM,EMAX,EM,EQ,IBIT)

4 and 5 are same as QUAN and RECHN documented in Section II (DPCMCH). The difference is that here parameters EM,EMAX, EXPM, LEVEL and IBIT are passed by the Subroutine rather than using a common statement.

6. CNLER (IZ,IZ$\emptyset$,IIX,IBIT,II)

As documented in Section II (DPCMCH).

V. MSE

Definition; Finds mean square error between the original ERTS data and the encoded ERTS data.

Specification; Original ERTS data on Units, 1, 2, 3, 4.
Encoded ERTS data on Units 11, 12, 13, 14.

Output; on Unit 6

1. Mean square (MSE) for each band.
2. $\frac{(MSE)}{\text{Signal Energy}}$ x 100 for each band
3. Peak-to-peak signal to rms noise for each band.
4. Average of the above values over all 4 bands.

Data Sets	Usage
DTFST	SPXT for forward transform
DTRST	SPXT for inverse transform
DT5PCM	DPCMCH for 0.5 bit/pixel
DT1PCM	DPCMCH for 1 bit/pixel
DT2PCM	DPCMCH for 2 bits/pixel
DT5HYB	HYBCH for 0.5 bit/pixel
DT1HYB	HYBCH for 1.0 bit/pixel
DT]HYB	HYBCH for 2.0 bits/pixel
DT5T3	TRB3D for 0.5 bit/pixel
DT1T3	TRB3D for 1.0 bit/pixel
DT2T3	TRB3D for 2.0 bits/pixel

The above data sets specify the bit rate as well as the type of transformation and the bit-error rate in the channel.